Departement für Kleintiere
Klinik für Kleintiermedizin
der Vetsuisse-Fakultät Universität Zürich

Direktorin: Prof. Dr. med. vet. Claudia Reusch, Dipl. ECVIM-CA

Arbeit unter der Leitung von:
Prof. Dr. med. vet. Felicitas Boretti, Dipl. ACVIM & ECVIM-CA
Prof. Dr. med. vet. Nadja Sieber-Ruckstuhl, Dipl. ACVIM & ECVIM-CA

Gene expression changes in peritoneal adipose tissue of healthy dogs after long term glucocorticoid exposure

Inaugural-Dissertation

zur Erlangung der Doktorwürde der
Vetsuisse-Fakultät der Universität Zürich

vorgelegt von

Isabelle Avital Martin

Tierärztin
aus Frankfurt am Main, Deutschland

genehmigt auf Antrag von

Prof. Dr. med. vet. Felicitas Boretti, Referentin
Prof. Dr. med. vet. Nadja Sieber-Ruckstuhl, Referentin
Prof. Dr. med. vet. Thomas Lutz, Korreferent

2020

To my family

Table of Contents

Abstract

Adipose tissue is a complex and essential organ system. It is mainly composed of adipocytes and functions in a very integrated unit with several hormones, especially glucocorticoids. Glucocorticoids (GC) have a large influence in the metabolic systems in humans and animals.

Aim of the present study was to evaluate the effects of chronic GC exposure (hypercortisolemia) in healthy beagle dogs on gene expression in adipose tissue.

Before and after implanting ACTH-releasing minipumps subcutaneously for a period of 25 weeks, visceral adipose tissue was taken and gene expression changes analyzed using next generation sequencing.

Long term ACTH treatment resulted in the expected hypercortisolism with the characteristic clinical signs (e.g. muscle loss, fat mass redistribution). Hypercortisolemia was confirmed by a positive LDDS and ACTH stimulation test. A total of 1442 genes with significant transcriptomic alterations could be identified; of these, 507 genes were up- and 935 down-regulated. Chronic hypercortisolemia had a highly significant impact on genes involved in lipid and protein metabolism and led to a suppression of genes involved in the immune system. Moreover, genes encoding factors involved in insulin signaling, angiogenesis and collagen metabolism were significantly influenced.

With further studies the biological significance of these findings should be evaluated.

Zusammenfassung auf Deutsch

Fettgewebe ist ein komplexes Organsystem. Es besteht grösstenteils aus Adipozyten und interagiert mit verschiedenen Hormonen, insbesondere Glukokortikoiden. Glukokortikoide (GC) beeinflussen verschiedene Stoffwechselsysteme bei Menschen und Tieren.

Ziel der Studie war, den Einfluss einer chronischen GC-Behandlung (Hyperkortisolismus) auf die Genexpression im Fettgewebe bei gesunden Beagle Hunden zu untersuchen.

Vor und nach 25 Wochen nach Implantierung von subkutanen ACTH-freisetzenden Minipumpen, wurde viszerales Fettgewebe entnommen und die Genexpression mithilfe von “next generation sequencing“ analysiert.

Die ACTH-Behandlung führte zum erwartenden Hyperkortisolismus mit den charakteristischen Symptomen (z.B. Muskelatrophie, Fettumverteilung.) Die Hyperkortisolämie wurde anhand eines positiven Dexamethason Suppression- und positiven ACTH-Stimulationstests bestätigt. Es konnten 1442 Gene mit signifikanten transkriptomischen Veränderungen identifiziert werden, von denen 507 hoch- und 935 runterreguliert waren. Die chronische Hyperkortisolämie hatte einen hochsignifikanten Einfluss auf Gene, die am Lipid- und Proteinstoffwechsel beteiligt sind, und führte zu einer Unterdrückung von Genen, die am Immunsystem beteiligt sind. Darüber hinaus wurden Gene, die Faktoren der Insulinsignalisierung kodieren, die bei der Angiogenese und dem Kollagenstoffwechsel beteiligt sind, signifikant beeinflusst.

Durch weitere Studien sollte die biologische Bedeutung der Resultate evaluiert werden.

Abbreviations

ACTH	adrenocorticotropic hormone
ACSL4	Long-chain-fatty-acid—CoA ligase 4
ADH	adrenal-dependent hyperadrenocorticism
ADIPOQ	adiponectin
AGPAT3	1-Acylglycerol-3-Phosphate O-Acyltransferase 3
AGT	Angiotensinogen
ANG	II Angiotensin II
AP-1	Activator protein 1
cAMP	cyclic adenosine monophosphate
CAPN11	calcium-dependent cysteine protease 11
CCR2	C-C chemokine receptor type 2
CKM	creatine kinase M-type
COL	collagens
CoV	coefficient of variation
CRH	corticotropin releasing hormone
CYP	cytochrome P450
CYP2B6	cytochrome P450 2B6
DGAT1	Diacylglycerol O-acyltransferase 1
DKK1	Dickkopf-1
DLA-DRA	MHC class II DR alpha chain
DLA-DQB1	MHC class II DQ beta 1
EC	endothelial cell
EIF4BP1	eIF4E-binding protein 4E-BP1
ELOVL5	Elongation of very long chain fatty acids protein 5
FA	fatty acid
fc	fold change
FDR	FALSE discovery rate
FoxO	forkhead box O
FKBP5	FK506 binding protein 5
GC	glucocorticoid
GL	glycerolipids
GP	glycerophospholipids
GR	glucocorticoid receptor
G6PC	glucose-6 phosphatase catalytic subunit
HAC	hyperadrenocorticism
HLA-DRB1	HLA class II histocompatibility antigen, DRB1 beta chain
HMGCS2	hydroxymethylglutaryl-CoA synthase
HOAC	hypoadrenocorticism
HPA	hypothalamic pituitary axis
HSD	hydroxysteroid dehydrogenase
11β-HSD1	hydroxysteroid dehydrogenase 11 beta 1
ICAM	intercellular adhesion molecule
IFN	interferon
IGF-1	insulin like growth factor 1
IL	interleukin
INSIG	insulin induced gene
IRF	interferon regulatory factor
ITGAV	Integrin alpha-V

LEP	leptin
LIPE	hormone sensitive lipase
Log2	logarithm
LPL	lipoprotein lipase
LUM	lumican
MCP-1	monocyte chemoattractant protein 1
MHC	major histocompability complex
MR	mineralocorticoid receptor
mRNA	messenger RNA
NF-κB	nuclear factor 'kappa-light-chain-enhancer'
NGS	next generation sequencing
NO	nitric oxide
NR3C1	glucocorticoid receptor
NR3C2	mineralocorticoid receptor
PCOLCE	procollagen C-endopeptidase enhancer 1
PDH	pituitary-dependent hyperadrenocorticism
PG	phosphatidylglycerol
PGF2	Prostaglandin F2
PI	phosphatidylinositol
PI3	peptidase inhibitor 3
PIK3R1	Phosphoinositide-3-Kinase Regulatory Subunit 1
PKA	protein kinase A
RAS	renin-angiotensin system
RETN	resistin
RNA	seq RNA sequencing
RNF213	Ring finger protein 213
RPS	ribosomal protein S
RPS6KA1	ribosomal protein S6-kinase 1
rRNA	ribosomal RNA
SCP5	sterol carrier protein 5
sFRP	secreted frizzled-related protein
SCD5	Stearoyl-CoA desaturase 5
SRD5A1	steroid reductase 5A1
SULT1A1	sulfotransferase family 1A member 1
TAG	triglycerides
Th	T- helper cell
TLR	toll- like receptor
TLS	tube like structure
TNF	Tumor necrosis factor
Tregs	regulatory T cell
VCAM	vascular adhesion molecule
VEGF	vascular endothelial growth factor
VLDL	very low-density lipoprotein
WAT	white adipose tissue
WIF1	Wnt inhibitory factor-1

Chapter One

Introduction

1.1 Adipose tissue

The general composition of adipose tissue is divided into white and brown adipose tissue. White adipose tissue (WAT) adipocytes consists of cells with single triglyceride droplets, whereas brown adipose tissue consists of multilocular lipid droplets (Radin et al., 2009). Traditional functions of WAT are energy storage and physical support. Brown adipose tissue is directed towards functioning in thermogenesis. In addition to energy storage and insulation this organ shows significant endocrine activity. Studies on humans acknowledge that white adipose tissue acts as an endocrine organ, interacting with the brain in addition to neighboring tissues through secretion of various hormones (Trayhurn et al., 2006). Besides mature adipocytes the tissue also consists of other components such as preadipocytes, fibroblasts, and endothelial cells, all of which support fat tissue being called an “adipose organ” (Infante et al. 2017).

The endocrine function of WAT was established through the discovery of the cytokine-like hormone, leptin, which is in charge of signaling appetite and energy saturation. Additionally, a number of other protein hormones and signals are secreted by WAT; a diverse range of factors, termed adipokines, are released from adipocytes (Eisele et al., 2005).

1.2 Adipokines

Adipokines, which derive from adipocytes, are a summation of signaling factors and proteins. These biologically active substances include cytokines (e.g. TNFα), chemokines (e.g. MCP-1), alternative complement system proteins (e.g. adipsin), and proteins involved in vascular hemostasis (e.g. plasminogen activator inhibitor-1), blood pressure level proteins (e.g. angiotensinogen) and angiogenesis factors (e.g. vascular endothelial growth factor). Being so diverse, they are also involved in the regulation of lipid (e.g. cholesteryl ester transfer protein) and glucose metabolism (e.g. adiponectin) (Trayhurn et al., 2006). Through metabolic regulation, WAT is involved in intensive communication with other organs. Intensively researched adipokines include leptin, resistin and adiponectin.

Adiponectin (ADIPOQ), a major adipocyte-derived hormone, is directly involved in the regulation of energy steadiness. According to what is known, adiponectin is produced almost exclusively by mature adipocytes and its gene is one of the most highly expressed genes in WAT (Radin et al., 2009). Its secretion is triggered by insulin,

resulting in higher insulin sensitivity. It also enhances anti-inflammatory properties so that the formation of atherosclerosis can be suppressed (Radin et al., 2009). In dogs it has the same effect as in humans, where diet-induced obesity causes a decrease in circulation of the hormone concentration (Eisele et al., 2005).

Leptin (LEP), is a cytokine like prototypic adipokine, secreted mainly by adipocytes and to a lesser extent also by other organs. The gene is expressed in both immature and mature adipocytes in multiple WAT depots. The main function of leptin is control of energy storage by suppression of appetite and by increasing thermogenesis. There is a correlation of leptin concentration and body fat mass in dogs, as has been described in humans and rodents (Radin et al., 2009). High-fat diets as well as weight gain result in higher gene expression in dogs. Glucocorticoid (GC) administration in dogs can also influence leptin concentrations depending on the type and dose of GC used. Whereas orally administered prednisolone does not affect circulating leptin levels, dexamethasone causes a postprandial peak. Interestingly, the effect of methylprednisolone seems to be dose-dependent with an inverse correlation between dose and leptin concentration (Radin et al., 2009).

Another adipokine secreted by adipocytes is resistin (RETN); however, there seem to be large species differences in the expression and secretion of resistin: in contrast to rodents, it is predominantly expressed and secreted by macrophages in humans, while in cattle and pigs, in addition to fat, is has been shown in mammary tissue and leukocytes, respectively (Radin et al., 2009). So far, no studies in dogs are available, which is assumed to be the result of technical and analytical problems with its detection. Resistin secretion follows the same pattern as leptin, with a concentration increase occurring with increasing body mass or following a meal. Its pro-inflammatory effects lead to an increase in vascular adhesion molecules as well as a stimulation of cytokine secretion by macrophages. Atherosclerosis is a correlated effect in humans (Lazar, 2007).

Angiotensinogen (AGT) is part of the renin-angiotensin system (RAS) and is also involved in normal adipocyte differentiation. In WAT fat depots the RAS functions mainly by secreting angiotensinogen. In mice however, elevated angiotensinogen expression was only found in peritoneal fat (Rahmouni et al., 2004). Weight gain and excess WAT causes increased production of angiotensinogen, resulting in more enzyme activity. After conversion of excess AGT into Angiotensin II (ANG II) in perivascular adipose tissue, its vasoconstrictor activity may result in renal and cardiovascular dysfunction in rodents (Engeli et al., 2003).

1.3 Glucocorticoids

1.3.1 Endogenous Glucocorticoids

Glucocorticoids (GCs) are catabolic steroid hormones which derive from the cortex of the adrenal gland, with cortisol being the most important endogenous human GC. Almost no stimuli can directly impel the zona fasciculata cells to produce cortisol. GC secretion depends entirely on adrenocorticotropic hormone (ACTH) deriving from the anterior pituitary gland. ACTH on the other hand is controlled by corticotrophin releasing hormone (CRH) secreted by the hypothalamus. Following ACTH stimulation, cortisol is released by the cells of the zona fasciculata. These glands are together known as the hypothalamic pituitary axis (HPA) which operates by a feedback inhibition loop (Klein, et al., 2010). In general GCs have a huge impact not only on the production and distribution but also on the storage and utilization of substrates used for energy metabolism (Sukumaran et al., 2012). In humans as well as in animals, GCs are effective regulators of inflammation through activation of a series of consecutive stimuli which are necessary for recovery.

1.3.2 Therapeutic usage of Glucocorticoids

Beside endogenous glucocorticoids, synthetic GCs are popular and often used in human and veterinary therapy because of their wide-ranging potent anti-inflammatory and immunosuppressive effects. Their anti-inflammatory effects are mainly mediated by stabilizing lysosomal membranes to reduce the release of proteolytic enzymes by damaged cells as well as by depressing the phagocytic abilities of white blood cells to reduce further release of inflammatory materials (Mooney and Peterson, 2004). Their immunosuppressive effects are mediated by interference with signaling from the key inflammatory transcriptional regulators (NF-kB and AP-1) (Heck et al., 1994). Indications for the use of synthetic GCs in humans and animals are numerous, but they are most commonly used in allergic, inflammatory, and autoimmune diseases.

1.3.3 Clinical disease induced by increased glucocorticoid concentrations

Hyperadrenocorticism (HAC) is nowadays one of the most common endocrinopathy in dogs and results from prolonged exposure to high plasma concentrations of cortisol. (Mooney and Peterson, 2004). HAC can be naturally occurring or iatrogenic (chronic treatment with GCs).

Iatrogenic HAC is the result of chronic exogenous GC treatment for allergic, autoimmune, inflammatory or neoplastic diseases in dogs. In naturally occurring HAC, high levels of endogenously produced cortisol cause a disturbance in the hypothalamic-pituitary adrenal axis. The abnormality lies in either the pituitary or the adrenal glands, causing elevated serum cortisol concentrations. In about 85% of cases a pituitary tumor in the anterior lobe autonomously secretes corticotropin (ACTH) which stimulates the

adrenal gland to secrete cortisol (pituitary-dependent hyperadrenocorticism, PDH). In only 15% of HAC cases do adrenal tumors autonomously secrete cortisol, of which 50% are malignant (adrenal-dependent hyperadrenocorticism, ADH) (Behrend et al., 2001). Clinical symptoms are wide-ranging; however, the general conditions of polydipsia, polyuria, polyphagia, and lethargy are often observed in combination with muscle loss, weakness, alopecia, wound healing disturbances and systemic hypertension. In humans and animals, HAC is often concomitantly diagnosed with diabetes mellitus (Miceli et al., 2017). Iatrogenic and naturally occurring HAC cannot be differentiated on the basis of clinical symptoms.

1.4 Mechanism of action of Glucocorticoids: GC- and Mineralocorticoid-Receptors

GCs act by binding to glucocorticoid receptors (GR), which are widely distributed throughout the body in the cytoplasm of the cells. GCs bind to the GR and the complex is then translocated to the nucleus, where by binding to glucocorticoid responsive elements (GRE), it can lead to an activation or repression of genes.

GCs can also bind to another receptor, the mineralocorticoid receptor (MR), which has a high affinity for endogenous GCs. Endogenous GCs are normally higher in concentration than mineralocorticoids. The mechanism of how the body is protected against an overactivation of the MR by GC is through the enzyme 11β-HSD type 2 that converts cortisol to the inactive form cortisone. 11β-HSD2 is primarily located in the colon, salivary gland, distal tubules of the kidney and several other epithelial tissues (Morgan et al., 2014; Odermatt et al., 2012) in which mineralocorticoid activity is important. 11β-HSD has another isoform 11β-HSD type 1 (11β-HSD1), which is primarily located in adipose tissue as well as liver, fibroblasts, muscle and immune cells, and transforms inactive cortisone into active cortisol (Tomlinson et al., 2004; Odermatt et al., 2012).

In adipose tissue, GCs bind to GRs as well as to MRs. MRs and GRs have an essential role in adipose tissue and metabolism, as they have a high affinity towards binding GCs and thus affecting metabolism. Through activation of the receptors, preadipocytes are fully differentiated into mature adipocytes. However, comparing studies on primary cultures the importance of receptors differs in humans and animals (Caprio et al. 2007; Lee et al., 2018). In a study on mice, GC overexpression triggered preadipocyte differentiation into mature adipocytes through increased activation of 11β-HSD1, the enzyme that converts inactive cortisone to active cortisol. This over-amplification induces obesity and associated metabolic disorders (Desarzens et al., 2016). On the other hand, through increased activation of 11β-HSD2, active cortisol is converted to its inactive form cortisone, as mentioned above.

To what extent MR or GR is more involved in adipose biology is not yet fully understood. Several studies have demonstrated controversial findings. In a study with human adipocyte cell cultures, GR expression was more dominant than MR. When cortisol was

added, preadipocyte differentiation was promoted, silencing GR blocked proadipogenic functions, which was not shown by silencing MR (Lee et al., 2018).

Another study with rodent cell cultures suggested that MR plays a critical role in 3T3-L1 cells, which are responsible for adipose differentiation (Caprio et al., 2007). This finding was supported by a different study by Marzolla and coworkers (Marzolla et al., 2012). The study claimed that transient knockdown of MR can inhibit dexamethasone-induced 3T3-L1 adipose conversion, whereas GR down-regulation does not, indicating that MR is the main contributor to corticosteroid-induced adipogenesis (Marzolla et al., 2012). Additionally, MR in contrast to GR is also expressed in brown adipose tissue, which also has metabolic and endocrine functions and is a target for mineralocorticoid actions (Hoppmann et al., 2010). To our knowledge, there have been no studies on the adipose tissue of dogs or canine adipocyte cell lines.

1.5 Effects of chronic glucocorticoid elevation

1.5.1 GCs and lipid metabolism

Adipose tissue plays an important regulatory role in normal substrate metabolism by storing and liberating energy compounds when the body requires them. GCs are one of the key regulators of energy flux within adipocytes and act in a catabolic as well as anabolic pattern according to the current situation.

In terms of lipid breakdown, which is governed by the lipase enzymes such as LPL, LIPE, PNPLA2 or PLCD4, GCs are believed to mediate many of their effects through interactions with the GC receptor. Lipases are involved in catalyzing the hydrolysis of triacylglycerol which enables the release of fatty acids and monoacylglyceride. In mammals, GCs are also known to induce expression of FoxO (Forkhead box O) transcription factors, which are genes responsible for influencing lipase activity (Guia and Herzig, 2015). Wang et al., 2012, state that FoxO production might be stimulated by GCs, which as a consequence triggers the enzymatic lipolytic pathway.
Xu et al., 2003, observed, in a study involving rats, that GC treatment increased lipolysis in mature adipocytes as a consequence of elevations in transcriptional levels and promoted secretion of lipase proteins. GCs possibly have an influence on the β-adrenergic pathway by activating cyclic adenosine monophosphate (cAMP) and protein kinase A (PKA), which allows the initiation of lipase activity (Xu et al., 2003). However, it is still unclear whether the effects occur through a genomic mechanism such as increased transcription, or through non-genomic effects that alter the enzyme activity directly. In addition, many effects also only occur after a certain period of GC exposure. The increased production of 11β-HSD1 promotes the production of cortisol in humans and dogs, and corticosterone in rodents. Through elevating levels of 11β-HSD1, GC levels rise, and visceral fat accumulation increases. Reports state that 11β-HSD1 and GR are more present in visceral fat depots in comparison with subcutaneous fat depots, and visceral adipocytes show a greater ability to bind GCs (Peckett et al., 2011). As a

consequence, these findings suggest that GCs possess a pro-adipogenic function and have a larger influence on abdominal / visceral adipose tissues in comparison to other locations (Guia and Herzig, 2015).

In terms of adipogenesis, GCs can also promote storage of FAs. Through increased corticosterone concentrations in rats, preadipocytes are stimulated to differentiate into mature adipocytes as an adipogenic effect (Campbell et al., 2009). Adipocytes are transformed into hyperplastic and hypertrophic shapes through increased synthesis and/or differentiation processes. These alterations, impacted by GC treatment, cause adipose tissue mass to grow and thus promote the development of obesity.

De novo lipogenesis and lipid storage are both known to be promoted by GCs through producing lipids from nonlipid substrates, such as glucose. Lipogenesis in the liver is well documented, however little work has been done on human and rodent adipose tissues so far (Peckett et al, 2011). Other studies describe conflicting arguments, stating that GCs cause FA synthetase to decrease as well as acetyl CoA carboxylase, which are the rate-limiting enzymes of lipogenesis in WAT in rats (Volpe et al., 1975). Further research is needed in order to determine how much impact GC treatment really has on lipogenesis in general.

Overall, GCs have a strong impact on adipose tissue, appearing to act in both pro-lipolytic as well as anti-lipolytic mechanisms, inhibiting the breakdown of adipose tissue (Peckett et al., 2011; Campbell et al., 2009). Metabolic effects differ depending on dose and duration of GC treatment. Investigations on humans and rodents carried out by Peckett and Campell report that increased hormonal expression of ATGL and HSL promote enzymatic breakdown, whereas reductions on cAMP levels suppress it. However, there is no clear hypothesis as yet, and findings are not compelling enough in terms of GCs and lipid homeostasis. For reliable data, more documented studies are required to determine the differences between various fat depots, whether the effects are genomically or non-genomically caused and a range of other factors that may have an influence on lipid metabolism. Several reports on studies in humans and rodents that have analyzed lipid metabolism changes induced by GCs also revealed insulin metabolism changes (Hochberg et al., 2015; Infante et al., 2017; Hazlehurst et al., 2013). Insulin resistance is described as the suppressed capability of insulin to regulate how nutrients are distributed into target organs (Geer et al., 2014). Insulin loses its ability to limit lipolysis and upsurges in glucose uptake. Glucocorticoids, especially cortisol, are powerful insulin antagonists and oppose insulin actions by inhibiting glucose utilization and causing redistribution of adipose tissue from peripheral to central depots. As a consequence, circulating glucose concentrations are elevated, and adipose tissue depots are expanded. Hazlehurst et al., 2013, describes that GCs have different effects on insulin sensitization and resistance in humans and rodents. To conclude, chronic glucocorticoid overexposure impairs insulin metabolism and actions resulting in hyperglycemia and dyslipidemia (Geer et al., 2014; Infante et al., 2017).

1.5.2 GCs and myopathy

Glucocorticoids are closely correlated to muscle metabolism. They are capable of suppressing protein synthesis and promoting protein catabolism, resulting in loss and atrophy of muscles. Different mechanisms participate in this process such as inhibition of amino acid transport within the muscle and inhibition of insulin stimulation and of amino acids. But also, activation of the ubiquitin-proteasome system, lysosomal system (cathepsins) and calcium-dependent system (calpains) are main causes of muscle proteolysis in rats and humans. (Hasselgren, 1999; Pereira et al., 2010). Especially myofibrillar proteins are dissociated from actin and myosin to be then broken down by the ubiquitin-proteasome system. In studies with humans, GCs also inhibit muscle development by causing suppression of insulin-like growth factor I (IGF-1). IGF1 can stimulate myogenesis and promote protein formation (Menconi et al., 2007; Pereira et al., 2010). Pereira and coworkers, 2010, observed the increase of myostatin, which downregulates protein synthesis and induces muscle atrophy. Mitochondrial dysfunction is another mechanism which is induced through reduced oxidative capacity by enlarged and aggregated mitochondria caused by long term GC treatment (Pereira et al., 2010). Menconi and coworkers, 2007, claim that FoxO transcription factors are influential in muscle atrophy as well as being monitored in various mammalian cells. The authors observed a significant transcriptional increase when muscle wasting occurred.

1.5.3 GCs and immune response

As mentioned above, GCs function in an immunosuppressive and in an anti-inflammatory manner. Several types of immune cell actions are especially affected and altered with GC therapy. In the human body, macrophages remove cellular debris and induce the elimination of microorganisms by phagocytosis (Oppong et al., 2015). Macrophages can be suppressed by GCs in their signaling pathways, resulting in dampening of the inflammatory response. Pro-inflammatory cytokines, such as interferon gamma (IFNγ), interleukin-1α and interleukin-1β (IL-1α and IL-1β) are also inhibited at genetic and protein levels. Inflammatory cytokines such as interleukin-6 (IL-6) and tumor necrosis factor alpha (TNF-α) are affected in a decreasing manner by GCs. Nearly all subtypes of T lymphocytes are sensitive to the actions of GCs, which potentially induce their cell death via an intrinsic or extrinsic pathway (Flammer et al., 2011). The pattern of how T cells are divided into distinct subtypes influenced by GCs and their induced cell death is well documented in the investigation made by Distelhorst, 2002.

There are reports that GCs also exert non-genomic actions in these cells by modulating kinase activities such as phosphorylation alterations (Oppong et al., 2015). The authors also mention that GCs increase survival time and accumulation of neutrophils, which are recruited for phagocytosis and destruction of invading organisms at inflammatory sites. The molecular details involved in the actions of anti-inflammation and

immunosuppression are still not yet completely understood since GCs exert diverse effects in different cells as described above.

1.5.4 GCs and vascular development

Glucocorticoids have essential effects on vascular development, and their mechanisms have been studied for many years in humans and animals (Small et al., 2005; Logie et al., 2010). Glucocorticoid receptors (GRs) mediate most of the regulation of adhesion molecules such as VCAM-1, ICAM-1, chemokine production (interleukins) as well as vasodilators (nitric oxide, NO) and vasoconstrictors (angiotensin II, endothelin-1). All these factors affect vascular growth, morphology, proliferation and maintenance of vascular tone. In addition, especially blood pressure regulation is directed via GRs in the vasculature (Burford et al., 2017). GCs can inhibit angiogenesis dependent on GRs by the induction of the anti-angiogenic protein thrombospondin-1. In an in vitro study on human endothelial cells by Logie et al., 2010, they focused on the unrevealed mechanism that causes suppression of angiogenesis under the influence of GC (physiological doses of cortisol and dexamethasone). GCs can directly inhibit new tube formation in human endothelial cells (Rae et al., 2009). GCs are, further, able to inhibit multiplication and the reshaping of endothelial cells, so it may be most likely the case that these alterations affect the inhibition of vascular development (Logie et al., 2010). Importantly, Logie and coworkers, 2010, found that GCs also block VEGF and PGF2 genes, which in turn cause suppression of new tube-like structure (TLS) formation. However, this inhibition of TLS was without measurable reduction in endothelial cell migration or proliferation.

1.5.5 GCs and collagen metabolism

Collagen and its crosslinks are the main parts of tendons and collagenous tissue in general and affect their mechanical and biological properties. Collagenous tissue is formed by covalent bonds between molecules as a result of enzymatic oxidative deamination of lysine and hydroxylysine by lysyl oxidase (Taguchi et al., 2016). These enzymatic crosslinks influence the strength of collagen fibers directly. Taguchi and coworkers, 2016, found that GC-treated rats produce abnormal intermolecular crosslinking of bone collagen which leads to decreased bone strength. GC treatment causes tensile strength to be low, impairs enzymatic crosslink formation and keeps collagen fibers in an immature state with a small diameter. Furthermore, synthetic GC treatment increases collagenolytic and proteolytic activities in fibroblast cultures in animal as well as in human tissues (Cutroneo et al., 1981). With both hydroxyproline and procollagen this results in being synthesized less. All these factors result in decreased collagen content and strength due to GC therapy.

1.6 Canine model of chronic GC exposure

As mentioned, GCs are widely used in human and veterinary medicine. Beside their beneficial effects, side effects, especially after long-term treatment, are inevitable. Side effects of GCs on different aspects of metabolism have been investigated in cell culture experiments. However, there are very few in vivo studies in humans and, to our knowledge, no studies in dogs evaluating the effect of chronic GC exposure on adipose tissue have been published so far. Moreover, there seem to be differences between subcutaneous adipose tissue und visceral adipose tissue. In humans it is difficult to obtain visceral adipose tissue after chronic GC treatment or in patients with naturally occurring hyperadrenocorticism. Also, it is not possible to take adipose tissue samples before starting therapy. As dogs are more similar in cortisol metabolism to humans and have a naturally occurring form of HAC, it is clear that the dog can function as a good experimental model with several advantages over a rodent model.

1.7 Aims of the study

Based on the information given above, two objectives were addressed in the present study:

Firstly, to characterize the gene expression in visceral adipose tissues of healthy beagle dogs using an RNA sequencing method.

Secondly, to evaluate the effect of chronic hypercortisolemia (induced by continuous ACTH stimulation) on gene expression changes of the adipose tissue of healthy beagle dogs.

Chapter Two

Materials and Methods

2.1 Animals/adipose tissue

Five Beagle dogs (3 males, 2 females) with a median age of 71.5 months (range 23-88mos) and a median body weight of 15.85kg (range 14-19.8kg) were included. They were considered healthy on the basis of a physical examination, and normal results of a complete blood count and biochemical analysis of serum and urine. The dogs were housed in small groups of 2-4 in standard dog kennels at the university facilities, fed dry adult maintenance dog food (Josera, Adult Sensitive, Kleinheubach, Germany), and given access to water ad libitum.

All dogs were infused with minipumps that were implanted into the subcutaneous area of the dorsolateral neck for 25 weeks with synthetic tetracosactide (Bachem AG, Bubendorf, Switzerland, catalogue number: 4042686). The minipumps (model: 2ML4, Alzet, Durect Corporation, Cupertino, CA, USA) were replaced every 4 weeks by new ones with increasing doses of tetracosactide, as described in more detail in Spoerel S. 2017 and Sieber-Ruckstuhl et al., 2019. Hypercortisolemia (iatrogenic HAC) was confirmed by a positive ACTH stimulation test and a positive low-dose dexamethasone suppression test after 25 weeks of tetracosactide treatment; data shown in Sieber-Ruckstuhl et al., 2019.

Visceral adipose tissue was removed under general anesthesia from the abdominal area of each dog during celiotomy, immediately snap frozen in liquid nitrogen and stored at -80°C for further RNA preparation (Spoerel, 2017). The first surgical procedure was performed prior to treatment (Pre-ACTH samples) and the second after 25 weeks of tetracosactide treatment (Post-ACTH samples).

2.2 RNA Extraction

Total RNA was separated from the adipose tissue using the RNeasy lipid tissue mini kit (Qiagen GmbH, Hilden, Germany). The adipose tissue was extracted according to the manufacturer´s instruction. Each sample of 30mg fat from the peritoneal area was transferred into each 2ml Eppendorf tube and incubated with 1ml Qiazol lysis reagent. The phenol/guanidine-based reagent contributes to higher yields of total RNA and improves the efficiency of further purification steps. In the next step the adipose tissues were disrupted and homogenized with 5mm stainless steel beads, using the Tissue Lyser II (Qiagen GmbH, Hilden, Germany) for a total of 2 times, with 2 minutes per time, at a frequency of 20-30 Hz. The homogenate was then incubated at room temperature

for 5 minutes, 200µl chloroform added, shaken for 15 seconds and again incubated again (5 min., room temp.). Each sample was then centrifuged for 15 minutes at 12.000 RCF (g), at 4 degrees Celsius. The upper hydrous phase was then placed into a new tube and 1 volume of 70% ethanol was added and vortexed. 700µl of the probe was relocated to the RNeasy mini spin column in 2ml collecting tubes and centrifuged for 15 seconds at 8000 RCF (g). The flow-through was discarded every time. 700µl buffer RW1 was added, centrifuged and the flow-through discarded. 500µl buffer RPE was added with the same procedure. The RNeasy tube content was transferred into a new tube and centrifuged for another “dry” round. RNeasy columns were then moved into new 1.5 ml Eppendorf tubes, 30µl RNase-free water added, and centrifuged for 1 minute, 8000 RCF (g). This time the flow-through contained the valuable RNA in each sample.

The RNA purity and quantity were measured with a Nano Drop 2000C (R) spectrophotometer (Thermo Fischer Scientific AG, Reinach, Switzerland) (Zatta et al., 2017). The measurements ranged from 732ng/30µl up to 1722ng/30µl (median 1512ng/30µl). RNA integrity was assessed with the Agilent 2200 TapeStation system (Agilent, Waldbronn, Germany) (Zatta et al., 2017) The RNA integrity number (RIN) measured a value between 7.6 and 7.8.

2.3 RNA sequencing and data evaluation

Samples were further analyzed via next generation sequencing (NGS). The RNA-seq library chosen in our experiment prior to sequencing was created by diminishing total RNA of the many ribosomal RNAs available.

2.4 Library preparation

The quality and quantity of isolated RNA was determined using a Qubit ® (1.0) Fluorometer (Life Technologies, California, USA) and a Bioanalyzer 2100 (Agilent, Waldbronn, Germany) as described (Zatta et al. 2017). The TruSeq Stranded mRNA Sample Prep Kit (Illumina, Inc., California, USA) was used in the following steps (Zatta et al., 2017). Briefly, total RNA samples (100 ng-1000 ng) were ribosome depleted and in the following step converted via reverse-transcription into double-stranded cDNA with actinomycin (Zatta et al., 2017) The newly formed cDNA then underwent fragmentation, fixation, and polyadenylation before connection to TruSeq adapters. After ligation, the fragments were amplified via PCR. The samples were quality controlled using Qubit ® (1.0) Fluorometer and the Bioanalyzer 2100 (Agilent, Waldbronn, Germany). The general fragment size contained10 bp. The collected samples were standardized to 10nM in Tris-HCl 10 mM, ph 8.5 with 0.1% Tween 20.

2.5 Cluster generation and sequencing

The TruSeq SR Cluster Kit v3-cBot-HS or TruSeq PE Cluster Kit v3-cBot-HS (Illumina, Inc., California, USA) was used for cluster generation, using 8 pM of pooled normalized libraries on the cBOT.“ (Rehrauer et al., 2018). The Illumina NovaSeq 6000 single end 150 bp continued with sequencing in combination with the TruSeq SBS Kit (Illumina, Inc., California, USA).

2.6 RNA-seq analysis

Raw read data were screened with Fastqc and FastqScreen to certify that libraries were of high quality and free of unwanted material. Reads were aligned with the STAR-aligner using the Ensembl dog genome build CanFam3.1, with the gene annotations downloaded on 2017-06-07 from Ensembl. The STAR alignment options were "--outFilterType BySJout --outFilterMatchNmin 30 --outFilterMismatchNmax 10 --outFilterMismatchNoverLmax 0.05 --alignSJDBoverhangMin 1 --alignSJoverhangMin 8 --alignIntronMax 100000 --alignMatesGapMax 100000 --outFilterMultimapNmax 50". (Zatta et al., 2017). Expression counts were generated using the function featureCounts of the R package Rsubread. The options for featureCounts were a minimum mapping quality of 10, minimum feature overlap of 10 base pairs, counts of multi mapping reads, counts of only primary alignments, and counts of reads also if they overlap with multiple genes. Genes were considered as expressed in a sample if they had at least 10 reads assigned.

2.7 Statistical analysis

Differential expression was assessed using the Bioconductor package DESeq2. We considered a gene as significantly differentially expressed if the p-value was ≤ 0.01, log2 ratio >1 or <-1, and false discovery rate (FDR) < 0.05.

Chapter Three

Results

3.1 Transcriptomic analysis of dogs before and after ACTH treatment

In the samples after ACTH treatment we identified 1442 genes with significant transcriptomic alterations; of these, 507 genes were upregulated and 935 downregulated.

We detected and analyzed various metabolic alterations in genes participating in lipid, glucose and protein metabolism

Some genes involved in immune function regulations, angiogenesis, collagen fibril organization and insulin resistance were also altered. We concentrated on general gene transcriptomic changes, with a special focus on individual significant gene alterations. These will be described in more detail in the subsequent chapters.

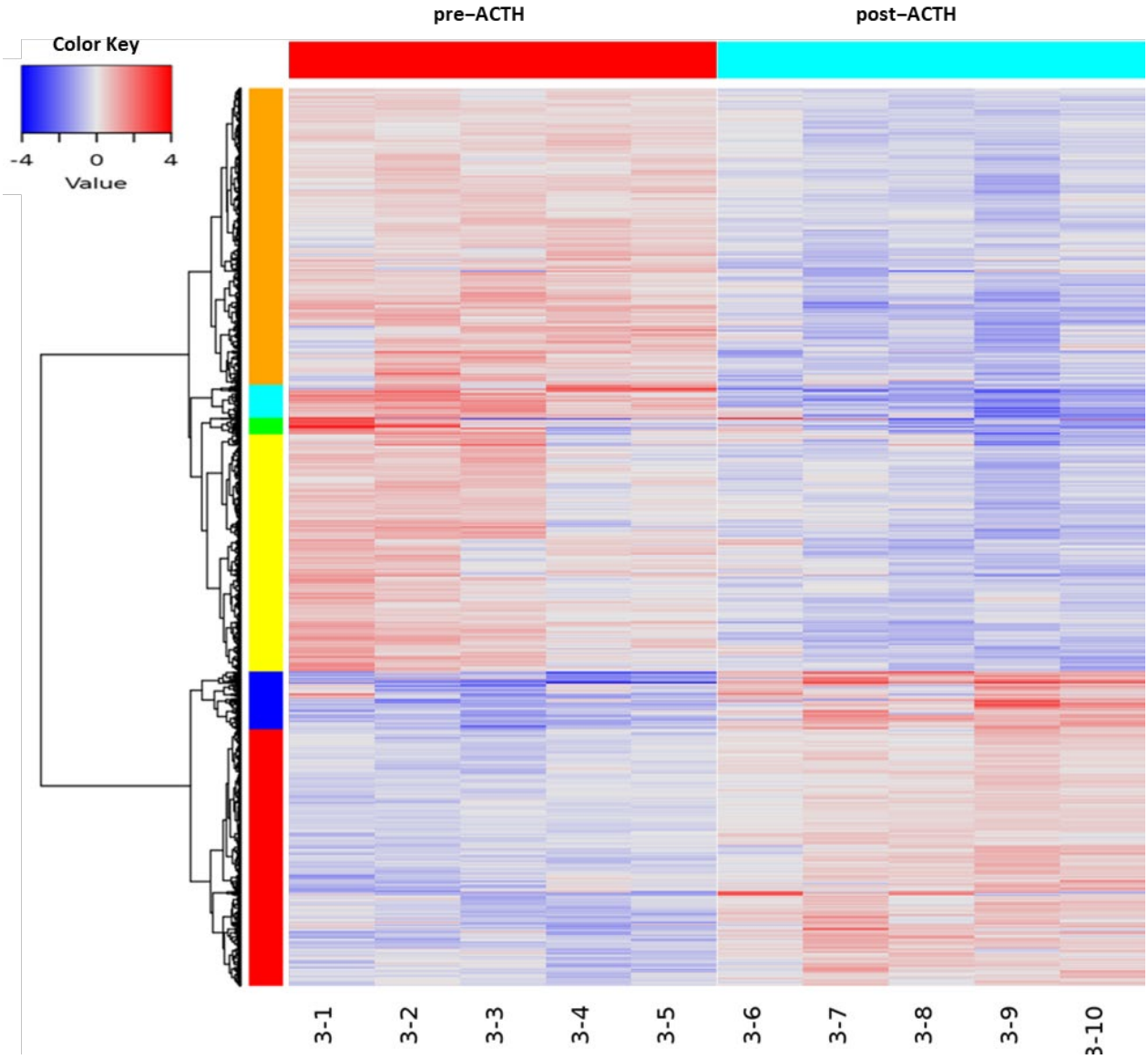

Figure 1: Heatmap presenting genetic transcript changes of visceral adipose tissue from 5 dogs before (pre ACTH) and after ACTH (post ACTH) treatment (3.1-3.5: pre ACTH; 3.6-3.10: post ACTH, x-axis). Clusters of cellular/biological/molecular gene functions (y-axis). blue: downregulated genes, red: upregulated genes.

	#significants	FDR	fc >= 1	fc >= 1.5	fc >= 2	fc >= 3	fc >= 4	fc >= 8	fc >= 10
p < 0.1	4045	0.3107000	4045	1683	802	321	172	55	40
p < 0.05	3181	0.1975000	3181	1524	757	319	171	54	40
p < 0.01	2002	0.0627100	2002	1238	625	294	166	53	39
p < 0.001	1199	0.0104400	1199	917	493	238	145	52	38
p < 1e-04	780	0.0016060	780	666	387	186	121	44	33
p < 1e-05	553	0.0002235	553	505	322	160	104	40	29

Figure 2: Total number of significant gene expressions according to p-value, fold change (fc) and false discovery rate (FDR) pre to post ACTH treatment. (p-value: significance level/ probability value; FDR: number of false positives; fc: quantity change between baseline and following measurements)

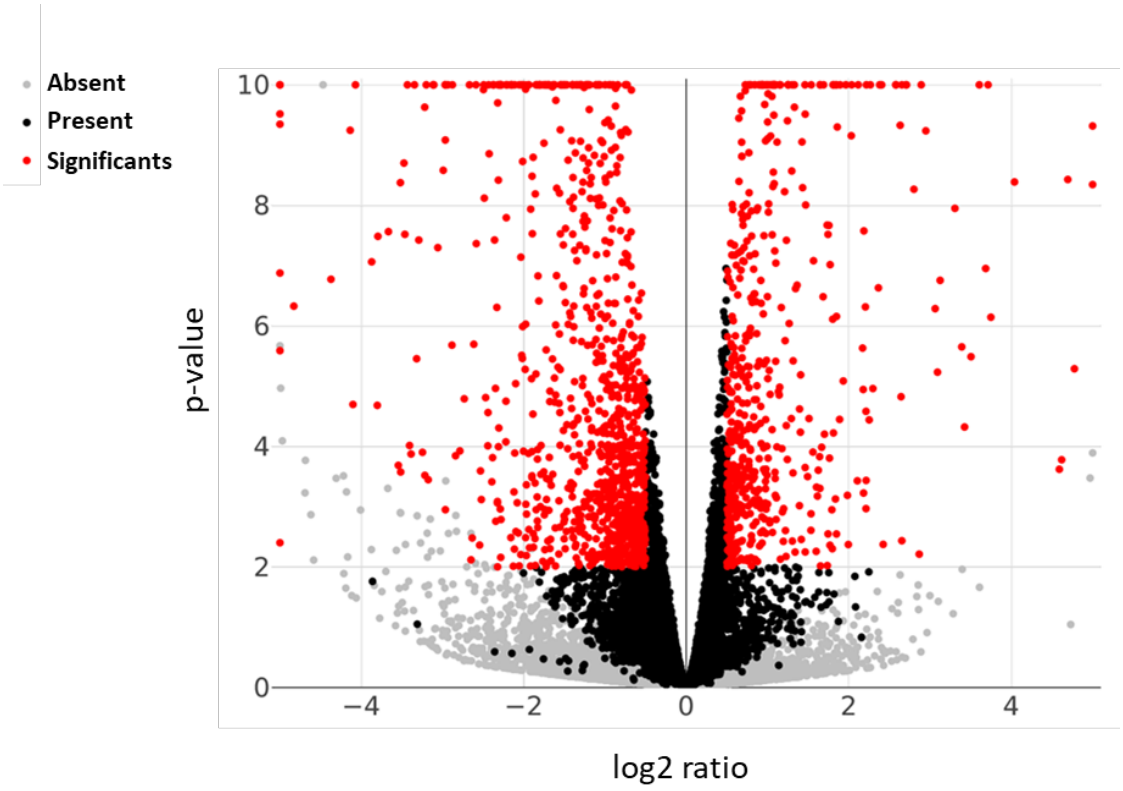

Figure 3: Volcano plot depicting the total number of genes according to p-value (-log10) and log2 ratio pre to post ACTH treatment. Genes with a p-value ≤0.01 (y-axis, -log10) and log2 ratio of >1 or <-1 (x-axis) were identified as significant. red: statistically significant genes, black: genes with no significant value, grey: genes that were absent post ACTH treatment.

3.3 Gene expression alterations

3.3.1 Genes involved in lipid metabolism

In this category, 34 out of 118 genes were significantly changed, with 23 out of the 34 being downregulated. We observed a mild but significant decrease of the glucocorticoid receptor (NR3C1) and the mineralocorticoid receptor (NR3C2) after ACTH treatment. Also, the gene coding for the hydroxysteroid dehydrogenase 11 β-HSD 1 (11 β-HSD1), an enzyme which controls the conversion of cortisone into active cortisol was significantly upregulated (Fig.4). Resistin (RETN), leptin (LEP) and adiponectin (ADIPOQ), hormones produced by adipocytes, were all downregulated, although not to a statistically significant level. ACSL4, which functions in fatty acid synthesis, was significantly upregulated. Stearoyl-CoA desaturase 5 (SCD5), which is involved in fatty acid desaturation and a necessary gene for de novo fatty acid synthesis, was also significantly downregulated (Fig.5). Genes involved in triglyceride synthesis, such as DGAT1 and AGPAT3 were significantly upregulated after long-term ACTH treatment. Additionally, we observed the following genes responsible for lipolysis, which were all upregulated on a significant level. Lipoprotein lipase (LPL), which liberates fatty acids from triglycerides, as well as hormone sensitive lipase (LIPE) and triglyceride lipase (PNPLA2) were all elevated at transcriptional level. Phospholipase C delta 4 (PLCD4), which is in charge of the lipid catabolic processes was highly significantly upregulated (Fig.6).

Upregulated Genes

Gene name	**Description**	**p-value**
PLCD4	Phospholipase C Delta 4	3.688E-27
DGAT1	diacylglycerol O-acyltransferase 1	4.679E-14
ACSL4	acyl-CoA synthetase long-chain family member 4	0.000002287
LIPE	lipase E, hormone sensitive type	0.000005841
AGPAT3	1-acylglycerol-3-phosphate O-acyltransferase 3	0.0002671
HSD11B1	hydroxysteroid 11-beta dehydrogenase 1	0.0009693
PNPLA2	patatin like phospholipase domain containing 2	0.002119

LPL	lipoprotein lipase	0.006239

Downregulated Genes

Gene name	**Description**	**p-value**
SCD5	Stearoyl-CoA desaturase 5	5.993E-07
NR3C1	nuclear receptor subfamily 3 group C member 1: glucocorticoid receptor	0.00002292
NR3C2	nuclear receptor subfamily 3 group C member 2: mineralocorticoid receptor	0.0001037
ELOVL5	ELOVL fatty acid elongase 5	0.008749
RETN	resistin	0.4831
ADIPOQ	adiponectin, C1Q and collagen domain containing	0.6022
LEP	leptin	0.8203

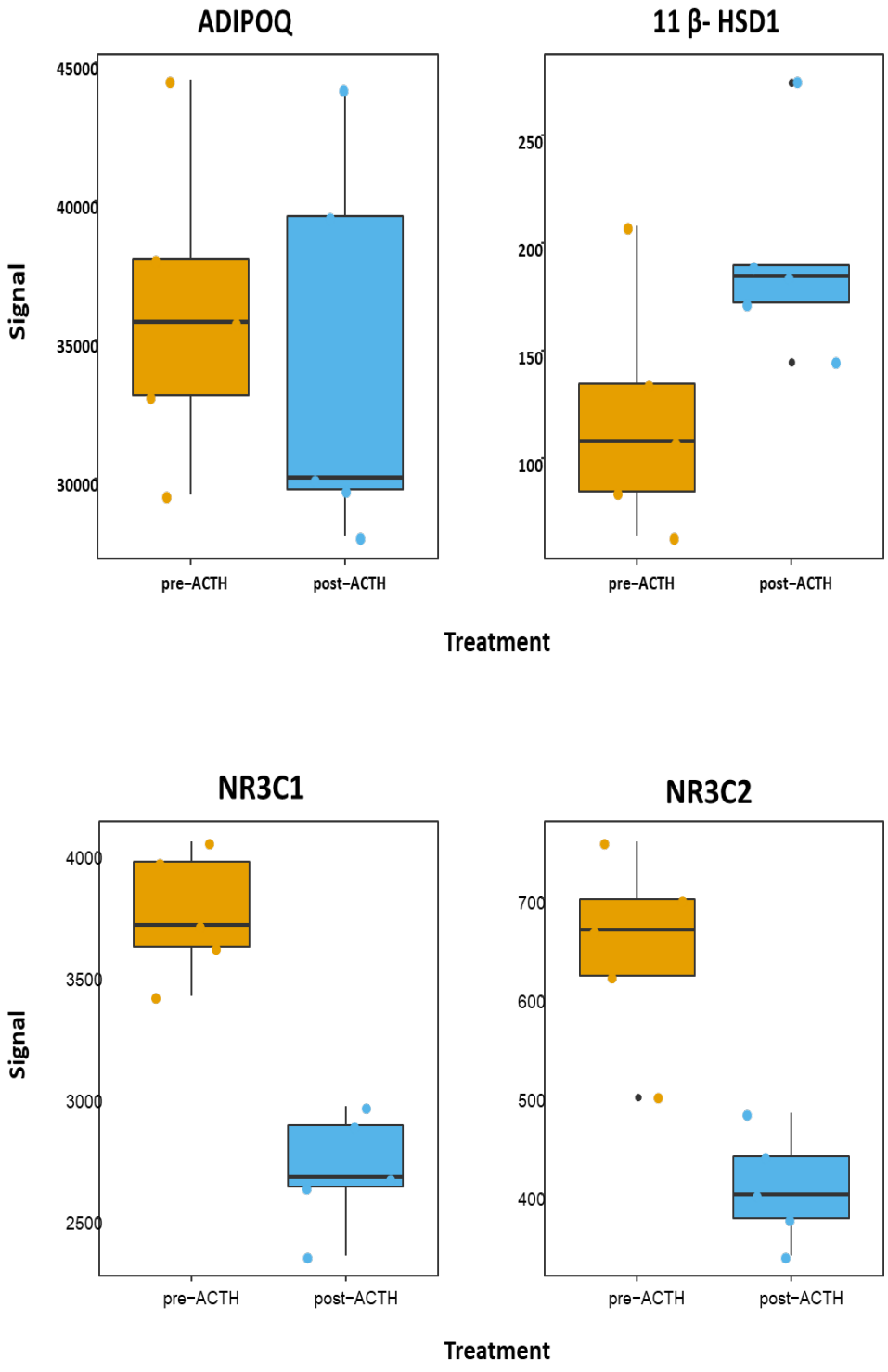

Figure 4: Boxplots depicting genes involved in lipid metabolism before and after ACTH treatment. Genetic signal strength/ activity (y-axis) pre and post ACTH treatment (x-axis).
ADIPOQ: adiponectin; 11 β-HSD 1: 11 β-hydroxysteroid dehydrogenase; NR3C1: glucocorticoid receptor; NR3C2: mineralocorticoid receptor.

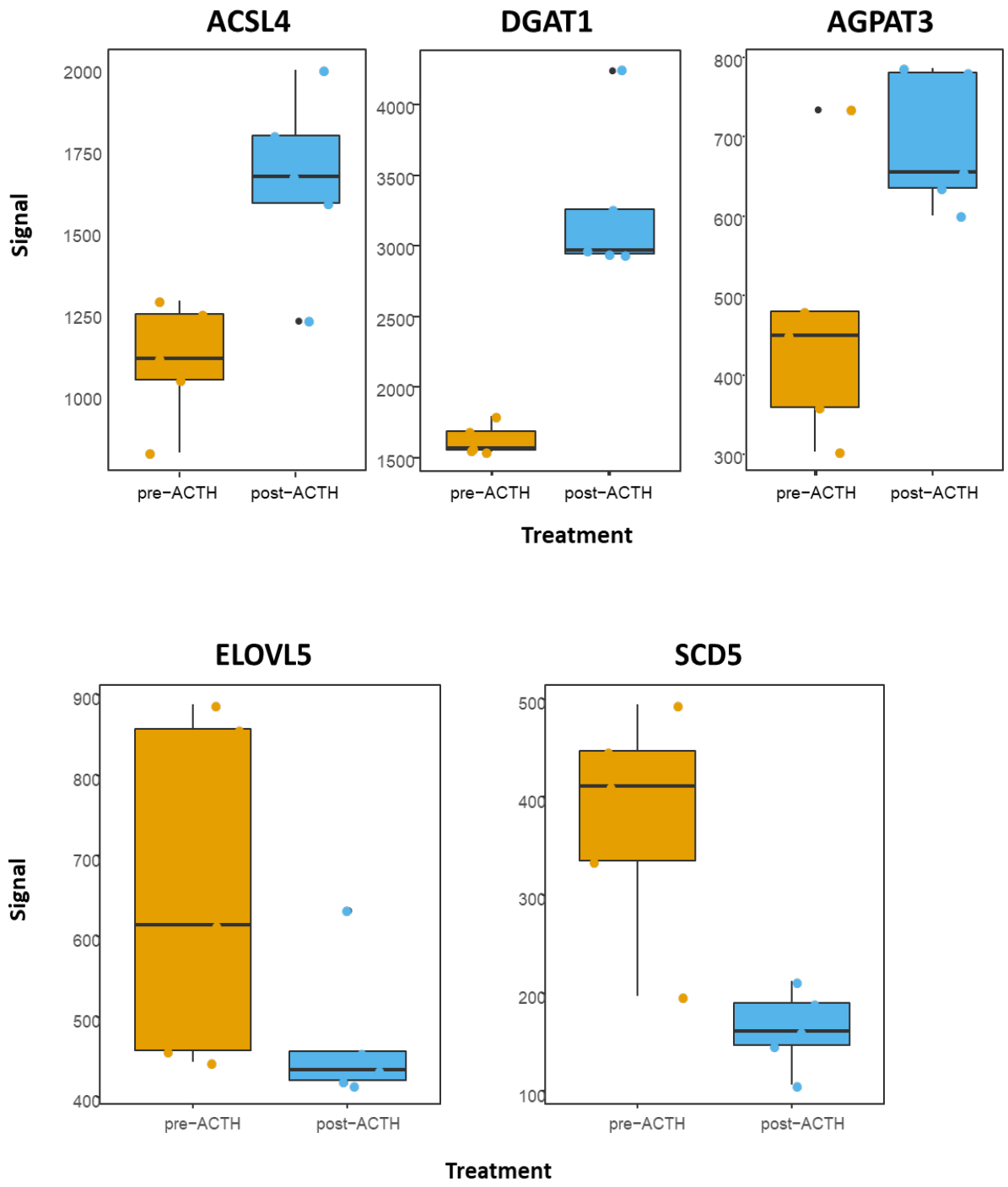

Figure 5: Boxplots depicting genes responsible for fatty acid and triglyceride composition pre and post ACTH treatment.
ACSL4: acyl-CoA synthetase long-chain family member 4; DGAT1: diacylglycerol O-acyltransferase 1; AGPAT3: 1-acylglycerol-3-phosphate O-acyltransferase 3; ELOVL5: fatty acid elongase 5; SCD5: Stearoyl-CoA desaturase 5.

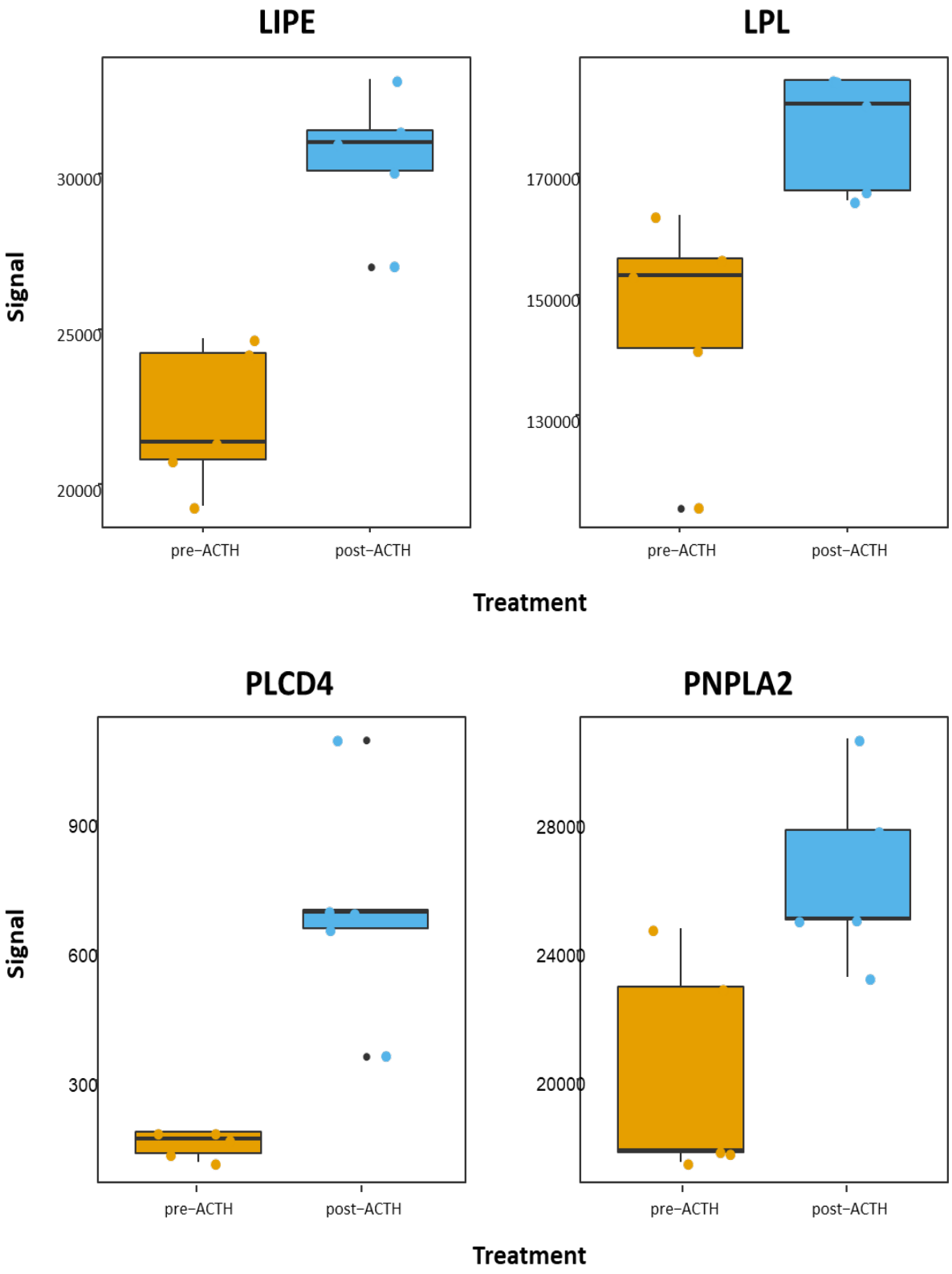

Figure 6: Boxplots depicting genes involved in lipid catabolic process pre and post ACTH treatment. LIPE: lipase E, hormone sensitive type; LPL: lipoprotein lipase; PLCD4: Phospholipase C Delta 4; PNPLA2: patatin like phospholipase domain containing 2.

3.3.2 Genes involved in protein metabolism

In this category, 71 out of 189 translational genes were significantly altered, with 70 out of 71 being upregulated by a gene ratio of 0.400 (Fig.9). These gene subtypes function in protein anabolism and biosynthesis (Zhou et al., 2015) (Fig 7.1, 7.2).

In terms of the genes responsible for protein metabolism, the results show that protein homeostasis was strongly affected after ACTH treatment. Multiple genes that encode for translational processes, such as ribosomal protein S (RPS) as well as ribosomal protein L (RPL), were all elevated. The mRNA concentration of creatine kinase M-type (CKM) was significantly elevated with a log2 ratio of 3.605 and FDR of 1.25E-47, corresponding to a 3-fold upregulation. CKM is responsible for loss of filament in muscle, muscle necrosis and increase of protein catabolism (Fernandez-Sola et al., 1993). The calcium-dependent cysteine protease (CAPN11) catalyzes hydrolysis of peptides and was downregulated in our results. Elafin, also known as peptidase inhibitor 3 (PI3), on the other hand, reduces the activity of any peptidase and prevents hydrolysis. In our results PI3 was significantly upregulated with a log2 ratio of 3.713 and FDR of 5.88E-31, corresponding to an 8-fold upregulation. The results display inconsistent and non-uniform transcriptomic results of both significant concentrations of anabolic and catabolic functioning genes (Fig.8).

Focusing on glucocorticoid-induced myopathy and muscle weakness, protein coding genes IGF-1, EIF4E-BP1, RPS6KA1, calpain11, and CKM have direct effects on atrophy of the muscle (Pereira et al., 2010). Protein catabolism is supported by inhibition of insulin-like growth factor (IGF-1), EIF4EBP1 and ribosomal protein S6-kinase 1 (RPS6KA1). Our results accordingly display a downregulation in IGF-1 and RPS6KA1; however, EIF4EBP1 was slightly elevated (Fig. 10).

The catabolic effects of GCs are triggered by the activation of cellular proteolytic systems such as ubiquitin-proteasome system, lysosomal system (cathepsins) and calcium-dependent system (calpains) (Hasselgren, 1999). Calpain 11 was significantly downregulated with a log2 ratio of -2.668, and FDR of 1.93E-18 (Fig.11). Forkhead box O1 (FoxO1), a substantial atrogene, is important for muscle wasting and potentially regulated by GCs in humans and rodents (Menconi et al., 2007; Brocca et al., 2016). In our results it was significantly upregulated (Fig.8).

Upregulated Genes

Gene name	**Description**	**p-value**
CKM	creatine kinase M-type	9.94E-52
PI3	elafin precursor	1.40E-34
RPL3	60S ribosomal protein L3	3.13E-11

RPL18	ribosomal protein L18	3.58E-10
EIF4EBP1	eukaryotic translation initiation factor 4E binding protein 1	8.91E-10
RPS7	ribosomal protein S7	4.60E-08
RPS12	ribosomal protein S12	6.67E-08
RPL10a	ribosomal protein L10a	8.21E-07
RPL28	ribosomal protein L28	1.29E-06
RPS18	40S ribosomal protein S18	2.35E-06
RPS6	ribosomal protein S6	0.0002637
FoxO1	forkhead box O1	0.0154

Downregulated Genes

Gene name	**Description**	**p-value**
CAPN11	calpain 11	1.93E-18
RPS6KA1	ribosomal protein S6 kinase A1	0.000133
IGF1	Insulin-like growth factor I	0.0002607

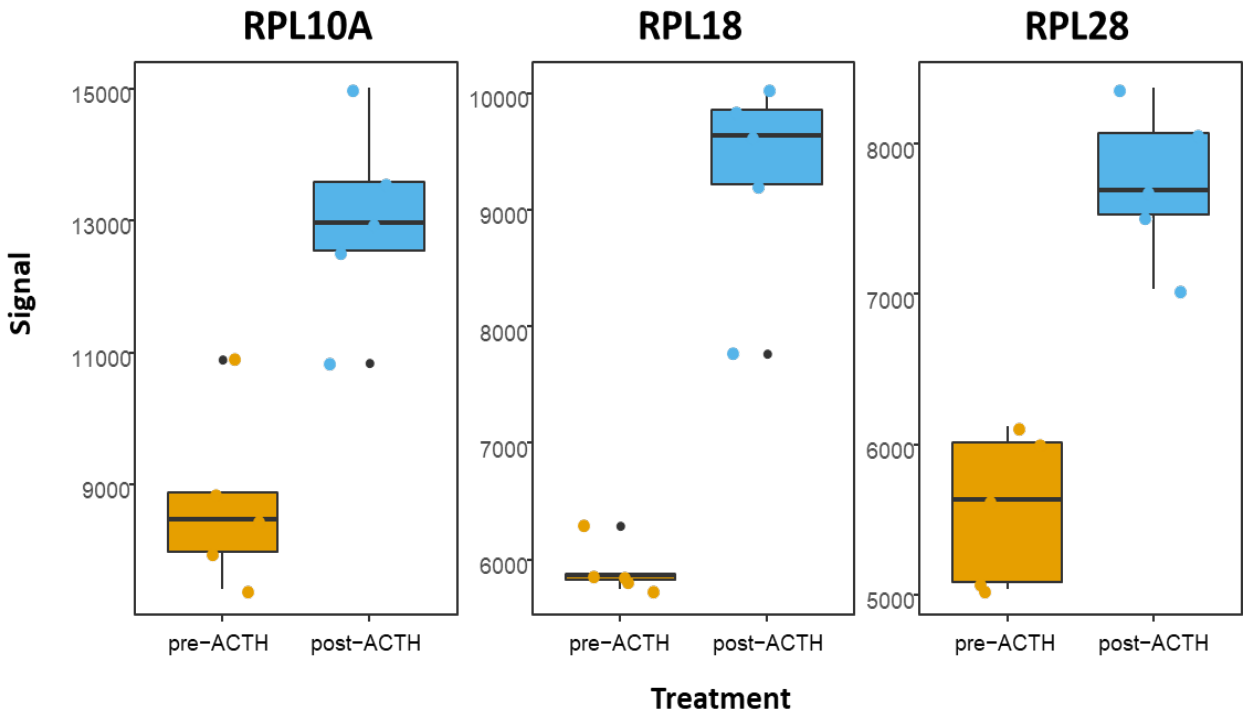
RPL10A
RPL18
RPL28
Signal
15000
13000
11000
9000
10000
9000
8000
7000
6000
8000
7000
6000
5000
pre−ACTH
post−ACTH
Treatment

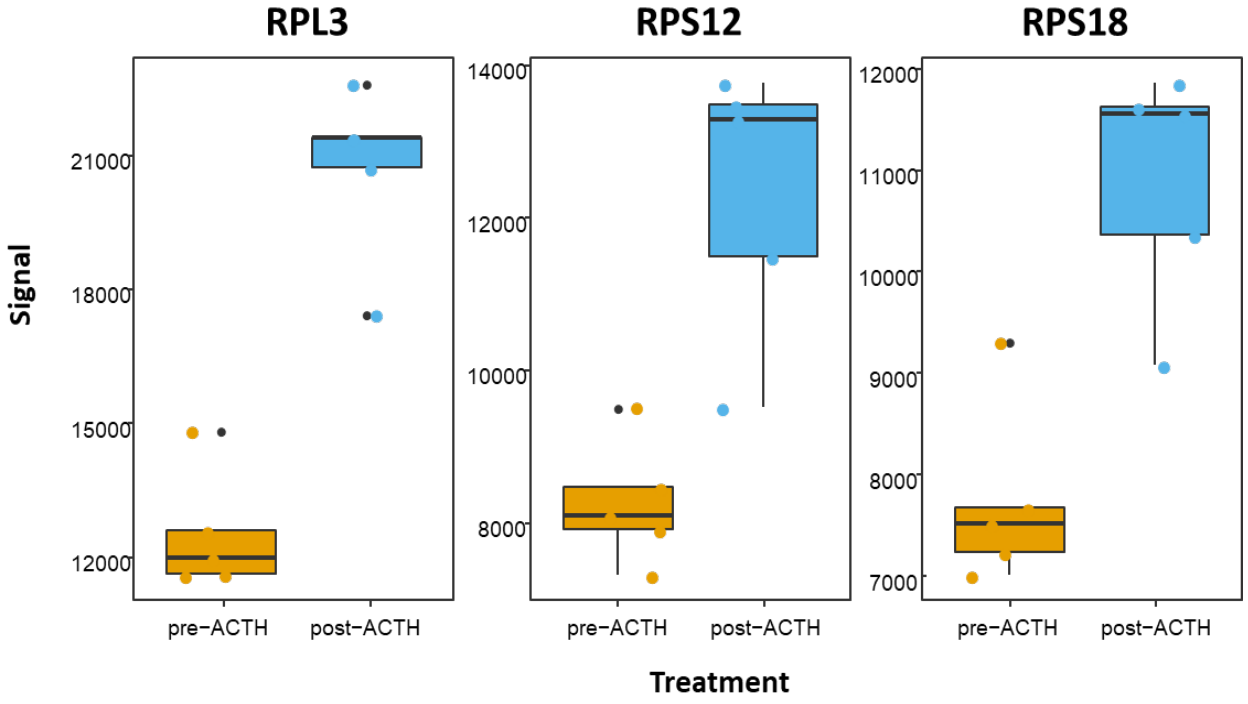
RPL3
RPS12
RPS18
Signal
21000
18000
15000
12000
14000
12000
10000
8000
12000
11000
10000
9000
8000
7000
pre−ACTH
post−ACTH
Treatment

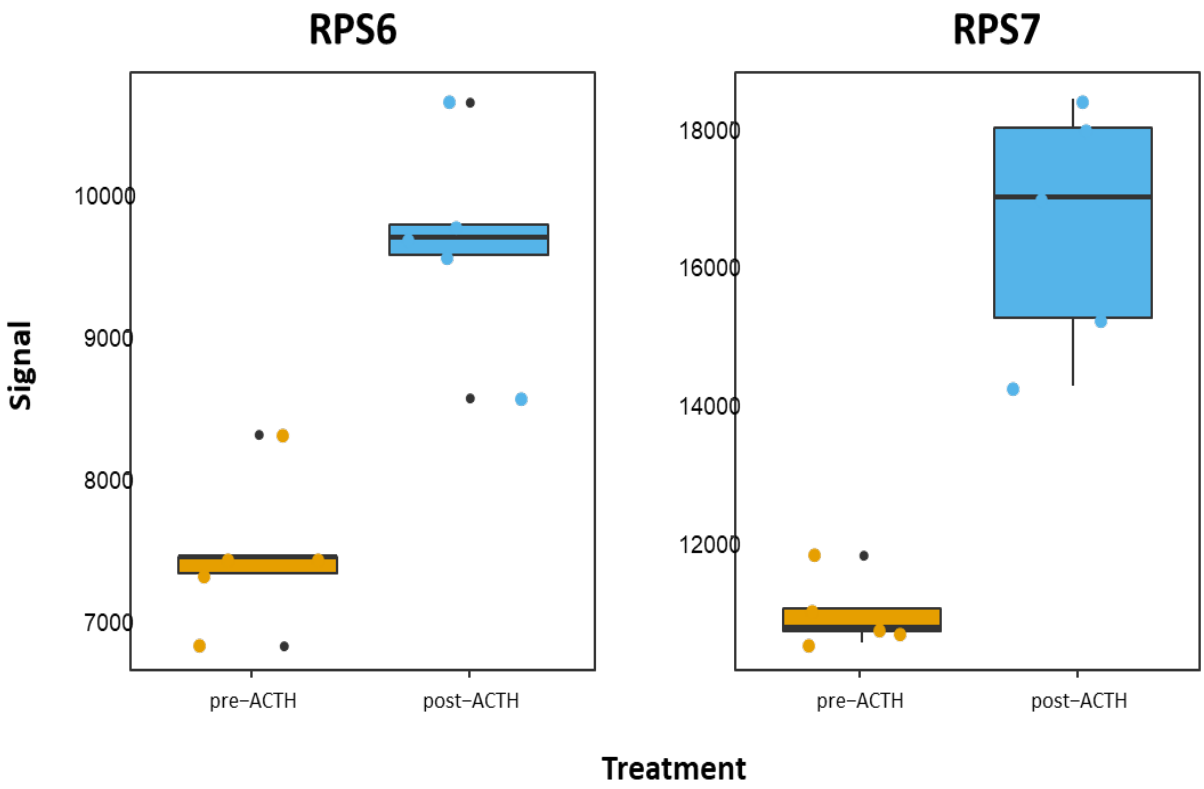

Figure 7.1: Boxplots depicting ribosomal protein genes pre and post ACTH treatment. PRL10A: ribosomal protein L10a; RPL18: ribosomal protein L18; PRL28: ribosomal protein L28; RPL3: 60S ribosomal protein L3; RPS12: ribosomal protein S12; RPS18: 40S ribosomal protein S18; RPS6: ribosomal protein S6; RPS7: ribosomal protein S7.

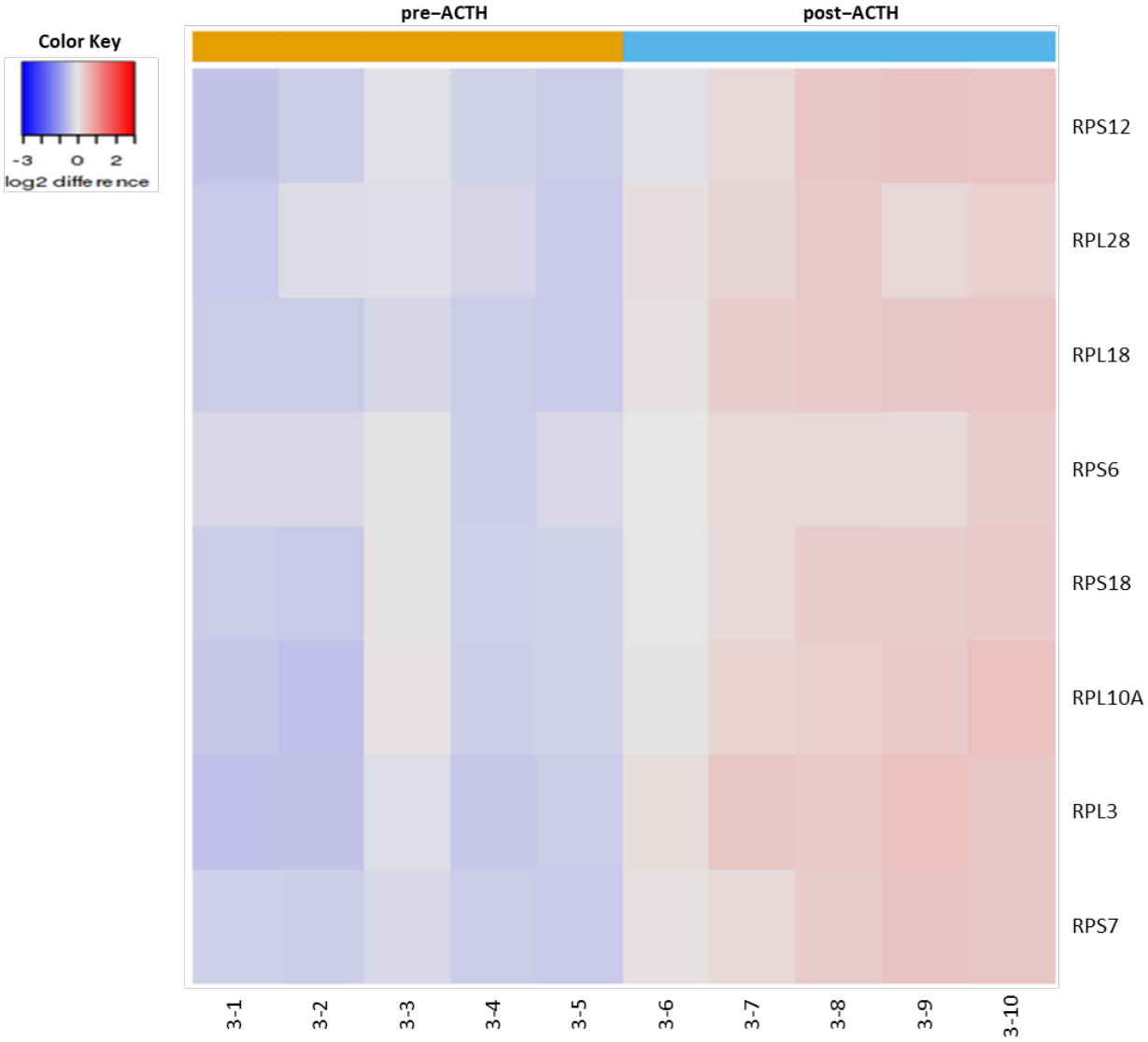

Figure 7.2: Heatmap presenting signal activity changes of ribosomal proteins from 5 dogs before (pre ACTH) and after (post ACTH) treatment. (3.1-3.5: pre ACTH; 3.6-3.10: post ACTH, x-axis). Ribosomal gene codes (y-axis). blue: downregulated genes, red: upregulated genes.
RPS12: ribosomal protein S12; RPL28: ribosomal protein L28; RPL18: ribosomal protein L18; RPS6: ribosomal protein S6; RPS18: 40S ribosomal protein S18; RPL10A: ribosomal protein L10a; RPL3: 60S ribosomal protein L3; RPS7: ribosomal protein S7.

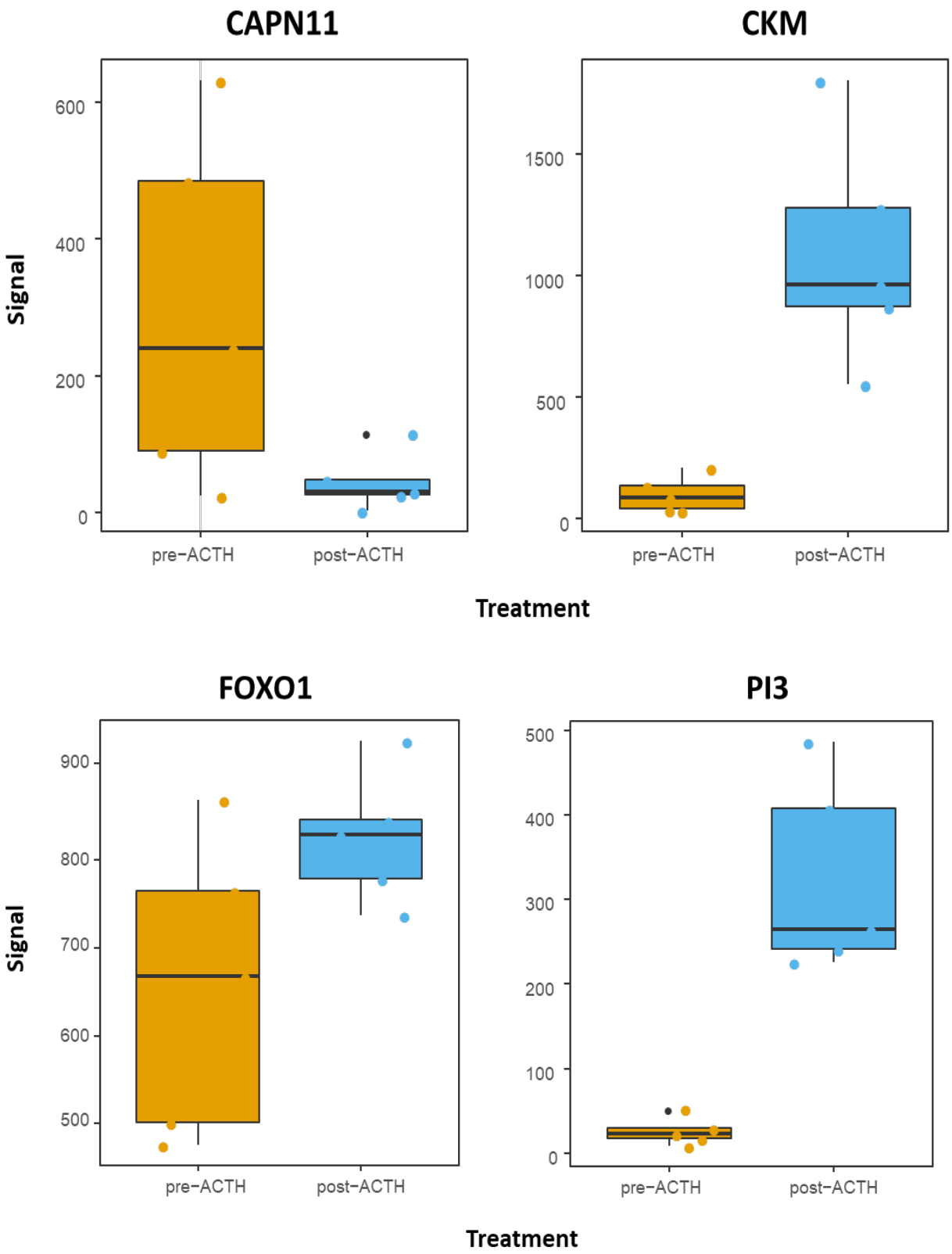

Figure 8: Boxplots depicting genes involved in protein metabolism pre and post ACTH treatment. CAPN11: calpain 11; CKM: creatine kinase M-type; FoxO1: forkhead box O1; PI3: elafin precursor.

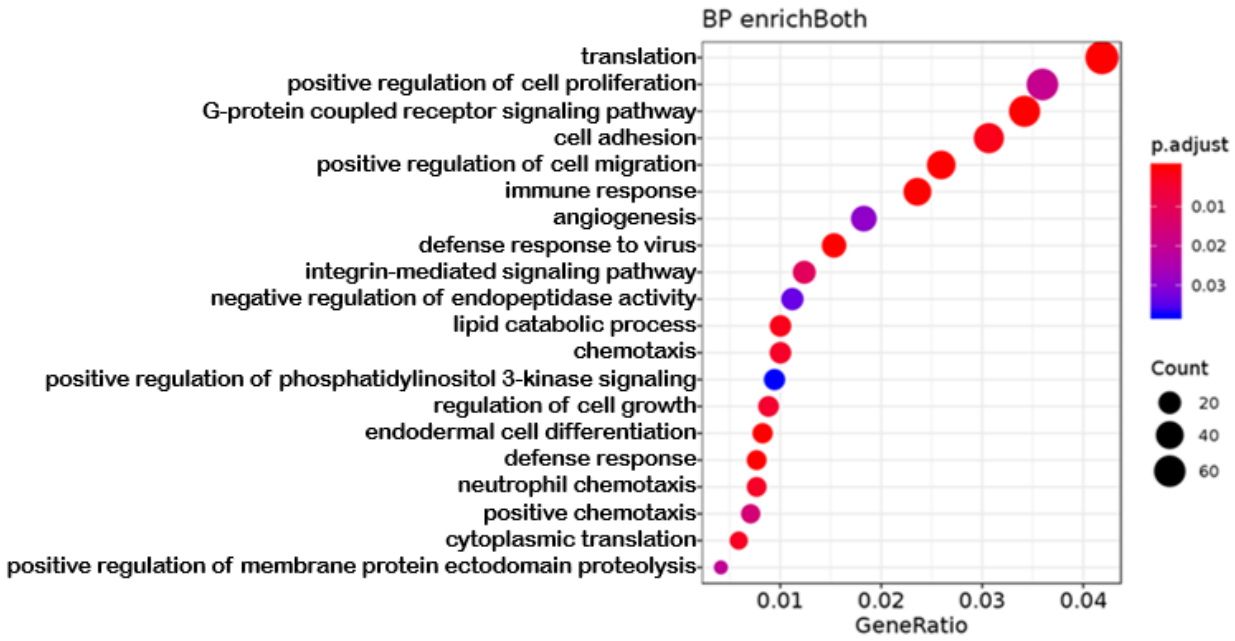

Figure 9: Biological processes of genes with the most significant signal activity (y-axis) in correlation to gene ratio (number of genes that are significantly altered in this category / number of genes in this category; x-axis) pre to post ACTH treatment. Count: circle size refers to number of genes. P adjust: with higher significance the color scheme changes from blue to red.

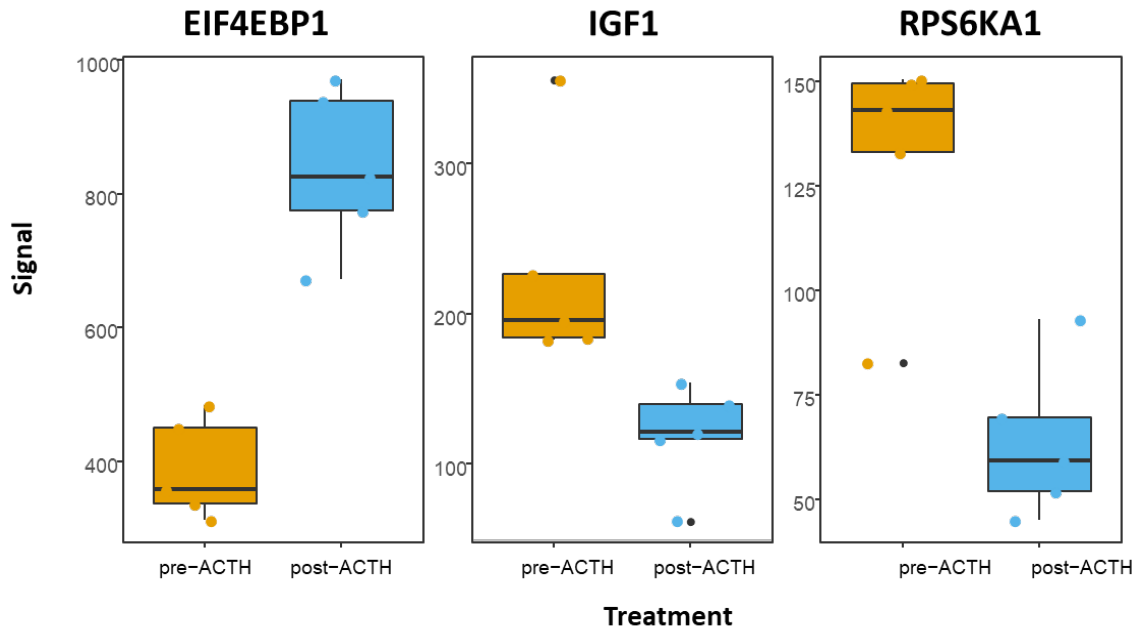

Figure 10: Boxplots depicting genes coding for protein catabolism in muscle necrosis pre and post ACTH treatment. EIF4EBP1: eukaryotic translation initiation factor 4E binding protein 1; IGF1: Insulin-like growth factor I; RPS6KA1: ribosomal protein S6 kinase A1.

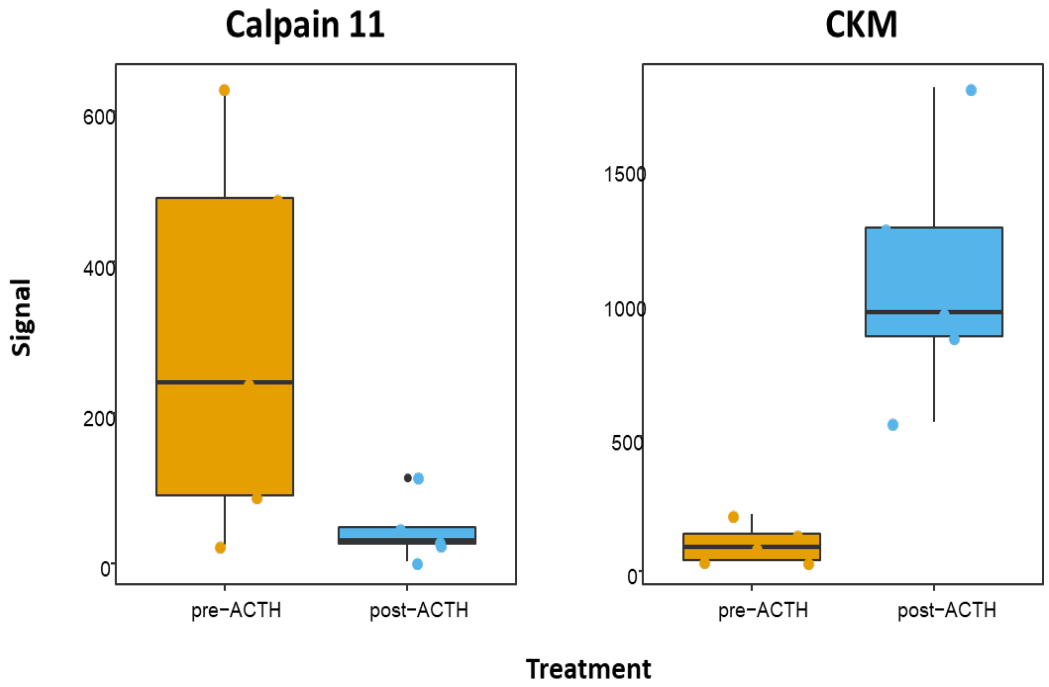

Figure 11: Boxplots depicting genes involved in cellular proteolytic activation pre and post ACTH treatment.
CAPN11: Calpain 11; CKM: creatine kinase M-type.

3.3.4 Genes involved in immune response

We identified 40 out of 107 genes in this category that were significantly altered, of which 32 genes were downregulated (Fig.12). As leukocyte infiltration is dependent on a fully functioning immune system and reacts to changes within the tissue we observed decreases in Interleukins (IL), Toll-like receptors (TLR), interferon gamma genes (IRF), and genes that form the class II major histocompatibility complex (MHC II) (Hochberg et al., 2015). Notably we measured a downregulation of MHC II genes such as HLA-DRBI, DLA-DRA, DLA-DQB1, which are in charge of presenting antigens for T-cell recruitment (Fig. 13). IL33, a member of the IL1 family, acts in inducing helper T cells, mast cells, and other lymphocytes to produce type 2 cytokines (Hochberg et al., 2015). It has important functions in the inflammatory response and was also nearly 4-fold downregulated in our samples. Another gene, TLR7, which functions in pathogen recognition and induction of the innate immune system was significantly reduced. Similar results were found with CCR2, a receptor for monocyte chemoattractant protein-1 (MCP-1), which specifically mediates monocyte chemotaxis especially in inflammatory diseases (Fig. 14) (Cain et al., 2017). Together, these data support a homogenous image of GCs suppressing the immune system in adipose tissue.

Downregulated Genes

Gene name	Description	p-value
IL33	interleukin 33	2.42E-20
DLA-DQB1	major histocompatibility complex, class II, DQ beta 1 precursor	1.20E-10
DLA-DRA	major histocompatibility complex, class II, DR alpha	9.28E-10
HLA-DRB1	DLA class II histocompatibility antigen, DR-1 beta chain precursor	2.97E-08
CCR2	C-C motif chemokine receptor 2	2.73E-08
TLR7	toll like receptor 7	3.763E-08

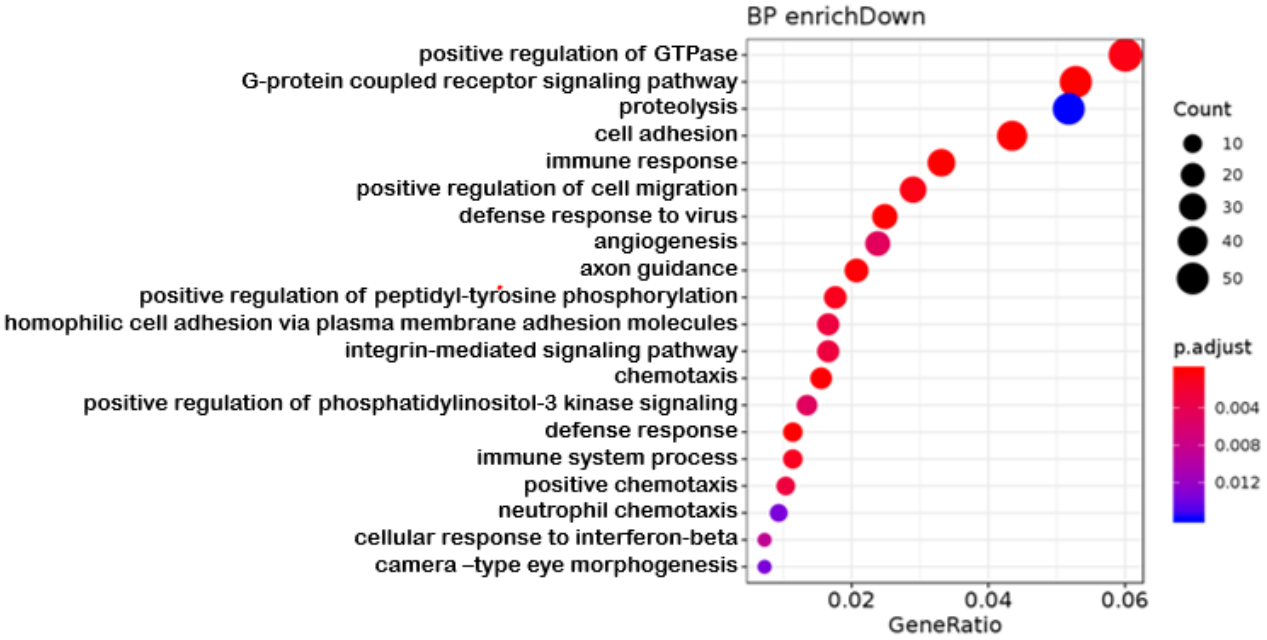

Figure 12: Biological processes of the most significantly downregulated genes (y-axis) in correlation to gene ratio (number of genes that are significantly altered in this category /number of genes in this category; x-axis) pre to post ACTH treatment.

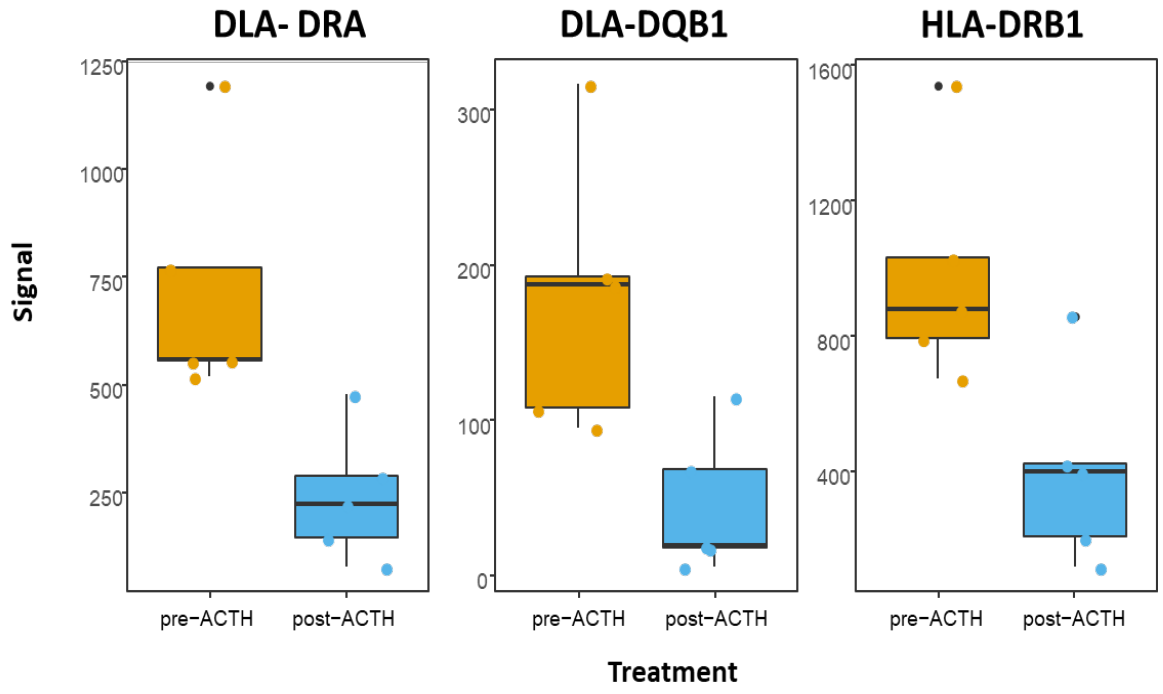

Figure 13: Boxplots depicting genes responsible for major histocompatibility complex formation pre and post ACTH treatment.
DLA-DRA: major histocompatibility complex, class II, DR alpha; DLA-DQB1: major histocompatibility complex, class II, DQ beta 1 precursor; HLA-DRB1: DLA class II histocompatibility antigen, DR-1 beta chain precursor.

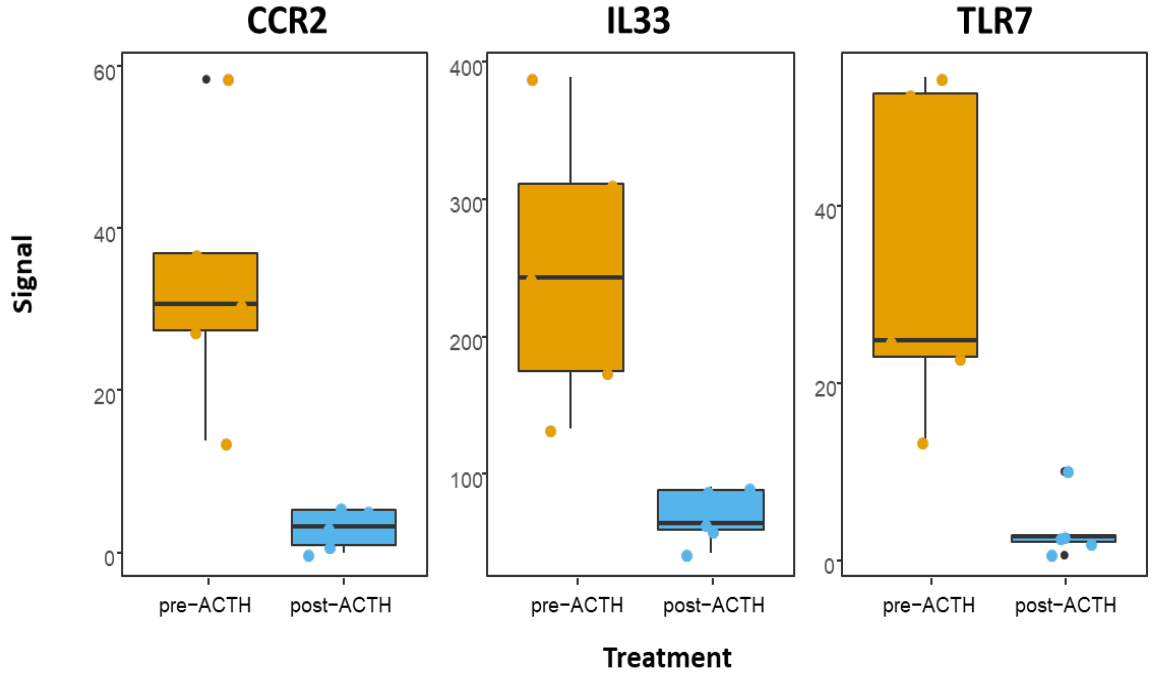

Figure 14: Boxplots depicting genes involved in regulation of the immune system pre and post ACTH treatment.
CCR2: C-C motif chemokine receptor 2; IL33: interleukin 33; TLR7: toll like receptor 7

3.3.5 Genes involved in angiogenesis

In total, 31 out of 101 genes in this category were significantly altered and 23 out of 31 were downregulated. Results display that there is an overall suppression of genes involved in angiogenesis and vascular development (Fig. 12). Specific genes such as HEY1, ENPEP, ITGAV, RNF213, and VEGFC are all examples of genes that function in new blood vessel formation and resulted in similar downregulations after long-term treatment with ACTH. ANGPT4, however, is a protein that acts as a significant factor in new blood vessel formation and was significantly upregulated in our transcriptomic analysis. With a p-value of 3.333E-34 and a log2 ratio of 2.71 it was nearly 8 times increased in its signal concentration (Fig.15).

Downregulated Genes

Gene name	**Description**	**p-value**
ENPEP	glutamyl aminopeptidase	3.65E-12
RNF213	ring finger protein 213	6.83E-08
HEY1	hes related family bHLH transcription factor with YRPW motif 1	2.86E-05
ITGAV	integrin subunit alpha V	8.78E-05
VEGFC	vascular endothelial growth factor C	0.0001135

Upregulated Genes

Gene name	**Description**	**p-value**
ANGPT4	angiopoietin 4	3.33E-34

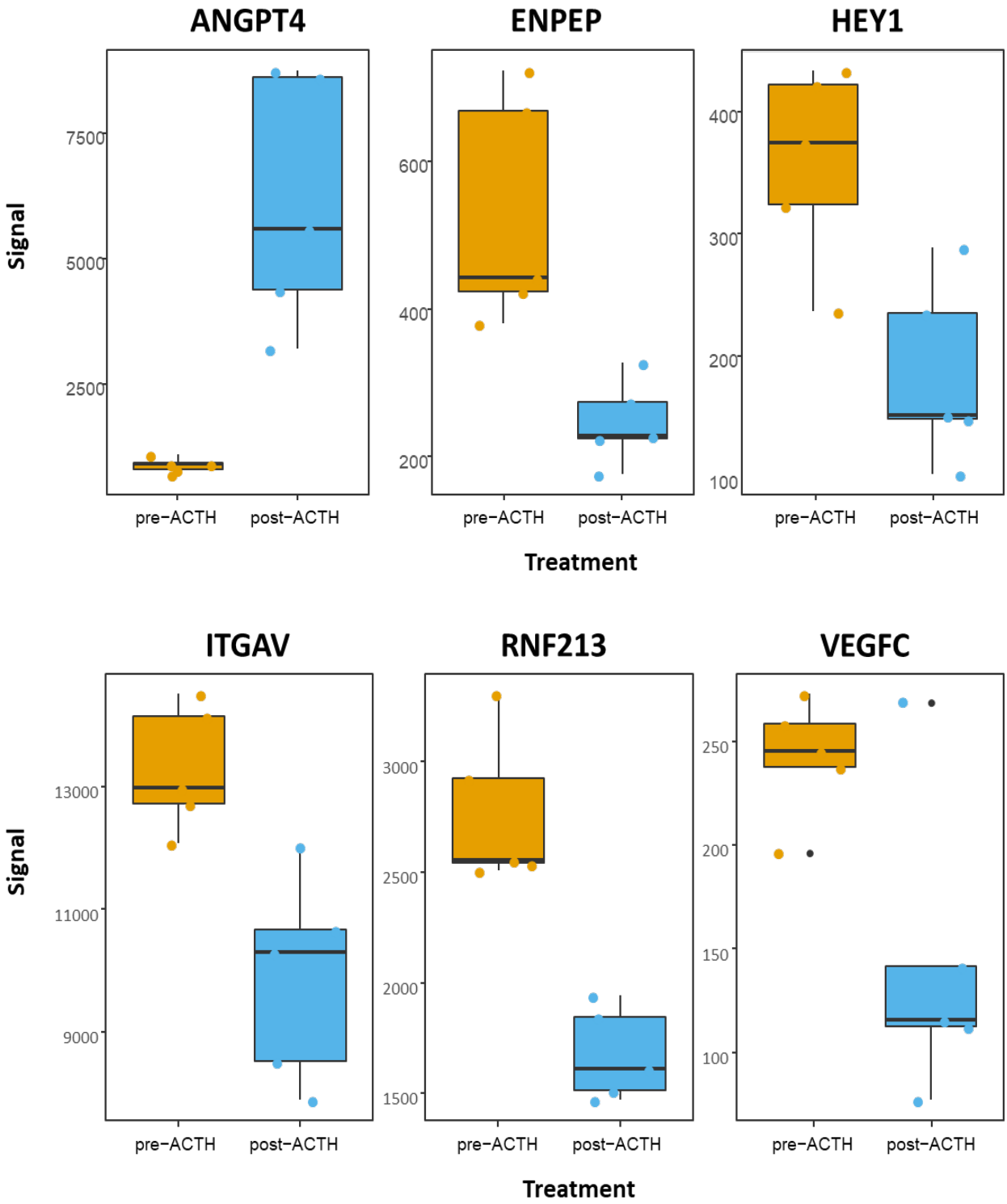

Figure 15: Boxplots depicting genes involved in angiogenesis pre and post ACTH treatment.
ANGPT4: angiopoietin 4; ENPEP: glutamyl aminopeptidase; HEY1: hes related family bHLH transcription factor with YRPW motif 1; ITGAV: integrin subunit alpha V; RNF213: ring finger protein 213; VEGFC: vascular endothelial growth factor C.

3.3.6 Genes involved in collagen metabolism

In this category, 9 out of 26 transcriptional genes displayed significant alterations. All 9 genes were downregulated, COL3A1, COL4A2/A3/A6/A5, PCOLCE, and LUM. These are procollagens, which function in fibrillogenesis regulation and tissue repair (geneontology.org; FGCZ). Results with significant concentration signals showed a uniform suppression in terms of forming new collagen fibrils (Fig. 16).

DKK1 and WIF1 are Wnt signaling inhibitory factors as well as sFRP, which function in osteoblast inhibition and induce osteoporosis in rats (Zhou et al., 2017). These 3 genes were significantly changed in our results and 2 out of 3 showed upregulations. We measured a high signal concentration in WIF1, which was nearly 8-fold downregulated (log2: -2.93; p value: 1.08E-18). DKK1 was more strongly elevated (log2: 4.61), however with less significance level (p-value: 0.00016). Another protein gene coding for Wnt inhibition, SFRP5, was also significantly upregulated (log2: 2.89; p-value: 4.16E-11) (Fig. 17).

Downregulated Genes

Gene name	**Description**	**p-value**
COL14A1	collagen type XIV alpha 1 chain	5.388E-34
PCOLCE	procollagen C-endopeptidase enhancer	4.061E-29
LUM	lumican	1.749E-26
COL3A1	collagen type III alpha 1 chain	3.375E-25
WIF1	WNT inhibitory factor 1	1.084E-18
COL1A1	collagen alpha-1(I) chain precursor	4.668E-13
COL4A5	collagen type IV alpha 5 chain	9.06E-10

Upregulated Genes

Gene name	**Description**	**p-value**
SFRP5	secreted frizzled related protein 5	4.16E-11

DKK1	dickkopf WNT signaling pathway inhibitor 1	0.0001663

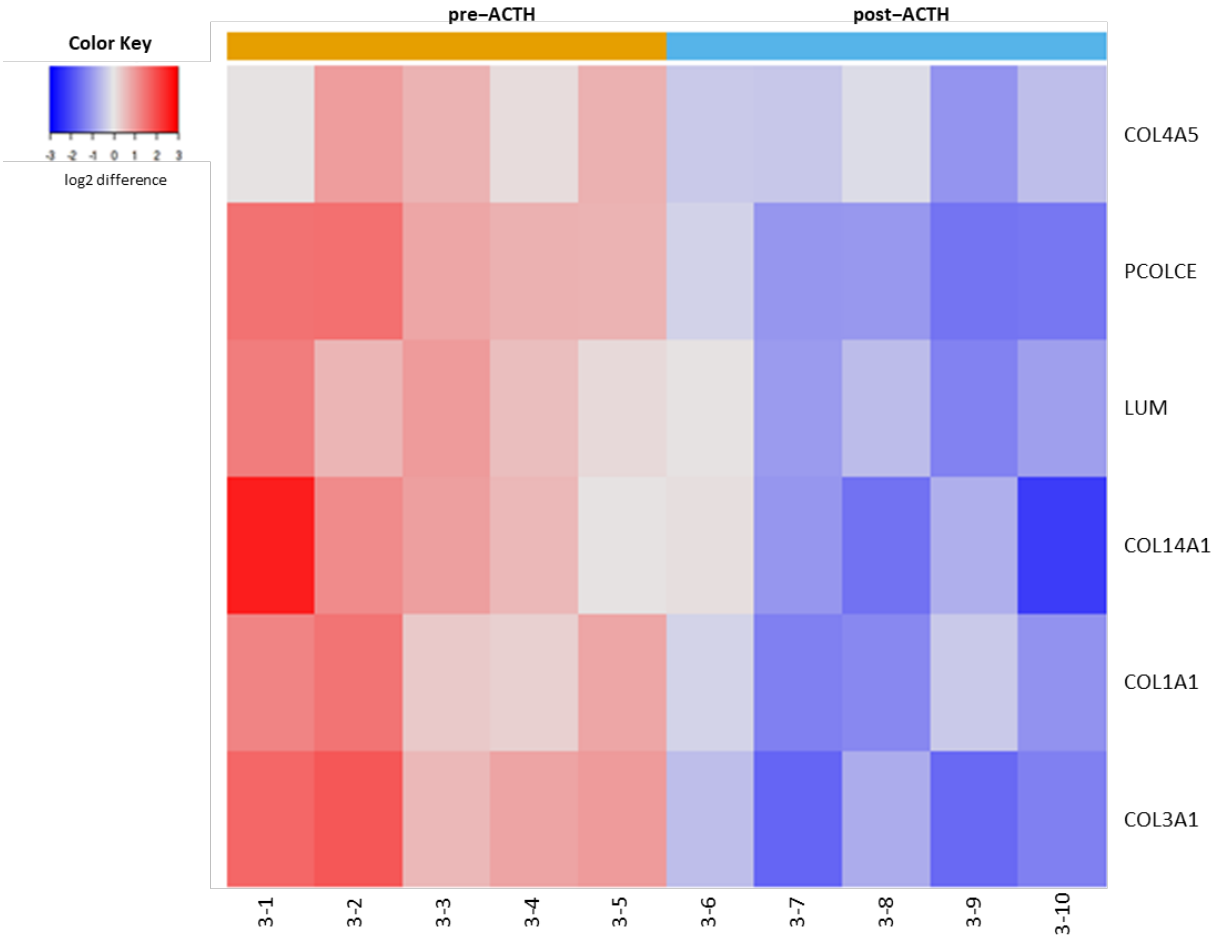

Figure 16: Heatmap presenting signal activity changes of fibrillar collagen type genes from 5 dogs before (pre ACTH) and after (post ACTH) treatment (3.1-3.5: pre ACTH; 3.6-3.10: post ACTH, x-axis). Fibrillar collagen gene codes (y-axis). blue: downregulated genes, red: upregulated genes.
PCOLCE: procollagen C-endopeptidase enhancer; LUM: lumican; COL14A1: collagen type XIV alpha 1 chain; COL1A1: collagen alpha-1(I) chain precursor; COL3A1: collagen type III alpha 1 chain.

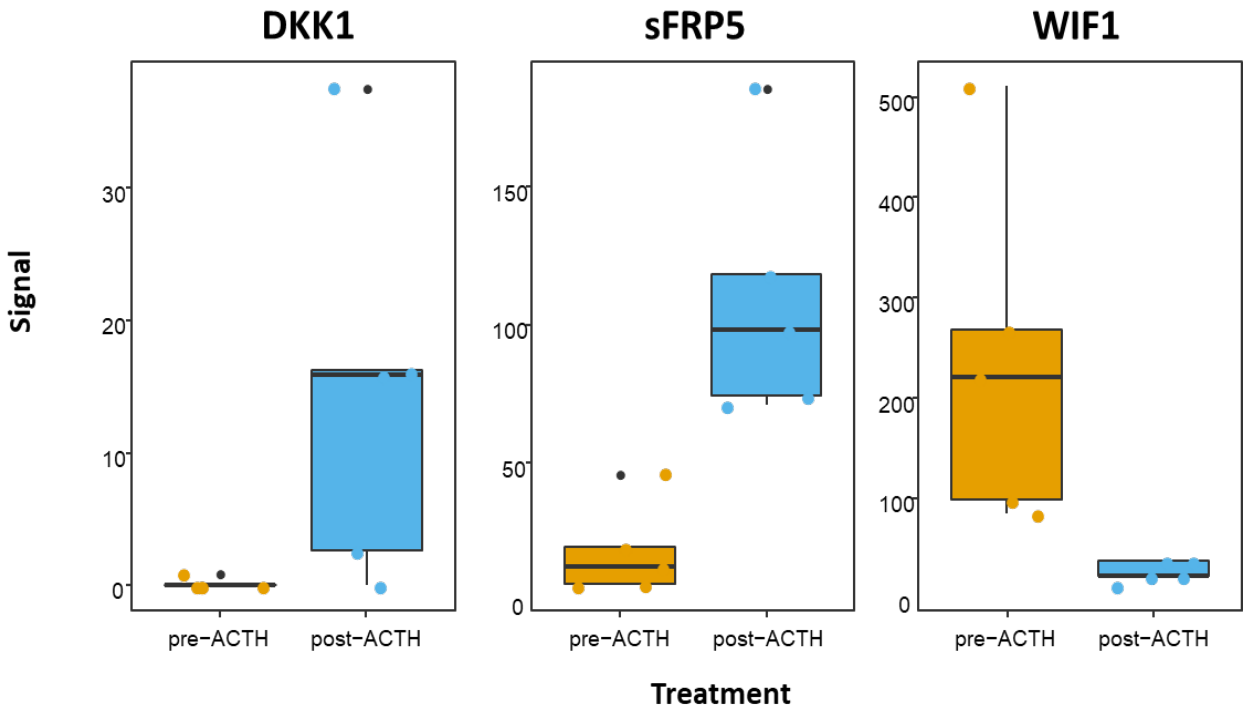

Figure 17: Boxplots depicting Wnt inhibitory signal genes pre and post ACTH treatment.
DKK1: dickkopf WNT signaling pathway inhibitor 1; sFRP5: secreted frizzled related protein 5; WIF1: WNT inhibitory factor 1.

3.3.7 Genes involved in insulin resistance

In this category, 7 out of 35 genes were significantly altered, and 6 out of 7 genes were elevated, namely PIK3R1, IRS1/ 2 (Fig.18). Also, FKBP5 was significantly upregulated (log2: 2.22; p value: 1.80E-20) (Fig.18). FKBP5 gene codes for the FK506-binding protein 5 (FKBP51), which is part of the immunophilins family. One of its functions is the regulation of glucocorticoid receptor activity by binding to its receptor and impairing it (Pereira et al., 2010).

Upregulated Genes

Gene name	Description	p-value
FKBP5	FK506 binding protein 5	1.802E-20
IRS2	insulin receptor substrate 2	5.924E-09
IRS1	insulin receptor substrate 1	1.188E-07
PIK3R1	phosphoinositide-3-kinase regulatory subunit 1	0.001966

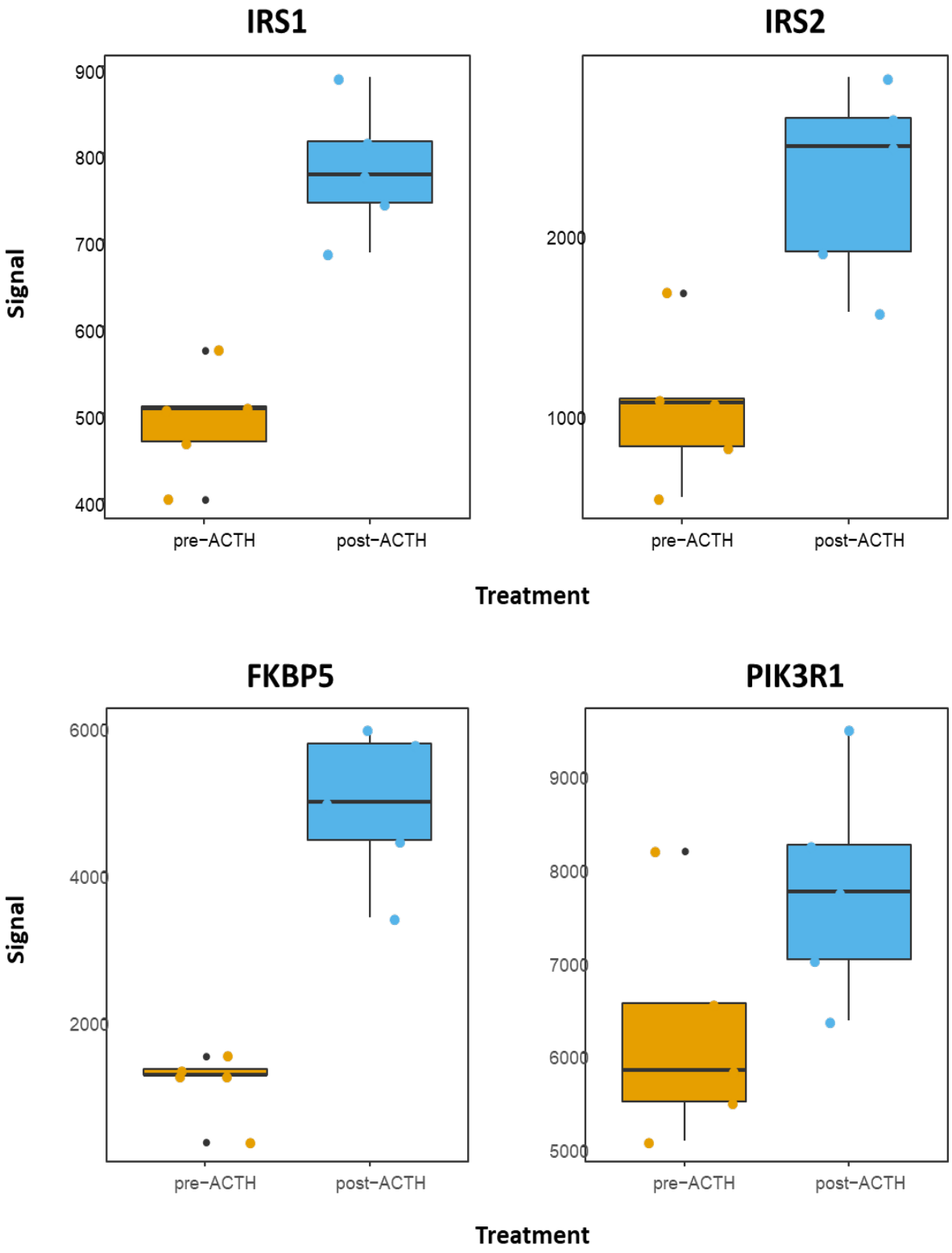

Figure 18: Boxplots depicting genes involved in insulin metabolism pre and post ACTH treatment. FKBP5: FK506 binding protein 5; PIK3R1: phosphoinositide-3-kinase regulatory subunit 1; IRS1: insulin receptor substrate 1; IRS2: insulin receptor substrate 2.

Chapter Four

Discussion

4.1 Experimental setting and methods

We used healthy beagle dogs and focused on keeping the group homogeneous in terms of breed and also of the origin/genetic background of the dogs, age, body-weight and gender population in order to obtain the most credible and significant outcomes. We are aware that despite this, we must expect a higher variance compared to using an inbred mouse strain. However, the dogs' advantage over rodents is the closer similarity to GC metabolism in humans. As stated above, in dog's cortisone is converted to cortisol as in humans, while in rodents the active form is corticosterone instead of cortisol. Moreover, in dogs naturally occurring, endogenous hyperadrenocorticism has signs similar to the metabolic syndrome observed in humans with hypertension and secondary diabetes mellitus. To our knowledge, this has not yet been described in rodents. With our model of implanting ACTH-releasing pumps, we were able to induce a state of chronic endogenous hypercortisolemia, as demonstrated clinically and also based on positive endocrine test results (Spoerel, 2017 and Sieber-Ruckstuhl et al., 2019). Therefore, we were able to evaluate, for the first time in a dog model, the effects of chronic endogenous GCs on gene expression in visceral adipose tissue.

In our study we chose to use a gene expression assay to investigate our samples. The basic steps of a gene expression assay can be done either via RNA sequencing or DNA microarrays. In both methods the RNA is firstly converted to cDNA and amplified gene transcripts are identified and quantified; then normalized data is analyzed to express differences in genes and pathways. However, DNA microarrays, such as the Affymetrix Gene chip, suffer from many technical issues such as cross hybridization, non-specific hybridization and limited range of detection of probes. RNA sequencing on the other hand, such as the Illumina Tru Seq mRNA sequencing assay, is not dependent on the selection of known genes and does not depend on the use of probesets and is therefore less limited by the saturation and sensitivity of the assay (Minnier et al., 2018). Upon investigation of other literatures and methods used to analyze genetic information, a next generation sequencing method proved to be the gold standard for transcriptome analysis due to its detailed objective performance. The extended dynamic range offered by RNA-Seq allows for the detection of larger fold changes, especially in a small sample size such as in our study with a group number of only 5 dogs.

In terms of RNA extraction, we decided to use the method of ribosomal RNA depletion instead of poly (A) + enrichment. Using this method, it is possible to characterize polyadenylated and non-polyadenylated RNAs, while requiring only small amounts of RNA in the sample (Sultan et al., 2014).

The statistical method applied in this trial, DESeq2, was chosen because it collects significant genetic data from the transcriptome and is therefore capable of achieving highly reliable results even in small sample sizes (Love et al., 2014). This advantage was especially important in our study as the dog number was limited to 5 animals, as mentioned above. Applications such as fold change, standard error approximation, and logarithm measurements are only a few positive examples of DESeq2 for improved quality control (Love et al., 2014). The analysis made in this study is part of a NGS two-group analysis, comparing the control group in terms of pre ACTH treated dogs with results of post ACTH treatment.

Statistical features such as p value, log2, fc, and FDR are significant for evaluation of the gene signals and for distinguishing the effects of glucocorticoid treatment on biological processes within the adipose tissue samples. The features chosen facilitate statistical analysis and provide more in-depth information for specific genetic expressions. Listing genes according to their concentration signal means that they can be easily used for follow up studies. Furthermore, the log2 transformation enables graphical illustration of differences, such as those used here in heatmaps and boxplots.

As we found 19856 features in total, we focused on a threshold and analyzed only counts above that limit. The counts then reduced to 12576. By deciding on a p-value threshold at/ or below 0.01, and a log2 ratio <-1 or >1 we were able to focus on the genes that had the largest impact pre ACTH to post ACTH treatment. We analyzed values of false discovery rates below 5%, or 0.05, to reduce technical bias influence on the results. Technical bias could occur due to extreme gene length or extreme glucocorticoid influence on specific genes. Also, overlapping genes could cause potentially false results. Hence, by keeping a low threshold on FDR we tried to keep the potentially false positives to a minimum.

4.2 Influence of chronic hypercortisolemia on gene expression

4.2.1 Genes involved in lipolysis, lipogenesis and adipogenesis

Our results demonstrate that chronic hypercortisolemia leads to both lipolytic and adipogenic gene changes. The induction of genes encoding for enzymes such as LPL, LIPE, PNPLA2 can potentially cause increased availability and uptake of FAs into the adipose tissue. Through LPL activity, TAGs are hydrolyzed and cause the release of FAs, which then can be taken up by surrounding tissues for storage.

Interestingly, the plasma lipase activity was significantly increased 25 weeks after ACTH-treatment (Sieber-Ruckstuhl et al. 2019). Moreover, also plasma triglycerides concentrations (TG) were significantly increased in these dogs (Sieber-Ruckstuhl et al. 2019). Clinically, all dogs showed a loss in body-weight, muscle loss and, in selected dogs, increased central obesity was observed (data not shown). These effects would probably be intensified by an altered food intake, as GCs contribute to an increase in

dietary intake. However, with a fixed feeding regimen as used for the dogs in our study, these effects could not be observed.

Along with higher FA availability, lipid synthesis is increased. According to a study by Minshull et al., 1985, corticosterone and insulin have been shown to increase lipid synthesis up to 66% in cultured adipose tissues in rats. However other studies claim that fatty acid synthesis and acetyl CoA carboxylase are rate-limiting enzymes of lipogenesis in adipose tissue of rats treated with GCs (Volpe et al., 1975). In our results, we have found signs of an increased lipolysis as well as lipogenesis. It is assumed that GCs act simultaneously by two independent pathways on lipid metabolism: Preadipocytes are stimulated to differentiate, which triggers adipogenesis. Parallel to that, lipolysis is increased through actions on mature adipocytes (Campbell et al., 2009).

With 11βHSD1 activity, through conversion of cortisone to the active ligand cortisol in humans and dogs, the enzyme amplifies the action of GCs in target tissues via the GR and MR. Our results show, however, that GR and MR gene expression were slightly suppressed, although 11βHSD1 gene was increased. Recent studies on metabolic effects of 11βHSD1 are not yet fully clarified and sorted out. In a mouse case study by Masuzaki et al., 2001, transgenic mice overexpressing 11βHSD1 experienced central obesity and an increased rate of adipogenesis in visceral adipose tissues. However, in another study with rodents that received GCs continuously, the elevated 11βHSD1 gene expression in visceral adipose tissue was closely related to a parallel elevation in lipolysis and diminished visceral adiposity (Campbell et al., 2009). Our beagle dogs` results would also more likely be explained by a reduced adipogenesis and increased lipolysis. Furthermore, one has to take into consideration that in the present study, only genes were detected, which does not necessarily reflect the protein level; i.e. not all genes are transcribed into proteins, a clear limitation of the study.

The role of MR and GR in connection with GCs has also not yet been fully investigated. Studies with rats however have claimed that GCs bind to MRs with a ten-fold higher affinity than to GRs, and MR expression is generally increased, especially during adipogenesis and obesity (Desarzens et al., 2016). In human adipocytes, GRs have been shown to be several 100 times higher than MRs. When silencing GR, but not MR, effects of cortisol on adipokine expression were blocked (Ferrau et al., 2015). As mentioned above, our beagle dogs have both MR and GR gene downregulations, with a more significant p-value in terms of the GR.

In humans and rodents, GC treatment generally has larger impact on visceral tissue than on subcutaneous tissue (Richelsen et al., 1991; Campbell et al., 2009). Campbell et al., 2009, claim that receptor density in visceral depots is higher. Richelsen et al., 1991 discuss an enhanced α_2-receptor activity in subcutaneous adipocytes that causes discrepancies. Peckett et al., 2011, mention cAMP alterations, as well as genomic and non-genomic causes as possibilities. Overall it is not yet fully clear what causes the discrepancy.

Adipokine gene expression levels such as leptin, adiponectin and resistin were insignificantly decreased as they showed only low signal activity. Significant p-values ranged from 0.01 or below, and our measured p-values ranged from 0.8-0.4 in all adipokine gene expressions. In humans treated with GCs (Fallo et al., 2004), adiponectin levels seem to act in an inverse pattern towards hydrocortisone injections. The authors of that study claim that GC administration has a direct effect on adiponectin inhibition, as a single intravenous hydrocortisone bolus injection into healthy human patients caused a direct but only transient decrease in circulating levels within 30 minutes. In another study with mice and hypercorticosteronemia, adipose tissues resulted in suppressed adiponectin at gene and protein levels (Shinahara et al., 2009). We cannot fully explain why our results did not measure significant signal concentration changes, however the rather long duration of ACTH treatment as well as limited number of dogs could have had an influence, so that results did not reach statistical significance.

4.2.2 Genes involved in insulin antagonism

GCs, and especially cortisol act as insulin-antagonistic hormones. Generally, peripheral glucose utilization is stimulated and hepatic glucose output suppressed. When GC levels are chronically elevated, fat is redistributed from peripheral to central deposits with insulin resistance and dyslipidemia being a common outcome in human patients (Rebuffe-Scrive et al., 1988). It is claimed that GCs result in whole-body insulin resistance in humans, however insulin action is not necessarily impaired in each tissue (Geer et al., 2014). A study by Hazlehurst et al., 2013, confirmed this statement by observing a tissue-specific interaction between GCs and insulin in humans and rodents.

According to our results, the insulin signaling pathway genes are significantly elevated in adipose tissue. In mice, there is the possibility that insulin resistance is active in a specific organ, such as liver or muscle and that visceral adipose tissue is not affected (Hochberg et al., 2015).

The immunophilin FKBP51 is associated with markers of insulin resistance and involved in attenuating GC action in general (Pereira et al., 2014). In a study with humans it was proven to be one of the genes with the most significant rise in expression after dexamethasone treatment in several adipose tissues (Pereira et al., 2014). Jääskeläinen et al., 2011, also support the theory that the gene is highly responsive to GC signaling in humans. In our results the FKBP51 gene was significantly elevated with a p-value of 1.802 E-20. For more detailed information, an insulin tolerance test would have been interesting in our beagle dogs to assess the functioning of the hypothalamic-pituitary-adrenal-axis. With this test we could have estimated how rapidly glucose would be cleared from the blood. This would have given us indications about whether insulin resistance was present in our dogs and to what extent. Unfortunately, this was not done in the present study but should clearly be considered in further experiments.

4.2.3 Genes involved in muscle wasting

GC treatment in humans, especially on a long-term basis, leads to direct catabolic effects on muscle, as a consequence of decreased protein synthesis (Menconi et al., 2007). IGF-1 and amino acids are in charge of the phosphorylation of the protein synthesis machinery, 4E-BP1 and RPS6KA1.

Our results identified this catabolic mechanism by the significant decrease in genes encoding for IGF-1 and RPS6KA1. Calpain 11 was also significantly reduced, which does not correspond to what happened in an experimental trial with rats (Hasselgren et al., 1999). Through catabolism, the most important cellular proteolytic systems, the ubiquitin-proteasome system, lysosomal system (cathepsins) and calcium-dependent system (calpains) should be activated (Pereira et al., 2010; Hasselgren et al., 1999). With CKM being significantly activated in our study, muscle is broken down in order to utilize energy in the form of ATP. This also correlates with the observed increased loss of body mass during the 25 weeks of ACTH treatment. It should be noted however, that GC induced myopathy varies greatly among human patients in terms of muscle weakness independently of duration and dosage (Pereira et al., 2010). FoxO1 functions as a main regulator in muscle atrophy and is a well-known atrogene (Brocca et al., 2016; Menconi et al., 2007). In a study by Brocca et al., 2016, knockout FoxO mice prevented muscle loss after 14 days of GC treatment. In our results FoxO gene expression is significantly elevated, supporting the observed muscle loss.

4.2.4 Genes involved in the function of the immune system

As GCs are potent regulators of inflammation, they influence the inflammatory response on three levels: when the signal for danger is triggered (alarm phase), during leukocyte migration (mobilization phase) and finally when the tissue is cleared (resolution phase) (Cain et al., 2017). TLR, IRF and IL, which represent genes acting in the alarm phase, are significantly suppressed in our results. In the mobilization phase our CCR genes represent an inhibited signal of chemokines and chemo-attractants which generally are in charge of recruiting leukocytes (Cain et al., 2017). In a human study by Ishmael et al., 2011, it is suggested that direct GR binding to chemokine-encoding mRNA transcripts promote their decay. In a different trial by Hochberg et al., 2015, mice with long-term dexamethasone treatment had several gene reductions that are in charge of forming the MHC II, such as HLA, DRA, DLA genes. These genes are responsible for T-cell recruitment. Our measurements show the same results, which supports the general claim of GCs having an important influence in the immune response. Hence, in the resolution phase GCs inhibit many wound healing processes, including collagen deposition, re-epithelialization and angiogenesis, which will be discussed below.

4.2.5 Genes influencing collagen, fibrillogenesis and bone formation

Collagen, which is the main component of tendons, connective tissues and skin, is strongly impacted in its function by GCs (Taguchi et al., 2016; Cutroneo et al., 1981). Generally, in an early stage of collagen fiber formation, enzymatic crosslinks must be formed in order to strengthen them. In a study by Taguchi et al, 2016, collagen was examined in Achilles tendons in rats that were treated long-term with GCs. Results of this study suggest that intermolecular crosslinking did not occur due to GC treatment, which prevented maturation of the fibers and consequently decreased tendon strength.

In our results genes encoding for proteins involved in fibrillogenesis and collagen biosynthesis were significantly downregulated. The meaning of this, especially as we evaluated adipose tissue, is unclear. The low collagen content observed in GC-treated skin or in tendons could be the result of a decreased synthesis, for example due to the inhibition of proline hydroxylase, or through an increased rate of collagen degradation (Cutroneo, et al., 1981). The main mechanisms behind the unified observation in several studies is not yet certain. The Wnt/β-catenin pathway is important for growth, development and maintenance of skeletal tissue and prevents osteoporotic progression in the bones (Zhou et al., 2017). It is regulated by the secreted antagonists sFRP, WIF1, DKK1 (Zhou et al., 2017). In a trial with rats by Zhou et al., 2017, the authors experienced a significant elevation of these genes which determine the Wnt signal pathway. DKK1 is also assumed to be the key receptor inhibitor in bone formation and development (Rossini et al., 2013). In our results we also measured significant elevations in DKK1, and sFRP5 signal concentrations, however not of WIF1. The data observed could be explained by the limited number of dogs used in the trial or their long-term treatment with ACTH.

4.2.6 Genes involved in angiogenesis and vascular functions

Angiogenesis is suppressed by high doses of GCs. In mice 11 βHSD-1 is expressed in adipose tissue, but when also present in blood vessel walls, it is able to modulate angiogenesis by determining the local regeneration of active GCs in the vessel wall (Small, et al., 2005). In a study by Michailidou et al., 2012, 11 βHSD-1 knockout mice showed enhanced angiogenesis, improved wound healing and oxygenation, which underlines the rather angiostatic or angiogenesis-inhibiting effect of 11 βHSD-1. The enzyme deficiency enhances peroxisome proliferator-activated receptor ɣ (PPAR-ɣ) activation and angiogenic factors such as VEGF. In our results the 11βHSD-1 gene was significantly increased after chronic GC influence, which could resonate with this theory, in addition to the hypoxia which mediates insulin resistance as was also observed. The reduction of VEGF, as in charge of vascular remodeling, leads to potential collagen deposition and inhibition of *de novo* collagen formation (Michailidou et al., 2012; Small et al., 2005). It could also be possible that the long-term GC treatment inhibited endothelial cell proliferation, migration and/or remodeling and thus prevented new tube formation, which is essential for new blood vessel formation (Logie et al., 2010). Angiopoietins,

such as ANGPT4 act primarily on vasculature, control of blood vessel development and stability. Although this gene is significantly elevated in our results, the role of ANGPT4 has not yet been extensively studied and does not have a substantial role in angiogenesis in comparison to other angiopoietins (Fagiani et al., 2013). ANGPT4 and ANGPT3 are orthologous in human and mice although structurally diverse, and both are able to induce angiogenesis (Fagiani, et al., 2013; Valenzuela et al., 1999).

4.3 Limitations and outlook

Several limitations of the study have already been mentioned above. Briefly, one of the main limitations is that we only evaluated gene expression levels. Therefore, we can draw no conclusions on what effects the up- or downregulation of the determined genes have on the protein level: not every up- and not every downregulation of a gene will lead to an up- or downregulation of the respective protein. However, to be biologically or clinically relevant, this information would be important. This should be considered in further studies.

We found genes coding for enzymes, for example involved in lipid metabolism, that were upregulated. However, we performed no studies to evaluate the activity of these enzymes. Therefore, even if we had protein data, we could not say anything about their function or activity.

Also, the rather small sample size of 5 dogs used in this study limits the reliability and credibility of our results. The presence of biological variance, as the animals in this study were of different sexes and ages and were line-breed dogs, should clearly be taken into consideration; this is a limitation which has been discussed in the previous chapter.

We used every dog as its own control by referring all measured genes after ACTH exposure and comparing them to before treatment. However, we did not include a placebo control group treated with NaCl-containing minipumps. With this setting, we could have evaluated the effect of the pump implantation, which might have led to an irritation and chronic inflammation of subcutaneous tissue. We therefore cannot exclude a systemic inflammation induced by the pumps, influencing gene expression in visceral adipose tissue.

For more in-depth information about adipose tissue and its metabolic activity we could have measured and compared adipocyte sizes in visceral fat depots and compare it with that of subcutaneous adipose tissue. This methodological approach would give us more information about whether lipolysis or adipogenesis was more active during hypercortisolemia. Therefore, in further experiments, sampling of subcutaneous adipose tissue in addition to visceral tissue should be planned. Moreover, a proteomic approach in addition to RNA sequencing should be taken into consideration. Beside a multi-omic approach, other methods to evaluate adipose tissue, e.g. histology and immunohistology, would be important approaches to further steps in pathophysiology and evaluation of the influence of chronic hypercortisolemia on adipose tissue.

5. Conclusions

Dogs with ACTH-releasing pumps represent a good model to study effects of chronic hypercortisolemia on adipose tissue. Results are comparable to findings from in vitro and in vivo studies performed in rodents. We agree with other authors that the interaction between the different cell types contained in adipose tissue (e.g adipocytes, pre-adipocytes, endothelial and immune cells) cannot be studied in vitro, therefore in vitro studies cannot replace in vivo studies.

There are several advantages of dogs compared to rodents: dogs have been used as models to study metabolic obesity, diabetes, dyslipidemia and response to pharmacologic interventions. They show similar side effects, e.g. hyperlipidemia, hypertension, and a higher risk of developing type 2 diabetes mellitus, which has not yet been described in rodents. Another advantage of our dog model compared to rodents is the higher similarity of the cortisol metabolism of dogs to humans than that of rodents.

In our study we used ACTH to induce hypercortisolemia instead of a treatment with a synthetic GC such as prednisolone or dexamethasone. Using a synthetic GC has the disadvantage that in contrast to cortisol, it cannot be inactivated and cannot activate the MR receptor.

Several, especially older studies, have used microarrays for gene analyses. However, results of these studies cannot be directly compared to results of our study. We have used the next generation sequencing method, which proved to be the gold standard for transcriptome analysis due to its detailed objective performance.

Dyslipidemia is a frequently observed consequence of GC treatment and hypercortisolemia, typified by increased lipolysis, lipid mobilization, liponeogenesis, and adipogenesis and could be studied intensively in our model. We could show that visceral fat is a highly metabolically active tissue, which is severely influenced by hypercortisolemia, at least on the transcriptomic level.

Interestingly, our findings are in accordance with results of a recent study (Hayashi et al. Endocrinology, March 2019, 160(3):504–521) in human patients with hypercortisolemia induced by adrenal gland adenoma. In their study, periadrenal adipose tissue was dissected out immediately after resection of the adrenal tumor. Among others, they showed a suppression of both, synthesis and degradation of collagen, comparable to our findings and adipose expansion was associated with a dysregulation of tissue remodeling and preadipocyte proliferation. These are possible explanations for the observed visceral accumulation of adipose tissue in patients with CS or in chronically GC treated patients.

We think that this study including the methods (dog model, ACTH releasing pumps, RNA sequencing) and the results represent an optimal basis for further studies, with which the biological significance of our findings can be evaluated using additional methods such as a proteomic analysis and a function analysis of the detected proteins.

With this, pathomechanisms of hypercortisolemia induced metabolic disturbances as well as therapeutic targets can be evaluated in a translational manner.

References

Atzmon, G., Yang, X. M., Muzumdar, R., Ma, X. H., Gabriely, I., Barzilai, N., 2002, Differential Gene Expression Between Visceral and Subcutaneous Fat Depots: Horn Metab Res, v. 34, p. 622-628.

Burford, N.G , Webster, N.A., Cruz-Topete, D., 2017, Hypothalamic-Pituitary-Adrenal Axis Modulation of Glucocorticoids in the Cardiovascular System: Int.J.Mol.Sci,v. 18, p. 2150.

Behrend, E. N., Kemppainen, R. J., 2001, Diagnosis of Canine Hyperadrenocorticism: v. 31(5)

Brocca, L., Toniolo, L., Reggiani, C., Bottinelli, R., Sandri, M., Pellegrino, M. A., 2016, FoxO-dependent atrogenes vary among catabolic conditions and play a key role in muscle atrophy induced by hindlimb suspension: J Physiol, v. 594.4, p. 1143-1158.

Cain, D. W., Cidlowski, J. A., 2017, Immune regulation by glucocorticoids : Springer Nature, v.17, p. 233-247.

Campbell, J. E., Fediuc, S., Hawke, T. J., Riddell, M. C., 2009, Endurance exercise training increases adipose tissue glucocorticoid exposure: adaptations that facilitate lipolysis: Metabolism, v. 58, p. 651-660.

Caprio, M., Feve, B., Claes, A., Viengchareun, S., Lombes, M., Zennaro, M., 2007: Pivotal role of the mineralocorticoid receptor in corticosteroid-induced adipogenesis: The FASEB Journal, v. 21, p. 2185-2194.

Cutroneo, K., Rokowski, R., Counts, D.F., 1981, Glucocorticoids and Collagen Synthesis: Comparison of in vivo and Cell Culture Studies: Collagen Rel. Res., v.1, p.557-568.

Dardevet, D., Sornet, C., Taillandier, D., Savary, I., Attaix, D., Grizard, J., 1995, Sensitivity and Protein Turnover Response to Glucocorticoids Are Different in Skeletal Muscle from Adult and Old Rats: J. Clin. Invest., v. 96, p. 2113-2119.

Desarzens, S., Faresse, N., 2016, Adipocyte glucocorticoid receptor has a minor contribution in adipose tissue growth: Journal of Endocrinology, v. 230, p. 1-11.

Distelhorst, C.W., 2002, Recent insights into the mechanism of glucocorticoid-induced apoptosis: Cell Death Differ, v.9(1), p.6-19.

Eisele, I., Wood, I. S., German, A. J., Hunter, L., Trayhurn, P., 2005, Adipokine Gene Expression in Dog Adipose Tissues and Dog White Adipocytes Differentiated in Primary Culture: Horm Metab Res, v. 37, p. 474-481.

Engeli, S., Schling, P., Gorzelniak, K., Boschmann, M., Janke, J., Ailhaud, G., Teboul, M., Massierea, F., Sharma, A. M., 2003, The adipose-tissue renin-angiotensin-aldosterone system: role in the metabolic syndrome?: Int J Biochem Cell Biol, v.35, p.807–825.

Fallo, F., Scarda, A., Sonino, N., Paoletta, A., Boscaro, M., Pagano, C., Federspil, G., Vettor, R., 2004, Effect of glucocorticoids on adiponectin: a study in healthy subjects and in Cushing`s syndrome: European Journal of Endocrinology, v. 150, p. 339-344.

Fagiani, E., Christofori, G., 2013, Angiopoietins in angiogenesis: Science Direct, v.328(1), p. 18-26.

Fardet, L., Antuna-Puente, B., Vatier, C., Cervetera, P., Touati, A., Simon, T., Capeau, J., Feve, B., Bastard, J., 2013, Adipokine profile in glucocorticoid-treated patients: baseline plasma leptin level predicts occurrence of lipodystrophy: Clinical Endocrinology, v. 78, p. 43-51.

Fernandez-Sola, J., Cusso, R., Picado, C., Vernet, M., Grau, J., Urbano-Marquez, A., 1993, Patients with chronic glucocorticoid treatment develop changes in muscle glycogen metabolism: Journal of the Neurological Sciences, p. 117, p. 103-106.

Ferrau, F., Korbonits, M., 2015, Metabolic comorbidities in Cushing`s syndrome: European Journal of Endocrinology, v. 173, p. 133-157.

Flammer, J.R., Rogatsky, I., 2011, Minireview: glucocorticoids in autoimmunity: unexpected targets and mechanisms: Mol. Endocrinol., v. 25(7), p. 1075-86.

Functional Genomics Center Zurich, 2018, Eidgenössische Technische Hochschule Zürich, accessed april 2019, http://www.fgcz.ch

Guia, R.M., Herzig, S., 2015, How Do Glucocorticoids Regulate Lipid Metabolism?: Springer Science + Business Media New York, Chaper 6, p. 127-137.

Geer, E.B., Islam, J., Buettner, C., 2014, Mechanisms of Glucocorticoid- Induced Insulin Resistance: Endocrinol Metab Clin North Am, v. 43 (1), p. 75-102.

Hasselgren, P., 1999, Glucocorticoids and muscle catabolism: Current opinion in Clinical Nutrition and Metabolic Care, v. 2.

Hayashi, R., Okuno, Y., Mukai, K., Kitamura, T., Hayakawa, T., Onodera, T., Murata, M., Fukuhara, A., Imamura, R., Miyagawa, Y., Nonomura, N., Otsuki, M., Shimomura, I., 2019, Adipocyte GR Inhibits Healthy Adipose Expansion Through Multiple Mechanisms in Cushing Syndrome: Endrocinology, v.160 (3), p.504-521.

Hazlehurst, J. M., Gathercole, L. L., Nasiri, M., Armstrong, M. J., Borrows, S., Yu, J., Wagenmakers, A. J. M., Stewart, P. M., Tomlinson, J. W. 2013, Glucocorticoids Fail to Cause Insulin Resistance in Human Subcutaneous Adipose Tissue In Vivo: J Clin Endocrinol Metab, v. 98(4), p. 1631-1640.

Heck, S., M. Kullmann, A. Gast, H. Ponta, H. J. Rahmsdorf, P. Herrlich, and A. C. Cato, 1994, A distinct modulating domain in glucocorticoid receptor monomers in the repression of activity of the transcription factor AP-1: EMBO J, v. 13, p. 4087-95.

Hochberg, I., Harvey, I., Tran, Q.T., Stephenson, E.J., Barkan, A.L., Saltiel, A.R., Chandler, W.F., Bridges, D. 2015, Gene expression changes in subcutaneous adipose tissue due to Cushing's disease: Journal of Molecular Endocrinology, v. 55, p. 81-94.

Hoppmann, J., Perwitz, N., Meier, B., Fasshauer, M., Hadaschik, D., Lehnert, H., Klein, J., 2010, The balance between gluco-and mineralo-corticoid action critically determines inflammatory adipocyte response: Journal of Endocrinology, v. 204, p. 153-164.

Infante, M., Armani, A., Mammi, C., Fabbri, A., Caprio, M., 2017, Impact of Adrenal Steroids on Regulation of Adipose Tissue: Comprehensive Physiology, v. 7, p. 1425-1447.

Ishmael, F. T., Fang, X., Houser, K. R., Pearce, K., Abdelmohsen, K., Zhan, M.,Gorospe, M., Stellato, C., 2011, The human glucocorticoid receptor as an RNA-binding protein: global analysis of glucocorticoid receptor-associated transcripts and identification of a target RNA motif: J. Immunol.,v. 186 (2), p.1189-1198.

Jääskeläinen, T., Makkonen, H., Palvimo, J., 2011, Steroid up-regulation of FKBP51 and its role in hormone signaling: Current Opinion in Pharmacology, v.11, p. 326-331.

Kooistra, H. S., Galac, S., 2012, Recent Advances in the Diagnosis of Cushing´s Syndrome in Dogs: Topics in Compan An Med, v. 27, p. 21-24.

Klein, S. C., Peterson, M. E., 2010, Canine hypoadrenocorticism: Part I: Can Vet J, v. 51, p. 63-69.

Krsek, M., Rosicka, M., Nedvidkova, J., Kvasnickova, H., Hana, V., Marek, J., Haluzik, M, Lai, E. W., Pacak, K., 2006, Increased Lipolysis of subcutaneous abdominal adipose tissue and altered noradrenergic activity in patients with cushing`s syndrome: An in-vivo microdialysis study: Physiol. Res., v. 55, p. 421-428.

Lathan, P., Thompson, A. L., 2018, Management of hypoadrenocorticism (Addison´s disease) in dogs: Veterinary Medicine: Research and Reports, v. 9, p. 1-10.

Lazar, M. A., 2007, Resistin- and Obesity-associated Metabolic Diseases: Horm Metab Res, v.39, p.710-716.

Lee, R.A., Harris, C.A., Wang, J., 2018, Glucocorticoid Receptor and Adipocyte Biology:Nucl Receptor Res, v. 5.

Liu, D., Ahmet, A., Ward, L., Krishnamoorthy, P., Mandelcorn, E. D., Leigh, R., Brown, J. P., Cohen, A., Kim, H., 2013, A practical guide to the monitoring and

management of the complications of systemic corticosteroid therapy: Allergy, Asthma & Clinical Immunology, v. 9 (30).

Logie, J.J., Ali, S., Marshall, K.M., Heck, M., S., Walker, B.R., Hadoke, P.M.F., 2010, Glucocorticoid-Mediated Inhibition of Angiogenic Changes in Human Endothelial Cells Is Not Caused by Reductions in Cell Proliferation or Migration: PLoS ONE, v.5 (12): e14476.

Love, M., Huber, W., Anders, S., 2014, Moderated estimation of fold change and dispersion for RNA-seq data with DESeq2: Genome Biology, v.15(12), p.550.

Marzolla, V., Armai, A., Zennaro, M., Cinti, F., Mammi, C., Fabbri, A., Rosano, G., Caprio, M., 2012, The role of the mineralocorticoid receptor in adipocyte biology and fat metabolism: Molecular and Cellular Endocrinology, v. 350, p. 281-288.

Masuzaki, H., Paterson, J., Shinyama, H., Morton, N. M., Mullins, J.J., Seckl, J.R., Flier,J.S., 2001, A Transgenic Model of Visceral Obesity and the Metabolic Syndrome: Science, v. 294, p. 2166-2170.

Menconi, M. Fareed, M., O'Neal, P. Poylin, V., Wei, W. Hasselgren, P., 2007, Role of glucocorticoids in the molecular regulation of muscle wasting: Crit Care Med, v. 35 (9)

Miceli, D.D., Pignataro, O.P., Castillo, V.A., 2017, Concurrent hyperadrenocorticism and diabetes mellitus in dogs: Research in Veterinary Science, v. 115, p. 425-431.

Minnier, J., Pennock, N., D., Guo, Q., Schedin, P., Harrington, C. A., 2018, RNA-Seq and Expression Arrays: Selection Guidelines for Genome-Wide Expression Profiling: Methods in Molecular Biology, v.1783.

Michailidou, Z., Turban, S., Miller, E., Zou, X., Schrader, J., Ratcliffe, P. J., Hadoke, P. W. F., Walker, B. R., Iredale, J. P., Morton, N. M.,Seckl, J. R., 2012, Increased Angiogenesis Protects against Adipose Hypoxia and Fibrosis in Metabolic Disease-resistant 11β-Hydroxysteroid Dehydrogenase Type 1 (HSD1)-deficient Mice: Journal of biological chemistry, v. 287(6), p.4188-4197.

Minshull, M., Strong, C. R., 1985, The stimulation of lipogenesis in white adipose tissue from fed rats by corticosterone: Int. J. Biochem., v. 4, p. 529-532

Mooney, C. T., and M. E. Peterson, 2004, BSAVA Manual of Canine and Feline Endocrinology: Quedgeley, UK, British Small Animal Veterinary Association, v. 47, p. 240.

Morgan, S. A., McCabe, E. L., Gathercole, L. L., Hassan-Smith, Z. K., Larner, D. P., Bujalska, I. J., Stewart, P. M., Tomlinson, J. W., Lavery, G. G., 2014, 11β-HSD1 is the major regulator of the tissue-specific effects of circulating glucocorticoid excess: PNAS, E2482-E2491.

Nakae, J., Oki, M., Cao, Y., 2008, The FoxO transcription factors and metabolic regulation: FEBS Letters, v.582, p.54-67.

National Human Genome Research Institute, 1999-2019, accessed april 2019, http://www.geneontology.org

Odermatt, A., Kratschmar,D.V., 2012, Tissue-specific modulation of mineralocorticoid receptor function by 11beta-hydroxysteroid dehydrogenases: An overview: Mol Cell Endocrinol, v. 350, p. 168-186.

Oppong, E., Cato, A. C. B., 2015, Effects of Glucocorticoids in the Immune System: Springer Science + Business Media New York, Chapter 9, p. 217-233.

Peckett, A., J., Wright, D. C., Riddell, M. C., 2011, The effects of glucocorticoids on adipose tissue lipid metabolism: metabolism clinical and experimental, v. 60, p. 1500-1510.

Pereira, M., Palming, J., Svensson, M., Rizell, M., Dalenbäck, J., Hammar, M., Fall, T., Sidibeh, C., Svensson, P., Eriksson, J., 2014, FKBP5 expression in human adipose tissue increases following dexamethasone exposure and is associated with insulin resistance: Metabolism clinical and experimental, v. 62, p. 1198-1208.

Pereira, R.M, Carvalho, J.F., 2010, Glucocorticoid-induced myopathy: Joint Bone Spine, v.78, p.41-44.

Radin, M., Sharkey, L., Holycross, B., 2009, Adipokines: a review of biological and analytical principles and an update in dogs, cats, and horses: Veteromary Clinical Pathology, v. 38(2), p. 136-156.

Rae,M., Mohamad, A., Price, D., Hadoke, P.W.F., Walker, B. R., Mason, J. I., Hillier, S.G., Critchley, O.D., 2009, Cortisol Inactivation by 11 β- Hydroxysteroid dehydrogenase-2 May Enhance Endometrial Angiogenesis vie Reduced Thrombospondin-1 in Heavy Menstruation: J Clin Endocrinol Metab, v.94(4), p. 1443-1450.

Rahmouni, K., Mark, A.L., Haynes, W.G., Sigmund, C.D., 2004, Adipose depot-specific modulation of angiotensinogen gene expression in diet-induced obesity: Am J Physiol Endocrinol Metab, v.286, p.891–895.

Rebuffe-Scrive, M., Krotkiewski, M., Elfverson, J., Björntorp, P., 1988, Muscle and Adipose Tissue Morphology and Metabolism in Cushing`s Syndrome: J Clin Endocrinol Metab, v.76 (6), p. 1122-1128.

Rehrauer, H., Wu, L., Blum, W., Pecze, L., Henzi, T., Serre-Beinier, S., Aquino, C., Vrugt, B., de Perrot, M., Schwaller, B., Felley-Bosco, E., 2018, How asbestos drives the tissue towards tumors: YAP activation, macrophage and mesothelial precursor recruitment, RNA editing, and somatic mutations: Oncogene, v. 37, p. 2645-2659.

Richelsen, B., Pedersen S.B., Moller-Pedersen, T., Bak, J.F., 1991, Regional differences in triglyceride breakdown in human adipose tissue: effects of catecholamines, insulin, and prostaglandin E2: Metabolism, v. 40, p. 990-996.

Roohk, D. J., Mascharak, S., Khambatta, C., Leung, H., Hellerstein, M., Harris, C., 2013, Dexamethasone-Mediated Changes in Adipose Triaglycerol Metabolism Are Exaggerated, Not Diminished, in the Absence of a Functional GR Dimerization Domain: Endocrinology, v. 154(4), p. 1528-1539.

Rossini, M., Gatti, D., Adami, S., 2013, Involvement of WNT/β-catenin signaling in the treatment of osteoporosis: Calcif Tissue Int, v. 93, p. 121-132.

Schmid, F. D., 2017, Canine Lipoprotein Separation and Characterization of the Canine Lipidome in Healthy and Prednisolone Treated Beagles, Inaugural-Dissertation, Vetsuisse-Fakultät Universität Zürich.

Shinahara, M., Nishiyama, M., Iwasaki, Y., Nakayama, S., Noguchi, T., Kambayashi, M., Okada, Y., Tsuda, M., Stenzel-Poore, M. P., Hashimoto, K., Terada, Y., 2009, Plasma Adiponectin Levels are Increased Despite Insulin Resistance in Corticotropin-releasing Hormone Transgenic Mice, an Animal Model of Cushing Syndrome: Endocrine Journal, v. 56 (7), p. 879-886.

Sieber-Ruckstuhl, N., Burckhardt, W., Hofer-Inteeworn, N., Riond, B., Rast, I., Hofmann-Lehmann, R., Reusch, C., Boretti, F., 2015, Cortisol Response in Healthy and Diseased Dogs after Stimulation with a Depot Formulation of Synthetic ACTH: Journal of Veterinary Internal Medicine, v. 29, p. 1541-1546.

Sieber-Ruckstuhl, N., Burla, B., Spoerel, S., Schmid, F., Venzin, C., Cazenave-Gassiot, A., Bendt, A., Torta, F., Wenk, M., Boretti, F., 2019, Changes in the Canine Plasma Lipidome after Short- and Long-Term Excess Glucocorticoid Exposure: Scientific Reports, v., 9 (6015).

Small, G. R., Hadoke, P. W. F., Sharif, I., Dover, A. R., Armour, D., Kenyon, C. J., Gray, G. A., Walker, B. R., 2005, Preventing local regeneration of glucocorticoids by 11β-hydroxysteroid dehydrogenase type 1 enhances angiogenesis: PNAS, v. 102(34), p. 12165-12170.

Smara, J. S., Clark, M. L., Humphreys, S. M., MacDonald, I. A., Bannister, P. A., Frayn, K. N., 1998, Effects of physiological hypercortisolemia on the regulation of lipolysis in subcutaneous adipose tissue: Journal of Clinical Endocrinology and Metabolism, v. 83 (2)

Spoerel, S., 2017, Characterization of canine plasma lipidome alterations due to prednisolone or tetracosactide treatment of healthy beagle dogs, Inagural-Dissertation, Vetsuisse-Fakultät Universität Zürich.

Sukumaran, S., DuBois, D., Jusko, W., Almon, R., 2012, Glucocorticoid Effects on Adiponectin Expression: Vitam Horm, v. 90, p. 163-186.

Sultan,M., Amstislavskiy,V., Risch, T., Schuette, M., Dökel, S., Ralser, M., Balzereit, D., Lehrach, H., Yaspo, M., 2014, Influence of RNA extraction methods and library selection schemes on RNA-seq data: BMC Genomics, v. 15 (1).

Taguchi, T., Kubota, M., Saito, M., Hattori, H., Kimura, T., Marumo, K., 2016, Change of Collagen of Achilles Tendons in Rats With Systemic Administration of Glucocorticoids: Foot & Ankle International, v.37(3) , p.327-333.

Tomlinson, J.W., Walker, E.A., Bujalska, I.J., Draper, N., Lavery, G.G., Cooper, M.S., Hewison, M., Stewart, P.M., 2004, 11 beta-hydroxysteroid dehydrogenase type 1: A tissue specific regulator of glucocorticoid response: Endocr Rev, v.25, p. 831-866.

Trayhurn, P., Bing, C., Wood, I., 2006, Adipose Tissue and Adipokines-Energy Regulation from the Human Perspective: American Society for Nutrition, v. 136, p. 1935-1939.

Valenzuela, D. M., Griffiths, J. A., Rojas, J., Aldrich, T. H., Jones, P. F., Zhou, H., McClain, J., Copeland, N. G., Gilbert, D. J., Jenkins, N. A., Huang, T., Papadopoulos, N., Maisonpierre, P. C., Davis, S., Yancopoulos, G. D., 1999, Angiopoietins 3 and 4: Diverging gene counterparts in mice and humans: Proc. Natl. Acad. Sci., v. 96, p. 1904-1909.

Volpe, J. J., Marasa, J. C., 1975, Hormonal Regulation of fatty acid synthetase, acetyl coa carboxylase and fatty acid synthesis in mammalian adipose tissue and liver: Biochemica et Biophysica Acta, v. 380, p. 454-472.

Wang, J., Gray, N.E., Kuo,T., Harris, C.A., 2012, Regulation of triglyceride metabolism by glucocorticoid receptor: Cell & Bioscience, v. 2(19)

Yano, A., Yasuhisa, F., Iwai, A., Kageyama, Y., Kihara, K., 2006: Glucocorticoids Suppress Tumor Angiogenesis and In vivo Growth of Prostate Cancer Cells: Clin Cancer Res, v. 12(10), p. 3003-3009.

Zatta, S., Rehrauer, H., Gram, A., Boos, A., Kowalewski, M., 2017, Transcriptome analysis reveals differences in mechanisms regulation cessation of luteal function in pregnant and non-pregnant dogs: BMC Genomics, v. 18 (757).

Zhou, M., Wu, J., Yu, Y., Yang, Y., Jin, L., Cui, L., Yao, W., Yuyu, L., 2017, Polygonum multiflorm alleviates glucocorticoid-induced osteoporosis and Wnt signaling pathway: Molecular Medicine Reports, v. 17, p.970-978.

Zhou, X., Liao, W., Liao, J., Liao, P., Lu, H., 2015, Ribosomal proteins: functions beyond the ribosome: Journal of Molecular Cell Biology, v. 7(2), p. 92-104.

Xu, H., Barnes, G., Yang, D., Chou, C., Sole, J., Nichols, A., Ross, J., Tartaglia L., Chen, H., 2003, Chronic Inflammation in fat plays a crucial role in the development of obesity- related insulin resistance: Journal of Clinical Investigation, v. 112(12), p. 1821-1830.

Supplements

Gene name	Description	pValue	fdr	log2 Ratio
ABCA1	ATP binding cassette subfamily A member 1	3.90E-08	0.000001664	0.7463
ABCA13	ATP binding cassette subfamily A member 13	7.59E-09	3.98E-07	-2.486
ABCC8	ATP binding cassette subfamily C member 8	1.76E-07	0.000006379	3.124
ABLIM1	actin binding LIM protein 1	8.82E-08	0.000003401	-0.788
ACER2	alkaline ceramidase 2	1.12E-07	0.000004211	0.4895
ACKR3	Atypical chemokine receptor 3	0.000002849	0.0000779	-0.8653
ACP6	acid phosphatase 6, lysophosphatidic	1.20E-08	5.84E-07	0.8675
ACPP	acid phosphatase, prostate	0.000001032	0.00003142	-1.385
ACSL4	acyl-CoA synthetase long-chain family member 4	0.000002287	0.00006407	0.5858
ADAM12	ADAM metallopeptidase domain 12	0.000001819	0.00005235	-1.29
ADAM22	ADAM metallopeptidase domain 22	2.15E-07	0.000007688	-1.517
ADAMTS16	ADAM metallopeptidase with thrombospondin type 1 motif 16	9.35E-07	0.00002883	-1.976
ADAMTS18	ADAM metallopeptidase with thrombospondin type 1 motif 18	1.21E-11	1.44E-09	-1.509
ADCY2	adenylate cyclase 2	4.60E-08	0.000001923	-1.31
ADCYAP1R1	ADCYAP receptor type I	1.55E-16	4.44E-14	-2.588
ADD3	adducin 3	4.99E-11	5.06E-09	-0.728
ADGRG4	adhesion G protein-coupled receptor G4	6.53E-12	8.30E-10	-2.319
ADGRL3	adhesion G protein-coupled receptor L3	4.54E-08	0.000001908	-1.513
ADM	adrenomedullin	0.000004541	0.0001151	-0.8966
AEBP1	AE binding protein 1	2.17E-14	4.41E-12	-1.471
AGPS	alkylglycerone phosphate synthase	0.00000005	0.000002082	0.7103
AGRN	agrin	1.46E-11	1.70E-09	-1.111
AGT	angiotensinogen	3.09E-35	1.94E-31	-2.432
AHCTF1	AT-hook containing transcription factor 1	1.87E-07	0.000006746	0.5383
AHCY	adenosylhomocysteinase	1.34E-09	8.73E-08	0.77
ALDH1A1	retinal dehydrogenase 1	3.99E-23	2.64E-20	-2.15

ALDH1A3	aldehyde dehydrogenase 1 family member A3	1.46E-07	0.000005448	-1.597
ALPL	alkaline phosphatase, liver/bone/kidney	0.000003794	0.0000992	1.315
AMOT	angiomotin	1.78E-09	1.10E-07	-1.454
ANGPT4	angiopoietin 4	3.33E-34	1.05E-30	2.71
ANGPTL1	angiopoietin like 1	1.61E-15	3.75E-13	-1.806
ANKRD16	ankyrin repeat domain 16	9.07E-08	0.000003479	-0.7247
ANKRD29	ankyrin repeat domain 29	2.45E-08	0.000001116	-0.9134
ANKRD9	ankyrin repeat domain 9	1.49E-12	2.10E-10	1.301
ANTXR1	anthrax toxin receptor 1	1.00E-08	5.01E-07	-1.08
APEX2	apurinic/apyrimidinic endodeoxyribonuclease 2	1.14E-16	3.34E-14	1.851
APLNR	apelin receptor	2.35E-12	3.20E-10	-2.967
APOD	apolipoprotein D	1.87E-09	1.15E-07	-2.014
APOE	apolipoprotein E	1.35E-09	8.74E-08	-1.364
ARHGAP10	Rho GTPase activating protein 10	3.08E-08	0.000001353	1.057
ARHGAP20	Rho GTPase activating protein 20	7.52E-07	0.00002358	-0.9981
ARHGAP28	Rho GTPase activating protein 28	1.11E-09	7.29E-08	-1.201
ARHGEF4	Rho guanine nucleotide exchange factor 4	2.12E-11	2.36E-09	-1.692
arsb	arylsulfatase B	4.23E-07	0.00001411	-0.8865
ARSD	arylsulfatase D	0.000009528	0.0002191	-0.8681
ATP5D	ATP synthase, H+ transporting, mitochondrial F1 complex, delta subunit	0.000003	0.00008149	0.5918
ATP9A	ATPase phospholipid transporting 9A (putative)	2.63E-08	0.000001193	-0.8091
BAMBI	BMP and activin membrane bound inhibitor	9.92E-33	2.08E-29	2.701
BCAR3	breast cancer anti-estrogen resistance 3	9.37E-09	4.81E-07	-0.7901
BCL6	B-cell CLL/lymphoma 6	0.000001445	0.00004305	-0.7911
BHMT2	betaine--homocysteine S-methyltransferase 2	1.16E-08	5.68E-07	-1.915
BNIP3	BCL2/adenovirus E1B 19kDa interacting protein 3	0.000004777	0.0001199	0.7745
BSND	barttin CLCNK type accessory beta subunit	0.00000752	0.0001764	-1.904
BSPRY	B-box and SPRY domain containing	6.96E-07	0.00002205	1.848
C10orf107	chromosome 10 open reading frame 107	1.11E-12	1.63E-10	-1.188

C1orf162	chromosome 1 open reading frame 162	3.03E-08	0.000001336	1.744
C1S	complement C1s	0.000003808	0.00009935	-1.061
C9orf72	chromosome 9 open reading frame 72	4.59E-11	4.73E-09	1.251
CA13	carbonic anhydrase 13	2.84E-18	1.05E-15	-1.227
CACNA1A	calcium voltage-gated channel subunit alpha1 A	0.0000032	0.00008617	-1.076
CALML4	calmodulin like 4	0.000001658	0.00004836	-0.9792
CAPN11	calpain 11	1.93E-18	7.37E-16	-2.668
CCDC180	coiled-coil domain containing 180	9.85E-09	4.96E-07	-1.026
CCDC3	coiled-coil domain containing 3	8.66E-09	4.46E-07	-1.433
CCND2	cyclin D2	0.000008251	0.0001922	-0.9888
CCR2	C-C motif chemokine receptor 2	2.73E-08	0.000001229	-3.665
CD1B	T-cell surface glycoprotein CD1b precursor	1.33E-07	0.000004947	-6.369
CD1D	CD1d molecule	1.66E-17	5.50E-15	-3.116
CD200	CD200 molecule	2.30E-08	0.000001053	-1.248
CD74	CD74 molecule	3.01E-08	0.000001336	-1.397
CD83	CD83 molecule	2.24E-07	0.000007973	-1.512
CD93	CD93 molecule	1.50E-08	7.14E-07	-1.254
CDC42BPA	CDC42 binding protein kinase alpha	6.95E-07	0.00002205	-0.5907
CDK6	cyclin dependent kinase 6	5.29E-08	0.000002189	-1.234
CDKN2B	cyclin dependent kinase inhibitor 2B	0.000000328	0.00001127	1.683
CES2	carboxylesterase 2	1.12E-11	1.35E-09	-1.06
CFP	complement factor properdin	1.82E-11	2.08E-09	-2.372
CHAC1	ChaC glutathione specific gamma-glutamylcyclotransferase 1	0.000003241	0.00008709	3.503
CHD1L	chromodomain helicase DNA binding protein 1 like	0.000001094	0.00003316	0.7898
CHERP	calcium homeostasis endoplasmic reticulum protein	7.08E-10	5.00E-08	1.038
CHRDL1	chordin like 1	5.60E-07	0.00001819	-0.6517
CILP	cartilage intermediate layer protein	1.02E-19	4.59E-17	-3.432
CKB	Creatine kinase B-type	2.12E-10	1.77E-08	0.9652
CKM	creatine kinase M-type	9.94E-52	1.25E-47	3.605

CLDN15	claudin 15	0.000003865	0.0001002	1.1
CLEC4G	C-type lectin domain family 4 member G	4.52E-16	1.18E-13	2.265
CLIC1		0.000009687	0.0002214	-0.5425
CLVS2	clavesin 2	7.14E-28	8.17E-25	2.578
CNST	consortin, connexin sorting protein	3.45E-07	0.00001181	0.7945
COBLL1	cordon-bleu WH2 repeat protein like 1	3.73E-07	0.00001272	-0.5858
COL12A1	collagen type XII alpha 1 chain	0.000008194	0.0001912	1.932
COL14A1	collagen type XIV alpha 1 chain	5.39E-34	1.36E-30	-2.201
COL1A1	collagen alpha-1(I) chain precursor	4.67E-13	7.93E-11	-1.73
COL1A2	collagen type I alpha 2 chain	1.07E-23	7.46E-21	-1.69
COL23A1	collagen type XXIII alpha 1 chain	1.11E-10	9.95E-09	-1.258
COL3A1	collagen type III alpha 1 chain	3.38E-25	2.83E-22	-2.375
COL4A5	collagen type IV alpha 5 chain	9.06E-10	6.06E-08	-1.03
COL6A1	collagen type VI alpha 1 chain	8.40E-10	5.84E-08	-1.049
COL6A3	collagen type VI alpha 3 chain	2.16E-15	4.76E-13	-1.763
COPZ2	coatomer protein complex subunit zeta 2	8.46E-09	4.38E-07	-0.8158
COTL1	coactosin like F-actin binding protein 1	7.53E-09	3.96E-07	-1.068
CPA3	carboxypeptidase A3	0.000002572	0.0000711	-5.257
CPNE7	copine 7	1.37E-08	6.54E-07	0.6777
CPXM1	carboxypeptidase X, M14 family member 1	7.98E-13	1.24E-10	-6.414
CPXM2	carboxypeptidase X, M14 family member 2	0.000007724	0.0001809	-1.036
CXCL12	C-X-C motif chemokine ligand 12	1.98E-29	2.77E-26	-1.937
CXCL14	C-X-C motif chemokine ligand 14	5.09E-09	2.78E-07	1.431
CYGB	cytoglobin	0.000008461	0.0001956	0.7376
CYP27A1	cytochrome P450 family 27 subfamily A member 1	3.95E-10	3.07E-08	1.245
CYTB	Cytochrome b	0.000000011	5.47E-07	0.8792
CYYR1	cysteine and tyrosine rich 1	4.87E-09	2.68E-07	1.066
DCLK2	doublecortin like kinase 2	1.24E-11	1.46E-09	-0.9987
DCN	Decorin	5.76E-11	5.66E-09	-1.238
DDAH2	dimethylarginine dimethylaminohydrolase 2	5.82E-21	3.18E-18	-1.362

DGAT1	diacylglycerol O-acyltransferase 1	4.68E-14	8.92E-12	0.995
DLA DRA	major histocompatibility complex, class II, DR alpha	9.28E-10	6.18E-08	-1.752
DLA-DMB		0.000001362	0.00004078	-1.561
DLA-DQA1	major histocompatibility complex, class II, DQ alpha precursor	0.000002014	0.00005755	-2.615
DLA-DQB1	major histocompatibility complex, class II, DQ beta 1 precursor	1.20E-10	1.06E-08	-2.496
DMGDH	dimethylglycine dehydrogenase	2.62E-09	1.58E-07	-2.991
DMPK	dystrophia myotonica protein kinase	6.37E-07	0.00002043	-1.052
DNAH10	dynein axonemal heavy chain 10	7.65E-09	3.99E-07	-1.18
DNAJA4	DnaJ heat shock protein family (Hsp40) member A4	2.15E-08	9.90E-07	1.755
DOCK10	dedicator of cytokinesis 10	6.27E-09	3.34E-07	-1.56
DOCK2	dedicator of cytokinesis 2	6.63E-08	0.000002661	-1.105
DOCK4	dedicator of cytokinesis 4	9.43E-07	0.00002891	-0.699
DPYSL3	dihydropyrimidinase like 3	7.72E-16	1.87E-13	-0.9505
DSEL	dermatan sulfate epimerase-like	5.34E-13	8.73E-11	-2.005
DST	dystonin	1.22E-10	1.07E-08	-0.6758
EBF2	early B-cell factor 2	0.000005438	0.0001336	-0.6815
ECE1	endothelin converting enzyme 1	1.29E-08	6.21E-07	1.011
ECM2	extracellular matrix protein 2	1.50E-31	2.35E-28	-2.056
EDEM1	ER degradation enhancing alpha-mannosidase like protein 1	0.000006574	0.0001569	0.6021
EIF4A1	eukaryotic initiation factor 4A-I	3.07E-07	0.00001063	0.6333
EIF4EBP1	eukaryotic translation initiation factor 4E binding protein 1	8.91E-10	6.02E-08	1.117
EML5	echinoderm microtubule associated protein like 5	6.18E-09	3.31E-07	0.7734
ENDOU	endonuclease, poly(U) specific	3.19E-08	0.000001396	0.956
ENPEP	glutamyl aminopeptidase	3.65E-12	4.69E-10	-1.083
ENPP2	ectonucleotide pyrophosphatase/phosphodiesterase 2	7.31E-12	9.10E-10	-0.9309
EPB41L3	erythrocyte membrane protein band 4.1 like 3	4.75E-07	0.00001567	-1.108
EPN2	epsin 2	6.16E-08	0.000002507	0.6389

ERGIC1	endoplasmic reticulum-golgi intermediate compartment 1	6.38E-08	0.000002572	0.8467
F2R	coagulation factor II thrombin receptor	0.000003928	0.0001014	-0.6007
FAM105A	family with sequence similarity 105 member A	1.41E-10	1.21E-08	1.006
FAM129A	family with sequence similarity 129 member A	4.83E-10	3.62E-08	-0.9226
FAM13C	family with sequence similarity 13 member C	5.64E-08	0.00000232	-1.235
FAM149A	family with sequence similarity 149 member A	0.000002804	0.000077	-0.6544
FAM198B	family with sequence similarity 198 member B	1.03E-13	1.90E-11	-1.076
FAP	fibroblast activation protein alpha	7.32E-09	3.87E-07	-1.388
FAU	FAU, ubiquitin like and ribosomal protein S30 fusion	1.23E-07	0.000004607	0.5088
FBLN5	fibulin 5	7.83E-09	0.000000407	-1.11
FBLN7	fibulin 7	1.87E-13	3.31E-11	-2.285
FGD2	FYVE, RhoGEF and PH domain containing 2	1.84E-08	8.59E-07	-1.271
FGF1	fibroblast growth factor 1	2.64E-09	1.58E-07	-1.226
FGFBP1	fibroblast growth factor binding protein 1	1.60E-08	7.58E-07	-2.215
FIBIN	fin bud initiation factor homolog (zebrafish)	8.12E-18	2.76E-15	2.581
FKBP5	FK506 binding protein 5	1.80E-20	9.07E-18	2.216
FMOD	fibromodulin	5.03E-08	0.000002086	-3.057
FN1	fibronectin 1	0.000003465	0.00009214	-2.017
FNDC1	fibronectin type III domain containing 1	4.11E-07	0.00001381	-1.488
FOS	Fos proto-oncogene, AP-1 transcription factor subunit	2.13E-08	9.87E-07	1.733
FSCN1	fascin actin-bundling protein 1	0.000002179	0.00006173	-1.046
FSD2	fibronectin type III and SPRY domain containing 2	9.11E-07	0.00002815	1.266
FTH1	Ferritin heavy chain Ferritin heavy chain, N-terminally processed	3.96E-07	0.00001337	0.8587
GALNT12	polypeptide N-acetylgalactosaminyltransferase 12	0.000009579	0.0002198	-0.747
GALNT13	polypeptide N-acetylgalactosaminyltransferase 13	1.60E-09	1.00E-07	-1.884
GALNT16	polypeptide N-acetylgalactosaminyltransferase 16	3.78E-17	1.16E-14	-1.798
GALNT2	polypeptide N-acetylgalactosaminyltransferase 2	5.88E-18	2.05E-15	1.066
GCAT	glycine C-acetyltransferase	9.07E-08	0.000003479	1.102
GDI2	rab GDP dissociation inhibitor beta	1.62E-07	0.000005951	0.6573

GEM	GTP binding protein overexpressed in skeletal muscle	3.80E-08	0.000001629	1.232
GGH	gamma-glutamyl hydrolase	0.000001453	0.0000431	0.779
GLIPR2	GLI pathogenesis related 2	9.45E-09	0.000000483	1.014
GLRB	glycine receptor beta	1.61E-09	1.01E-07	-0.8137
GLUL	Glutamine synthetase	8.46E-13	1.28E-10	1.251
GOLM1	golgi membrane protein 1	0.000004891	0.0001218	-0.8258
GPC3	glypican 3	0.000002965	0.00008087	-0.7416
GPLD1	glycosylphosphatidylinositol specific phospholipase D1	0.00000529	0.0001302	-1.551
GPX3	glutathione peroxidase 3 precursor	7.18E-07	0.00002262	3.748
GRIA4	glutamate ionotropic receptor AMPA type subunit 4	0.000001782	0.00005141	0.7303
GRTP1	growth hormone regulated TBC protein 1	1.12E-08	5.53E-07	3.305
GSN	gelsolin	9.37E-12	1.16E-09	-1.108
GSTM3	glutathione S-transferase mu 3	1.11E-19	4.80E-17	1.843
GSTM4	glutathione S-transferase mu 4	1.24E-14	2.56E-12	1.537
GULP1	GULP, engulfment adaptor PTB domain containing 1	2.26E-10	1.87E-08	-0.8709
GUSB	glucuronidase beta	8.55E-08	0.00000332	0.7102
GXYLT2	glucoside xylosyltransferase 2	4.12E-09	2.32E-07	-0.9898
HDAC9	histone deacetylase 9	3.07E-09	1.80E-07	-0.9384
HERPUD1	homocysteine inducible ER protein with ubiquitin like domain 1	0.000001448	0.00004305	0.732
HHIP	hedgehog interacting protein	3.57E-12	4.68E-10	-3.106
HLA-DRB1	DLA class II histocompatibility antigen, DR-1 beta chain precursor	2.97E-08	0.000001324	-1.549
HMCN1	hemicentin 1	1.06E-12	1.57E-10	-1.401
HMCN2	hemicentin 2	8.24E-10	5.76E-08	-2.966
HMGCS2	3-hydroxy-3-methylglutaryl-CoA synthase 2	2.34E-07	0.000008271	2.364
HPCAL1	hippocalcin like 1	1.87E-13	3.31E-11	1.1
HPGD	15-hydroxyprostaglandin dehydrogenase	7.74E-07	0.0000242	1.801
HPN	hepsin	0.000001757	0.00005079	1.216
HTRA1	HtrA serine peptidase 1	0.000002273	0.00006396	-0.5703
HTRA3	HtrA serine peptidase 3	6.33E-07	0.00002035	0.9472

HYKK	hydroxylysine kinase	0.000006065	0.0001467	-0.7308
ICOS	Inducible T-cell costimulator	7.24E-08	0.000002844	-2.035
IDH2	isocitrate dehydrogenase (NADP(+)) 2, mitochondrial	8.51E-10	5.85E-08	0.9752
IFT122	intraflagellar transport 122	6.31E-08	0.000002553	-0.7497
IGFBP2	insulin like growth factor binding protein 2	4.82E-10	3.62E-08	6.037
IGFBP3	insulin like growth factor binding protein 3	3.96E-25	3.11E-22	1.815
IGFBP7	insulin like growth factor binding protein 7	0.000004028	0.0001036	-0.8091
IL1RL1	interleukin 1 receptor like 1	0.000002226	0.00006278	3.39
IL27RA	interleukin 27 receptor subunit alpha	6.88E-07	0.00002201	-0.9691
IL33	interleukin 33	2.42E-20	1.17E-17	-1.815
IMPDH2	inosine monophosphate dehydrogenase 2	3.53E-12	4.67E-10	0.795
IQGAP2	IQ motif containing GTPase activating protein 2	6.88E-11	6.61E-09	-1.214
IRF8	interferon regulatory factor 8	3.84E-08	0.000001642	-0.9994
IRS1	insulin receptor substrate 1	1.19E-07	0.00000446	0.6729
IRS2	insulin receptor substrate 2	5.92E-09	3.18E-07	1.21
IRX2	iroquois homeobox 2	5.90E-11	5.75E-09	2.653
ITGA11	integrin subunit alpha 11	8.10E-15	1.73E-12	-2.492
ITGA2	integrin subunit alpha 2	5.51E-11	5.50E-09	-2.295
ITGAL	integrin subunit alpha L	0.0000025	0.00006924	-1.724
ITGAX	integrin subunit alpha X	1.99E-10	1.67E-08	-2.32
ITGBL1	integrin subunit beta like 1	8.68E-11	8.15E-09	-1.74
ITIH1	inter-alpha-trypsin inhibitor heavy chain 1	0.000005852	0.0001421	3.091
ITIH3	inter-alpha-trypsin inhibitor heavy chain 3	2.91E-17	9.37E-15	1.689
ITIH4	inter-alpha-trypsin inhibitor heavy chain family member 4	1.88E-11	2.13E-09	2.404
ITPR1	inositol 1,4,5-trisphosphate receptor type 1	2.76E-08	0.00000124	-0.6792
IZUMO1R	IZUMO1 receptor, JUNO	1.99E-09	1.21E-07	-3.474
KAT2B	lysine acetyltransferase 2B	6.07E-10	4.39E-08	-0.7178
KCNK5	potassium two pore domain channel subfamily K member 5	2.41E-07	0.000008475	1.345
KCNQ5	potassium voltage-gated channel subfamily Q member	7.90E-11	7.52E-09	1.461

	5			
KCP	kielin/chordin-like protein	0.000004823	0.0001206	-1.579
KERA	keratocan	0.000001026	0.00003132	-2.013
KIF26B	kinesin family member 26B	8.29E-08	0.000003237	1.565
KITLG	Kit ligand Soluble KIT ligand Processed kit ligand	3.45E-09	2.00E-07	-1.394
KLHL25	Kelch-like family member 25	4.14E-10	3.19E-08	1.001
LAMA3	laminin subunit alpha 3	3.27E-13	5.64E-11	-1.206
LAMA4	laminin subunit alpha 4	2.86E-07	0.00001005	-0.5521
LAMB2	laminin subunit beta 2	3.60E-07	0.00001231	-0.7196
LAMC3	laminin subunit gamma 3	3.54E-09	2.04E-07	-0.9972
LBH	limb bud and heart development	3.45E-17	1.08E-14	-2.218
LCP1	lymphocyte cytosolic protein 1	1.64E-09	1.02E-07	-1.27
LDLRAD3	low density lipoprotein receptor class A domain containing 3	0.000006381	0.0001531	0.5734
LIMCH1	LIM and calponin homology domains 1	0.000003725	0.0000976	0.9873
LIPE	lipase E, hormone sensitive type	0.000005841	0.0001421	0.4694
LMO4	LIM domain only 4	5.53E-10	4.09E-08	-0.7453
LONP2	lon peptidase 2, peroxisomal	0.000008395	0.000195	-0.4814
LOXL2	lysyl oxidase like 2	1.98E-09	1.21E-07	-1.202
LPGAT1	lysophosphatidylglycerol acyltransferase 1	2.71E-10	2.18E-08	0.6797
LRAT	lecithin retinol acyltransferase (phosphatidylcholine-retinol O-acyltransferase)	3.04E-10	2.44E-08	-5.88
LRMP	lymphoid restricted membrane protein	1.39E-09	8.98E-08	-2.426
LRRC4	leucine rich repeat containing 4	0.000005262	0.00013	-1.982
LSAMP	limbic system-associated membrane protein	1.99E-11	2.23E-09	-6.583
LSP1	lymphocyte-specific protein 1	0.00000126	0.00003808	-0.7755
LTBP1	latent transforming growth factor beta binding protein 1	1.01E-14	2.11E-12	-1.292
LTBP4	latent transforming growth factor beta binding protein 4	0.000001084	0.00003293	-1.069
LUM	lumican	1.75E-26	1.69E-23	-1.493

LVRN	laeverin	6.21E-10	4.46E-08	-0.8084
LYZ	lysozyme precursor	0.000001752	0.00005078	-0.8953
MANBA	mannosidase beta	2.85E-09	1.68E-07	-0.8564
MAP1B	microtubule associated protein 1B	2.01E-15	4.52E-13	-1.345
MAP3K15	mitogen-activated protein kinase kinase kinase 15	0.000004759	0.0001197	-0.775
MAP3K5	mitogen-activated protein kinase kinase kinase 5	1.24E-08	5.98E-07	0.8002
MAPK13	mitogen-activated protein kinase 13	0.00000652	0.0001559	0.7695
MATK	megakaryocyte-associated tyrosine kinase	1.18E-10	1.05E-08	-1.977
MDFIC	MyoD family inhibitor domain containing	4.13E-08	0.000001755	-0.9375
ME3	malic enzyme 3	0.000004024	0.0001036	-1.11
MEST	mesoderm specific transcript	3.82E-09	2.18E-07	-2.312
MET	MET proto-oncogene, receptor tyrosine kinase	1.19E-08	0.000000582	-0.7348
METTL7A	methyltransferase like 7A	5.13E-13	8.49E-11	1.158
MFAP4	microfibrillar associated protein 4	4.22E-14	8.29E-12	-2.963
MFSD4A	major facilitator superfamily domain containing 4A	6.46E-09	0.000000343	-1.858
MICAL3	microtubule associated monooxygenase, calponin and LIM domain containing 3	8.31E-08	0.000003237	0.6959
MMP2	matrix metallopeptidase 2	1.78E-07	0.000006426	-1.152
MRC2	mannose receptor C type 2	2.38E-07	0.00000842	-1.258
MRPL37	mitochondrial ribosomal protein L37	0.000005271	0.00013	0.6833
MSX1	msh homeobox 1	4.36E-09	2.43E-07	1.081
MT3	metallothionein 3	4.09E-09	2.32E-07	4.038
MT-ND4	NADH-ubiquinone oxidoreductase chain 4	0.000001275	0.00003845	0.7757
MXRA5	matrix remodeling associated 5	4.29E-18	1.54E-15	-2.164
MXRA8	matrix remodeling associated 8	0.000007442	0.0001756	-1.273
MYLK	myosin light chain kinase	9.51E-09	0.000000484	0.7402
MYO5B	myosin VB	6.91E-10	4.94E-08	-0.7996
NAP1L1	nucleosome assembly protein 1 like 1	1.17E-08	5.72E-07	0.5725
NAV3	neuron navigator 3	2.92E-07	0.00001023	-1.074
NCLN	Nicalin isoform 1	5.74E-08	0.000002345	0.6722

NCOR1	nuclear receptor corepressor 1	0.000004179	0.0001068	0.4728
ND4L	NADH-ubiquinone oxidoreductase chain 4L	2.93E-07	0.00001023	0.8423
NDUFB7	NADH:ubiquinone oxidoreductase subunit B7	1.05E-08	5.22E-07	0.7
NEDD4	neural precursor cell expressed, developmentally down-regulated 4, E3 ubiquitin protein ligase	0.000005905	0.0001431	-0.5765
NET1	neuroepithelial cell transforming 1	3.42E-19	1.39E-16	0.9427
NLRP3	NLR family pyrin domain containing 3	5.67E-11	5.62E-09	-2.113
NOD1	nucleotide binding oligomerization domain containing 1	0.000001341	0.00004025	0.866
NOV	nephroblastoma overexpressed	2.42E-08	0.000001107	-1.486
NPR3	natriuretic peptide receptor 3	0.000001679	0.00004888	-1.112
NT5E	5'-nucleotidase ecto	1.81E-10	1.53E-08	-1.605
NTRK2	neurotrophic receptor tyrosine kinase 2	0.000007952	0.0001859	0.5062
NTRK3	neurotrophic receptor tyrosine kinase 3	2.37E-12	3.20E-10	1.149
NUP210	nucleoporin 210	1.76E-12	2.43E-10	-1.718
NYNRIN	NYN domain and retroviral integrase containing	0.000001549	0.00004541	-0.5442
OAF	out at first homolog	0.000000063	0.000002553	-0.9811
OAS1	2'-5'-oligoadenylate synthetase 1	0.00000977	0.0002226	-1.278
OAS2	2'-5'-oligoadenylate synthetase 2	0.000002094	0.00005945	-1.215
OGFRL1	opioid growth factor receptor like 1	1.55E-09	9.80E-08	-1.009
OGN	osteoglycin	1.07E-11	1.30E-09	-1.525
OLFML1	olfactomedin like 1	8.46E-10	5.84E-08	-1.41
OLFML2A	olfactomedin like 2A	1.07E-16	3.20E-14	-1.85
OLFML3	olfactomedin like 3	3.44E-09	2.00E-07	-1.17
OSMR	oncostatin M receptor	3.32E-12	4.44E-10	1.08
PABPC1	poly(A) binding protein cytoplasmic 1	0.00000331	0.00008875	0.4472
PABPC4	poly(A) binding protein cytoplasmic 4	0.000004854	0.0001211	0.5456
PACSIN1	protein kinase C and casein kinase substrate in neurons 1	0.000006928	0.000165	-1.014
PACSIN3	protein kinase C and casein kinase substrate in neurons 3	0.00001023	0.0002313	0.6319

PAM	peptidylglycine alpha-amidating monooxygenase	0.000001418	0.00004236	-0.671
PCBD1	pterin-4 alpha-carbinolamine dehydratase 1	8.87E-07	0.00002755	-0.6972
PCDH12	protocadherin 12	3.86E-07	0.00001307	-1.815
PCDH18	protocadherin 18	1.76E-13	3.20E-11	-1.307
PCOLCE	procollagen C-endopeptidase enhancer	4.06E-29	5.11E-26	-2.277
PCSK1	proprotein convertase subtilisin/kexin type 1	0.000001732	0.00005032	-1.391
PDE1A	phosphodiesterase 1A	1.51E-08	7.17E-07	0.753
PDGFRB	platelet derived growth factor receptor beta	2.27E-14	4.54E-12	-0.7512
PDGFRL	platelet derived growth factor receptor like	4.69E-07	0.00001555	-1.384
PDP1	pyruvate dehyrogenase phosphatase catalytic subunit 1	3.84E-16	1.03E-13	0.9285
PDXK	pyridoxal kinase	4.55E-11	4.73E-09	1.088
PEBP1	phosphatidylethanolamine binding protein 1	0.000004716	0.0001189	-0.7566
PELI2	pellino E3 ubiquitin protein ligase family member 2	5.53E-23	3.48E-20	1.805
PER3	period circadian clock 3	3.45E-08	0.000001495	-0.7243
PGLS	6-phosphogluconolactonase	2.14E-08	9.90E-07	0.6988
PHF5A	PHD finger protein 5A	0.000002215	0.00006261	0.5615
PI16	peptidase inhibitor 16	1.72E-32	3.08E-29	-3.345
PI3	elafin precursor	1.40E-34	5.88E-31	3.713
PICALM	phosphatidylinositol binding clathrin assembly protein	1.14E-07	0.000004309	0.8287
PIK3AP1	phosphoinositide-3-kinase adaptor protein 1	2.95E-08	0.000001321	-1.895
PKD1	polycystin-1 precursor	0.000002358	0.00006547	0.6829
PLAU	plasminogen activator, urokinase	6.89E-11	6.61E-09	-1.293
PLCB2	phospholipase C beta 2	8.65E-10	5.91E-08	-1.302
PLCD4	phospholipase C delta 4	3.69E-27	3.87E-24	2.115
PLCG2	phospholipase C gamma 2	0.000000902	0.00002794	-0.9054
PLEKHG3	pleckstrin homology and RhoGEF domain containing G3	0.000006988	0.0001661	0.6957
PLEKHG5	pleckstrin homology and RhoGEF domain containing G5	0.000004148	0.0001063	-0.8153
PLEKHS1	pleckstrin homology domain containing S1	5.80E-10	4.22E-08	2.948

PLXDC1	plexin domain containing 1	1.94E-15	4.43E-13	-1.639
PM20D2	peptidase M20 domain containing 2	7.85E-10	5.52E-08	1.001
PNKD	paroxysmal nonkinesigenic dyskinesia	2.81E-09	1.67E-07	1.071
POSTN	periostin	4.70E-10	3.56E-08	2.632
PPBP	platelet basic protein precursor	2.65E-08	0.000001199	2.185
PPM1K	protein phosphatase, Mg2+/Mn2+ dependent 1K	0.000005806	0.0001415	-0.6968
PPP1R12B	protein phosphatase 1 regulatory subunit 12B	0.000003913	0.0001013	0.5673
PPP1R15A	protein phosphatase 1 regulatory subunit 15A	0.00000571	0.0001394	0.6682
PPP2R1B	protein phosphatase 2 scaffold subunit Abeta	6.53E-16	1.61E-13	0.8427
PPP2R5A	protein phosphatase 2 regulatory subunit B'alpha	1.22E-09	7.99E-08	-0.9215
PRELP	proline and arginine rich end leucine rich repeat protein	4.25E-10	3.26E-08	-1.001
PREX2	phosphatidylinositol-3,4,5-trisphosphate dependent Rac exchange factor 2	1.22E-08	5.89E-07	-0.892
PRICKLE2	prickle planar cell polarity protein 2	9.26E-11	8.63E-09	-1.399
PRLR	prolactin receptor	4.90E-14	9.19E-12	1.648
PROM1	prominin 1	9.42E-07	0.00002891	-1.452
PRRX1	paired related homeobox 1	5.92E-09	3.18E-07	-1.283
PRSS35	protease, serine 35	4.93E-07	0.00001618	-2.331
PSAT1	phosphoserine aminotransferase 1	4.21E-07	0.00001407	0.9217
PTGDS	Prostaglandin-H2 D-isomerase	0.000009074	0.0002094	-2.1
PTP4A3	protein tyrosine phosphatase type IVA, member 3	4.84E-07	0.00001592	2.204
PTPN13	protein tyrosine phosphatase, non-receptor type 13	0.000004473	0.0001137	-0.6627
PTPRC	protein tyrosine phosphatase, receptor type C	0.000002832	0.0000776	-1.104
PTPRF	protein tyrosine phosphatase, receptor type F	0.000006287	0.0001515	0.6732
PTPRM	protein tyrosine phosphatase, receptor type M	0.000001617	0.0000473	-0.8007
PXDNL	peroxidasin like	7.44E-07	0.00002338	-1.163
PYGL	glycogen phosphorylase, liver form	3.63E-12	4.69E-10	-0.7411
RAC2	ras-related C3 botulinum toxin substrate 2 (rho family, small GTP binding protein Rac2)	0.000003076	0.00008337	-2.025
RACK1	receptor for activated C kinase 1	9.69E-09	4.92E-07	0.5651

RAN	GTP-binding nuclear protein Ran	0.000001958	0.00005621	0.5512
RAPH1	Ras association (RalGDS/AF-6) and pleckstrin homology domains 1	9.96E-11	9.14E-09	-0.8435
RASA2	RAS p21 protein activator 2	1.56E-10	1.32E-08	1.054
RASSF8	Ras association domain family member 8	0.000007368	0.0001742	-0.7341
RCAN2	regulator of calcineurin 2	8.28E-08	0.000003237	-1.346
REEP1	receptor accessory protein 1	5.60E-08	0.000002307	-1.375
REM1	RRAD and GEM like GTPase 1	4.40E-09	2.44E-07	-1.182
RETSAT	retinol saturase	3.23E-08	0.000001411	0.804
RFTN1	raftlin, lipid raft linker 1	1.71E-08	8.02E-07	0.6951
RGS6	regulator of G protein signaling 6	3.29E-09	1.92E-07	-1.898
RNF144B	ring finger protein 144B	9.66E-11	8.93E-09	1.091
RNF213	ring finger protein 213	6.83E-08	0.000002711	-0.7232
RPL10A	ribosomal protein L10a	8.21E-07	0.00002561	0.5786
RPL18	Ribosomal protein L18	3.58E-10	2.81E-08	0.647
RPL19	60S ribosomal protein L19	1.74E-07	0.000006326	0.4998
RPL22L1	ribosomal protein L22 like 1	0.000003853	0.0001001	0.8983
RPL23		0.000003719	0.0000976	0.6146
RPL28	ribosomal protein L28	0.000001291	0.00003883	0.4749
RPL3	60S ribosomal protein L3	3.13E-11	3.39E-09	0.7263
RPL32	60S ribosomal protein L32	6.70E-08	0.000002665	0.5977
RPL35	ribosomal protein L35	0.000002699	0.00007426	0.498
RPL7A	60S ribosomal protein L7a	1.57E-07	0.00000577	0.5134
RPL8	ribosomal protein L8	1.53E-09	9.79E-08	0.684
RPL9	ribosomal protein L9	4.00E-09	2.28E-07	0.6484
RPS11	40S ribosomal protein S11	5.80E-07	0.00001881	0.4594
RPS12	ribosomal protein S12	6.67E-08	0.000002661	0.5668
RPS14	40S ribosomal protein S14	0.000001511	0.00004449	0.5081
RPS15	ribosomal protein S15	8.30E-13	1.27E-10	0.7808
RPS17	Canis lupus familiaris ribosomal protein S17 (RPS17), mRNA.	0.000004905	0.0001219	0.4881

RPS18	40S ribosomal protein S18	0.000002348	0.00006532	0.4919
RPS21	ribosomal protein S21	9.54E-12	1.16E-09	0.762
RPS23	ribosomal protein S23	0.000001484	0.00004381	0.4797
RPS27	ribosomal protein S27	8.95E-10	6.02E-08	0.6813
RPS7	ribosomal protein S7	4.60E-08	0.000001923	0.5926
RPS8	ribosomal protein S8	8.66E-07	0.00002697	0.4928
RPS9	ribosomal protein S9	6.66E-08	0.000002661	0.5602
RPSA	ribosomal protein SA	1.25E-10	1.09E-08	0.7248
RTN4RL1	reticulon 4 receptor like 1	4.52E-09	0.000000249	6.481
SAMD9L	sterile alpha motif domain containing 9 like	0.000001543	0.00004535	-0.6418
SARDH	sarcosine dehydrogenase	2.04E-21	1.16E-18	-1.8
SBDS	SBDS, ribosome assembly guanine nucleotide exchange factor	0.000001965	0.0000563	-0.5531
SCD5	stearoyl-CoA desaturase 5	5.99E-07	0.00001938	-1.174
SCN1B	sodium voltage-gated channel beta subunit 1	0.000006485	0.0001553	1.407
SCN5A	sodium voltage-gated channel alpha subunit 5	1.55E-07	0.000005723	-0.868
SDC3	syndecan 3	4.24E-07	0.00001411	-0.8729
SEMA3C	semaphorin 3C	8.25E-11	7.80E-09	-1.546
SEMA4A	semaphorin 4A	3.76E-08	0.000001621	-2.36
SEMA5B	semaphorin 5B	3.02E-08	0.000001336	-3.463
SERPINE1	serpin family E member 1	7.00E-10	4.97E-08	2.03
SERPINF1	serpin family F member 1	3.49E-11	3.75E-09	-1.399
SERPINI1	serpin family I member 1	2.35E-10	1.92E-08	1.331
SESN1	sestrin 1	0.000007487	0.0001763	1.003
SESN3	sestrin 3	1.48E-09	9.49E-08	-1.13
SETBP1	SET binding protein 1	1.14E-10	1.02E-08	-0.8701
SFRP5	secreted frizzled related protein 5	4.16E-11	4.43E-09	2.891
SGPL1	sphingosine-1-phosphate lyase 1	0.000003368	0.00008992	0.6867
SH3BP5	SH3 domain binding protein 5	7.20E-08	0.000002838	-0.7242
SH3D19	SH3 domain containing 19	0.00001008	0.0002289	-0.6194

SHROOM1	shroom family member 1	0.000004681	0.0001184	0.8758
SIPA1L2	signal induced proliferation associated 1 like 2	0.00000751	0.0001764	-0.6438
SLC10A6	solute carrier family 10 member 6	0.000003105	0.00008397	-1.033
SLC1A2	solute carrier family 1 member 2	4.20E-09	2.35E-07	-3.518
SLC22A3	solute carrier family 22 member 3	4.70E-11	4.80E-09	1.039
SLC23A2	solute carrier family 23 member 2	5.22E-16	1.31E-13	0.9633
SLC25A6	solute carrier family 25 member 6	0.000004072	0.0001045	0.4515
SLC26A4	solute carrier family 26 member 4	1.12E-07	0.000004211	3.684
SLC37A1	solute carrier family 37 member 1	0.000004688	0.0001184	0.7514
SLC3A2	solute carrier family 3 member 2	3.27E-07	0.00001126	0.9985
SLC43A2	solute carrier family 43 member 2	1.12E-08	5.53E-07	-1.393
SLC4A4	solute carrier family 4 member 4	2.93E-11	3.21E-09	-0.9006
SLC5A6	solute carrier family 5 member 6	4.54E-14	8.79E-12	0.9841
SLC7A2	solute carrier family 7 member 2	0.000003596	0.00009461	-0.7787
SLCO2A1	solute carrier organic anion transporter family member 2A1	9.86E-09	4.96E-07	1.469
SLIT2	slit guidance ligand 2	4.85E-16	1.25E-13	-1.837
SLIT3	slit guidance ligand 3	5.06E-13	8.48E-11	-1.544
SMARCA2	SWI/SNF related, matrix associated, actin dependent regulator of chromatin, subfamily a, member 2	0.000002293	0.00006409	-0.6079
SMYD2	SET and MYND domain containing 2	1.03E-07	0.000003923	-0.681
SOAT1	sterol O-acyltransferase 1	2.96E-07	0.00001029	0.8333
SORL1	sortilin related receptor 1	0.000009495	0.0002187	-0.9536
SOX5	SRY-box 5	5.39E-11	5.42E-09	0.9399
SPOCK1	SPARC/osteonectin, cwcv and kazal like domains proteoglycan 1	3.72E-09	2.14E-07	4.694
SPSB1	splA/ryanodine receptor domain and SOCS box containing 1	1.47E-12	2.10E-10	1.072
SPTBN5	spectrin beta, non-erythrocytic 5	0.000008406	0.000195	-1.375
SRD5A2	3-oxo-5-alpha-steroid 4-dehydrogenase 2	5.02E-10	3.73E-08	1.858
SRGAP1	SLIT-ROBO Rho GTPase activating protein 1	2.02E-09	1.22E-07	-1.059

SRGAP3	SLIT-ROBO Rho GTPase activating protein 3	1.48E-07	0.000005498	-1.825
STAC2	SH3 and cysteine rich domain 2	5.40E-09	2.93E-07	2.801
STAMBPL1	STAM binding protein like 1	4.19E-07	0.00001406	-0.9594
STARD10	StAR related lipid transfer domain containing 10	2.94E-07	0.00001024	-1.265
STAT5B	signal transducer and activator of transcription 5B	0.000003533	0.00009325	0.4438
STBD1	starch binding domain 1	2.10E-07	0.000007551	-0.669
STEAP4	STEAP4 metalloreductase	1.69E-12	2.36E-10	-2.03
SUCLG1	succinate-CoA ligase alpha subunit	7.16E-07	0.00002261	0.4706
SVIL	supervillin	9.85E-08	0.000003754	0.6151
SYNC	syncoilin, intermediate filament protein	0.00000205	0.00005846	-1.155
SYNE3	spectrin repeat containing nuclear envelope family member 3	0.000000176	0.000006379	0.9169
SYT9	synaptotagmin 9	0.00001022	0.0002313	-0.6644
SZT2	seizure threshold 2 homolog (mouse)	0.000004958	0.000123	0.4772
TACR1	tachykinin receptor 1	3.12E-07	0.00001078	-1.099
TDRD7	tudor domain containing 7	2.20E-09	1.33E-07	-0.8545
TES	testin	0.000002287	0.00006407	-0.8059
TET1	tet methylcytosine dioxygenase 1	0.000006346	0.0001526	-0.9429
TGFB3	transforming growth factor beta 3	6.81E-12	8.56E-10	-2.279
THY1	thy-1 membrane glycoprotein precursor	5.57E-10	4.10E-08	-1.55
TLR7	toll like receptor 7	3.76E-08	0.000001621	-3.291
TMEM119	transmembrane protein 119	4.31E-08	0.000001819	-2.584
TMEM120A	transmembrane protein 120A	4.56E-11	4.73E-09	1.257
TMEM150C	transmembrane protein 150C	1.81E-08	8.45E-07	-1.218
TMEM47	Transmembrane protein 47	0.000002987	0.00008132	-0.6621
TMEM52	transmembrane protein 52	6.06E-13	9.78E-11	1.017
TNFAIP2	TNF alpha induced protein 2	9.65E-07	0.00002953	-1.607
TNFSF10	tumor necrosis factor superfamily member 10	1.09E-09	7.22E-08	-0.8721
TNIK	TRAF2 and NCK interacting kinase	1.62E-08	7.62E-07	-0.9373
TOM1L1	target of myb1 like 1 membrane trafficking protein	0.000006273	0.0001514	-1.85

TOP1	topoisomerase (DNA) I	0.000001462	0.00004326	0.6039
TOX2	TOX high mobility group box family member 2	0.000005138	0.0001272	4.775
TP53I3	tumor protein p53 inducible protein 3	6.96E-07	0.00002205	-1.422
TPD52	tumor protein D52	0.000005684	0.0001391	-0.8038
TPT1	tumor protein, translationally-controlled 1	0.000002616	0.00007216	0.4384
TRERF1	transcriptional regulating factor 1	6.06E-07	0.00001955	-1.434
TRIM22	tripartite motif containing 22	7.59E-13	1.19E-10	-3.2
TSC22D3	TSC22 domain family member 3	4.26E-08	0.000001804	0.5475
TSPAN11	tetraspanin 11	3.85E-10	3.00E-08	-0.9606
TTC21B	tetratricopeptide repeat domain 21B	0.000007299	0.0001731	-0.511
TTN	titin	8.90E-13	1.33E-10	-2.146
TUBB2A	tubulin beta 2A class IIa	2.57E-10	2.09E-08	-1.194
TUBB6	tubulin beta 6 class V	3.19E-10	2.52E-08	1.077
USP2	ubiquitin specific peptidase 2	9.63E-08	0.000003682	1.77
USP24	ubiquitin specific peptidase 24	0.000003444	0.00009177	0.5624
VASH1	vasohibin 1	0.000009685	0.0002214	-0.9078
VCAM1	vascular cell adhesion molecule 1	4.07E-07	0.00001371	0.8109
WDFY4	WDFY family member 4	0.000009702	0.0002214	-0.6406
WDPCP	WD repeat containing planar cell polarity effector	0.000003345	0.0000895	-0.7085
WDR66	WD repeat domain 66	7.56E-13	1.19E-10	1.893
WFDC1	WAP four-disulfide core domain 1	2.11E-07	0.000007563	1.363
WIF1	WNT inhibitory factor 1	1.08E-18	4.26E-16	-2.934
WIPI1	WD repeat domain, phosphoinositide interacting 1	0.000000231	0.000008205	0.5744
WISP2	WNT1 inducible signaling pathway protein 2	1.54E-15	3.65E-13	-2.303
WNK3	WNK lysine deficient protein kinase 3	3.61E-15	7.84E-13	1.329
XDH	xanthine dehydrogenase	2.83E-22	1.69E-19	1.645
YAF2	YY1 associated factor 2	0.000009828	0.0002235	0.8686
ZDHHC14	zinc finger DHHC-type containing 14	4.96E-07	0.00001618	-1.225
ZNF365	zinc finger protein 365	0.000003819	0.00009943	-1.027

Acknowledgments

I am grateful to all the people involved in the success of this thesis.
Firstly, I would like to thank and express my sincere gratitude to both of my advisors Prof. Dr. med. vet. Felicitas Boretti and Prof. Dr. med. Vet. Nadja Sieber-Ruckstuhl for their continuous support in my research, for their patience, motivation and contributing knowledge. I am very appreciative of their trust in me and furthermore for the thorough reading, generous advice and corrections on my thesis.
Besides my advisors, my sincere thanks also go to Prof. Dr. med. vet. Thomas A. Lutz for his time and the examination of this thesis.
Many thanks also to Prof. Dr. Claudia Reusch, director of the department for small animals, for accepting me as a graduate student and giving me this great opportunity to write my thesis in the internal medicine department for small animals.
Furthermore, I would like to thank Sabine Müller Mutschler for her coordination and administrative aid throughout my thesis.
Secondly, I would like to specially thank Dr. Hubert Rehrauer and Susanne Kreutzer from the Functional Genomics Center Zurich (FGCZ), who provided me with the opportunity to enter the world of next generation sequencing and guided me through transcriptomics no matter how many questions I had. Without their guidance and patience I would still be trying to figure out endless Excel sheets with a lot of question marks.
Furthermore, profound thanks go to Anke Willing, who assisted me with the laboratory work, guided me through the thesis and supported me wherever she could. Her great spirit always encouraged me to do more.
I am also grateful to Prof. Dr. Hofmann-Lehmann, who enabled me to use the Center for Clinical Studies (ZKS) as well as Marilisa Novacco, who showed me around and aided me with all facilities in the lab and their usage.
Moreover, many thanks go to Aymone Lenisa and Karol Agnieszka for their great team work, effort and guidance throughout the year in the ZKS laboratory.
Additionally, I would like to thank my predecessors Florence Schmid and Susanne Spoerel, who conducted the long-term animal experiment and provided me with the samples as well as necessary information. Without their diligent work I would not have been able to process the samples.
Many thanks go to my colleague and friend Sophie Schmidt, who always had an open ear for thoughts about my thesis during our daily lunch walks with the dogs.
Finally, I would like to especially thank my mother, as well as the rest of my family, who always stood behind me and encouraged me no matter when or where. Thank you for always being there for me.
Last but not least, heartfelt thanks go to my partner Renato Gabellone, who is not only a graphical design talent, but also an inspiration, and my greatest support.

Curriculum Vitae

Persönliche Daten:

Name, Vorname	Martin, Isabelle Avital
Geburtsdatum	25.06.1990
Geburtsort	Frankfurt am Main
Nationalität	Deutsch

Bildungsweg:

08/2000-05/2008	Elisabethengymnasium, Frankfurt am Main (DEU) Frankfurt International School, Frankfurt am Main (DEU)
06/2008	International Baccalaureate (IB), Frankfurt am Main (DEU)
08/2008-09/2011	Studium der Medien- und Kommunikationswissenschaften, Bachelor of Arts (B.A.), Herzliya (ISR)
09/2012-02/2018	Studium der Veterinärmedizin, Freie Universität Berlin (DEU)
02/2018	Approbation, Freie Universität Berlin (DEU)
05/2018-05/2020	Anfertigung der Dissertation unter Leitung von Prof. Dr. med. vet. Felicitas Boretti Prof. Dr. med. vet. Nadja Sieber-Ruckstuhl in der Klinik für Kleintiermedizin der Vetsuisse-Fakultät Universität Zürich (CH) Direktorin: Prof. Dr. med. vet. Claudia Reusch, Dipl. ECVIM-CA
05/2019-07/2020	Internship, Bessys Kleintierklinik, Regensdorf/ Watt (CHE)

Extracurriculäre Weiterbildung:

02/2019	LTK Modul 1, Vetsuisse Fakultät, Zürich (CHE)
09/2018-05/2019	Assistenzärztin im Nachtdienst, Klinik für Kleintiermedizin, Vetsuisse Fakultät, Zürich (CHE)